The role of CD22 and Bim expression as determinants for the regulation of antigen-specific adaptive immune responses

Daphne Yin-Wai Ma

A dissertation

submitted in partial fulfillment of the

requirements for the degree of

Doctor of Philosophy

University of Washington

2012

Reading Committee:

Edward A. Clark, Chair

Michael J. Gale

Jessica A. Hamerman

Program authorized to offer Degree:

Department of Immunology

University of Washington

Abstract

The role of CD22 and Bim expression as determinants for the regulation of antigen-specific adaptive immune responses

Daphne Yin-Wai Ma

Chair of the Supervisory Committee:
Professor Edward A. Clark
Department of Immunology

West Nile Virus (WNV) is a RNA virus of the family *Flaviviridae* and the leading cause of mosquito-borne encephalitis in the United States. Humoral immunity is essential for protection against WNV infection; however, the requirements for initiating effective antibody responses against WNV infection are still unclear. CD22 (Siglec-2) is expressed on B cells and regulates B cell receptor signaling, cell survival, proliferation and antibody production. Here we investigated how CD22 contributes to protection against WNV infection. We found that CD22 knockout (*Cd22*$^{-/-}$) mice were highly susceptible to WNV infection and had increased viral loads in the serum and central nervous system (CNS) compared to wildtype (WT) mice. This outcome was not due to a

defect in humoral immunity as *Cd22*$^{-/-}$ mice had normal WNV-specific antibody responses. However, *Cd22*$^{-/-}$ mice had decreased WNV-specific CD8^{+} T cell responses compared to WT mice. These defects were not simply due to reduced proliferation or increased cell death, but rather were associated with decreased lymphocyte migration into the draining lymph nodes (dLNs) of infected *Cd22*$^{-/-}$ mice. *Cd22*$^{-/-}$ mice had reduced production of the chemokine CCL3 in the dLNs after infection, suggesting that CD22 affects chemotaxis via controlling chemokine production. CD22 was not restricted to B cells but was also expressed on a subset of splenic DCIR2^{+} dendritic cells that rapidly expand early after WNV infection. Thus, CD22 plays an essential role in controlling WNV infection by governing immune cell migration and CD8^{+} T cell responses.

In addition to CD22, the lifespan of a DC also affects the quality of adaptive immune responses. We found that DCs from mice lacking Bim, a pro-apoptotic protein of the Bcl-2 (B cell lymphoma -2) family, had prolonged lifespan in culture. The loss of Bim expression resulted in inability of DCs to promote BCR and antigen –induced B cell proliferation, regardless of maturation status. Long-lived DCs from *Bim*$^{-/-}$ mice also produced more IL-6 and had reduced expression of genes encoding BAFF and APRIL, all cytokines that affect B cell proliferation and survival. Thus both CD22 and Bim are important regulators of adaptive immune responses, and can specifically affect DC-mediated regulation of antigen-specific T and B cell response.

Table of Contents

List of Abbreviations

AFC	Antibody Forming Cells
Akt/PKB	Ak thymoma /Protein Kinase B
APC	Antigen-presenting cell
APRIL	A Proliferation Inducing Ligand
BAFF/BLyS	B cell Activating Factor/B Lymphocyte Stimulator
Bak	Bcl-2 antagonist/killer
Bax	Bcl-2 associated X protein
Bcl-2	B cell lymphoma-2
BCL2L11	Bcl-2 like protein 11
Bcl-xL	B cell lymphoma extra large
BCR	B cell receptor
Bim	Bcl-2 interacting mediator
BMDC	Bone Marrow-derived dendritic cell
BrdU	Bromodeoxyuridine
CCR5	C-C motif Receptor 5
CD22L	CD22 ligand
CFSE	Carboxyfluorescein succinimidyl ester
CGG	Chicken Gamma Globulin
CLEC	C-type Lectin domain family
CLR	C-type Lectin Receptor
CNS	Central Nervous System
CTL	Cytotoxic Lymphocyte
DC	Dendritic cell
DCAL2	Dendritic Cell-Associated Lectin 2
DCIR2	Dendritic Cell Inhibitory Receptor 2
DC-SIGN	Dendritic Cell-Specific Intercellular adhesion molecule-3-Grabbing Non-integrin
dLN	Draining lymph node
DMEM	Dulbecco's Modified Eagle Medium
DNGR-1	DC, NK lectin Group Receptor-1
DNP-KLH	Dinitrophenol-Keyhole Limpet Hemocyanin
E	Envelope
Erk	Extracellular regulated kinase
FCS	Fetal Calf Serum
GM-CSF	Granulocyte Macrophage-Colony Stimulating Factor
Grb2	Growth factor-receptor bound protein 2
HBSS	Hank's Balanced Salt Solution
HEL	Hen Egg Lysozyme

ICAM-1	Intercellular Adhesion Molecule -1
ICS	Intracellular Cytokine Staining
IFN	Interferon
Ig	Immunoglobulin
IL	Interleukin
iNOS/NOS2	Inducible Nitric Oxide Synthase/Nitric Oxide Synthase 2
IPS-1	Interferon Promoter Stimulator-1
IS	Immunological synapse
ITGAX	Integrin, alpha X (complement component 3 receptor 4 subunit)
ITIM	Immunoreceptor Tyrosine-based Inhibitory Motif
JNK	c-Jun N-terminal Kinase
LC	Langerhans Cells
LCMV	Lymphocytic Choriomeningitis Virus
LPS	Lipopolysaccharide
mAb	Monoclonal antibody
MAPK	Mitogen Activated Protein Kinase
Mcl-1	Myeloid cell leukemia differentiation protein-1
MDA5	Melanoma Differentiation Antigen 5
MFI	Mean Fluorescence Intensity
MHC	Major histocompatability complex
MIP	Macrophage Inflammatory Protein
MOI	Multiplicity of Infection
MRL	Murphy Roths Large
MST	Mean Survival Time
MZ	Marginal Zone
NFAT	Nuclear Factor of Activated T cells
NFκB	Nuclear Factor κ light-chain-enhancer of activated B cells
NK	Natural killer
NP	4-Hydroxy-3-nitrophenylacetyl
OVA	Ovalbumin
p.i.	Post-infection
PBS	Phosphate Buffered Solution
pDC	Plasmacytoid dendritic cell
PFU	Plaque Forming Units
PI3K	Phosphoinositide 3 Kinase
PLCγ2	Phospholipase Cγ2
PMCA-4	Plasma Membrane Ca2+ ATP-ase 4
PRNT	Plaque Reduction Neutralization Titer
PtI-(4,5)P2	Phosphoinositol-(4,5) diphosphate
qPCR	Quantitative Polymerase Chain Reaction

RAG-1	Recombination Activating Gene-1
RANTES	Regulated on Activation, Normal T cells Expressed and Secreted
RIG-I	Retinoic acid Inducible Gene-I
RLR	RIG-I Like Receptor
RPMI	Roswell Park Memorial Institute
SAP	SLAM-Associated Protein
Shc	Src homology/collagen
SHIP	Src homology-2 domain-containing inositol polyphosphate-5'-phosphatase
SHP-1	Src homology 2 domain-containing phosphatase 1
Siglec	Sialic acid binding Ig-like lectin
sIgM	Secretory IgM
SLP65/BLNK	SH2 domain-containing phosphoprotein of 65 kDa/B-cell linker protein
SPF	Specific Pathogen Free
ST6GAL-I	β-galactosidase α2,6 sialyltransferase
Syk	spleen tyrosine kinase
TCR	T cell receptor
TdT	Terminal deoxynucleotidyl transferase
Th1	T helper 1
Th2	T helper 2
TLR	Toll-like receptor
TNF	Tumor Necrosis Factor
TSLP	Thymic Stromal Lymphopoietin
VSV	Vesicular Stomatitis Virus
WNV	West Nile Virus
WT	Wildtype

List of Figures and Tables

Acknowledgements

First, I have to say many thanks to Professor Edward Clark and his lab for taking on the challenge of training me. I joined the lab as a very young and inexperienced student. The rigor and intellectually-stimulating environment has provided me the skills and confidence to further develop my career as an independent researcher. I will never forget the things I have learned from the lab, and will carry these lessons for the rest of my life.

I'd like to thank the members of my thesis committee: Drs. Keith Elkon, Michael Gale, Jr., Jessica Hamerman and Carol Sibley. Thank you for always providing guidance, patience, support and encouragement through some very trying times. I must also thank members of Keith and Mike's labs for help and technical support, and in particular Dr. Mehul Suthar for really introducing me to the field of West Nile virus and mentoring me throughout in all things virology. I could not have accomplished this without your dedication and enthusiasm, and will always appreciate your friendship and jokes.

To the members of the Clark lab, past and present, you have all contributed to training me and providing a home for me to grow as a scientist. Thank you especially to Dr. Shinji Kasahara for guiding me in and out of the lab, and for teaching me so many important lessons in my life. You have helped me to grow and have impacted my life in Seattle in so many ways. 進司先生、ありがとうございます！おきゃん！Thank you also to Drs. Marianne Bryan and Craig Chappell, my office-mates, for laughing with me during fun times, and comforting my sorrows with a nice bowl of pho or boba drink. My thanks also go to Kevin Draves for endless technical guidance along with a laugh (or chocolate), and Jay Chaplin for your friendship.

I'd like to thank all of my friends in Seattle and abroad, and in particular, all of my classmates: Deborah Hendricks, Sarah Warren, Meghan Koch, Mark Headley, Steven Josefowicz, Nathan Yee, Sasha Astrakhan, Jordan Jarjour, and Deanna Santer. Sincere gratitude goes to Sylvia Chien and your entire family for your friendship, encouragement and a food care packages when I am sick or busy. Thank you also to all my friends at the UW Newman Catholic Center and eXitSpace School of Dance for keeping my body healthy and mind sane.

Thank you to my science teachers and mentors who inspired me to pursue immunology, including Bill Pence, my high school AP Biology teacher for introducing me to immunology and invoking my passion for science; Drs. James P. Allison and P'ng Loke for giving me my first research job and encouraging me to go to graduate school; Dr. Judith E. Allen for letting me train in Edinburgh, Scotland and opening my eyes to the world; and Dr. Laurent Coscoy for supporting me through my final year in college.

Finally, I am forever grateful to my family here in the US and back in Hong Kong: my parents, Alfred and Kathleen for making me who I am and giving me the opportunity to pursue my dreams. Thank you for teaching me how to be a good person, and instilling the grace of God in me and what I do. 多謝您們為我犧牲, 也教我許多東西。多謝您們讓我追求我的夢想，又教了我怎麼樣自己獨立生活。And thank you to my brother, Colin, for being a role model for me, for believing in me and teaching me to always stand up for myself. Thank you all!
~Daphne 馬妍卉

Chapter 1: Introduction

The mammalian immune response is comprised of numerous cellular and molecular responses that are intricately and precisely coordinated functions that must be able to protect the host against invading pathogens as well as maintain tolerance to self. In broad terms, the cellular and molecular responses that make up the immune response can be divided into two main branches: the innate immune response and the adaptive immune response. The innate immune response involves components including initial pathogen recognition, discrimination between self and non-self pathogens, rapid production of antimicrobial and inflammatory molecules, gross phagocytosis and cytolysis of pathogens and infected cells. These processes of the innate immune response are not specific to a particular pathogen, and generally resolve in the early days after initial contact with a pathogen.

The initiation of the adaptive immune response generally includes monoclonal cells recognizing specific antigens, production of antibodies, cytolysis of cells infected with a specific pathogen, and usually initiates days after an infection begins and can last for weeks and even months in a host. The adaptive immune response also includes the generation and maintenance of memory responses involving expansion of antigen-specific cell clones that retain recognition and reactivity to specific pathogens, thus providing long-lived protection to the host for a particular pathogen. Ultimately it is the dual efforts of both the innate and adaptive components that provide acute and long-lived immunity against a pathogen.

The programming of adaptive immune responses is one function of innate immune responses, which bridge and coordinate the two branches of immunity into effective protection against a myriad of pathogens. It is thus crucial to understand the determinants influencing innate immune responses that impart effective adaptive immune responses. A better understanding of the interaction between the innate and adaptive immune branches would improve current strategies aimed at manipulating T cell and antibody responses as therapies and vaccines against various pathogens, such as DC vaccines for generating tumor-specific cytotoxic lymphocytes (CTLs).

DCs initiate and regulate the adaptive immune response

Dendritic cells (DCs) are central to innate immune responses and can function to initiate adaptive immune responses. Conseza and coworkers initially identified a loosely-adherent splenic macrophage-like population that was more efficient than adherent macrophages at inducing activation of naive T cells *in vitro* [1-3]. It wasn't until Steinman and Cohn compared these populations with macrophages by histology and microscopy and coined the term 'dendritic cell' that DCs were defined as a population distinct from macrophages [4]. Since that time, numerous studies have characterized the DC as a highly efficient antigen presenting cell (APC) that in particular is superior to B cells and macrophages in activating naive T lymphocytes [5-11].

Cells of both hematopoietic and non-hematopoietic origin are constantly engaging and disengaging via transient cell-contact mediated interactions with each other in which each cell sends and receives bi-directional signals with their partner(s)

that influence the activity of the other. During engagement of a naive T cell with an APC, the naive T cell receives multiple crucial signals from an APC to become fully activated. Signal 1 describes the interaction of the antigen-specific T cell receptor (TCR) on T cells with processed antigenic peptide bound to major histocompatability complex (MHC) I or II on APCs, while signal 2 refers to the engagement of co-stimulatory molecules such as those of the B7 family (CD80, CD86) on APCs with the CD28 receptor on T cells [12]. Both signals are generally required for the full activation of a naive T cell and preventing anergy. After encountering pathogens, DCs efficiently process antigen and present peptides bound to MHC I and MHC II to provide signal 1 to naive T cells as well as provide signal 2 by upregulating surface expression of CD80/CD86 after antigen uptake [13-15]. DCs can also produce cytokines and chemokines that can activate and recruit naive T cells and other immune cells to the site of infection [16-18].

The focal contact site between a T cell and its APC occurs at the immunological synapse (IS) which is made of clusters of surface molecule pairs such as TCR-peptide MHC complexes, co-stimulatory molecules and their receptors (CD80/CD86-CD28), and various adhesion molecules such as integrins [19,20]. Initial contact between T cells and APCs is brief [21], and the strength and duration of TCR engagement and signaling at the IS is important for the robustness of T cell activation and determining the fate of T cell responses [22-27]. DCs express integrins such as CD11c (Integrin, alpha X (complement component 3 receptor 4 subunit) or ITGAX) and other adhesion molecules such as intercellular adhesion molecule -1, ICAM-1 (CD54) and dendritic cell-specific intercellular adhesion molecule-3-grabbing non-integrin, DC-SIGN (CD209) [28] that

participate in forming and stabilizing the IS to facilitate signal 1 and signal 2 interactions on the surface of T cells [26,29]. Signals downstream of TCR engagement to APC peptide-MHC complexes also induces conformational changes and clustering of integrins [20,30], which stabilizes and increases longevity of cell-cell contact between the T cell and the APC at the newly forming IS, thereby further inducing T cell effector functions such as production of IL-2 and proliferation [30]. It is also via this prolonged cell contact that APCs can receive signals from T cells such as CD40-CD40 ligand (CD40L/CD154) and CD80-CD28 that influence the activation, survival and upregulation of co-stimulatory molecules within the APC [31,32], which may go on to activate more naive T cells. Thus the interaction of the T cell and the APC during this bi-directional dialogue provides signals for the T cell to become activated and differentiate into an effector cell as well as for the APC to enhance its immunogenicity allowing it to further amplify the magnitude of the immune response.

DCs also serve as major players in determining whether $CD4^+$ T cells become T helper 1 (Th1) cells or helper 2 (Th2) cells [33]. Th1 polarization depends heavily on interleukin-12 (IL-12) signaling, and DCs are a major source of IL-12 produced in response to Toll-like receptor (TLR) agonists and other products of pathogens [33-36]. DCs have also been shown to be required for induction of Th2 responses [37], but the exact mechanisms involved are still unclear. The current understanding is that DC production of TSLP [38-40] and surface expression of OX40 ligand (CD252, glycoprotein 34 kD/GP34, tumor necrosis factor super family 4/TNFSF4) [41-43] are involved in induction

of Th2 cell differentiation. Nevertheless, it is well established that DCs play a prominent role in determining effector T cell fate.

Subset and lifespan are factors that affect DC-mediated regulation of T cell responses

There are several factors that influence how DCs regulate T cell responses. One important factor is the subset of DC that interacts with the naive T cell during priming. There are a number of distinct DC subsets found in various anatomical locations. This dissertation will focus on $CD8^+$ and $CD8^-$ DC subsets found in the peripheral lymphoid tissues. Our lab and others have defined three distinct non-plasmacytoid DC subsets in the spleen. $CD8\alpha^+$ DCs constitute around 20% of splenic DCs and express the C-type lectin receptor (CLR) CD205 (DEC205), C-type lectin domain family 9A, CLEC9A (DNGR-1) and CLEC12A (DCAL2) [44]. $CD8\alpha^-$ DCs can be subdivided into two distinct subsets: $DCIR2^+$ DCs comprise around 50% of splenic DCs and express the CLR DCIR2 but do not express the CLR DCAL2 [43,45]. $CD8\alpha^-$ $DCAL2^+$ DCs comprise the remaining 30% of splenic DCs and express DCAL2, but DCIR2 [43].

The anti-DCIR2 monoclonal antibody (mAb), 33D1, anti-DEC205 mAb and anti-DCAL2 mAb have been useful for identifying the anatomical location of the different subsets in the spleen. Witmer and Steinman initially used the 33D1 mAb to show that $DCIR2^+$ DCs reside principally in splenic marginal zones (MZs) and bridging channels [46]. Later, Dudziak and colleagues used the 33D1 mAb to show that it bound the CLR, DCIR2 [45]. They also showed that $CD8\alpha^+DEC205^+$ DCs reside in the T cell zones distinct from the location of $DCIR2^+$ DCs. $DCAL2^+$ DCs, which overlap with the $CD8\alpha^-CD4^-$

subset [43], are located in the splenic MZ, red pulp and T cell zones [47]. The distinct anatomical localizations of the three subsets shape the cell types that interact with and are regulated by each subset.

Indeed, these three DC subsets have distinct functions in the regulation of effector T cell responses, and the use of these cell surface markers have been extremely useful to target individual populations for functional analysis. Carter *et al.* targeted Dectin-1 on CD8α$^-$CD4$^-$CD11b$^+$ DCs and DEC205 on CD8α$^+$DEC205$^+$ DCs using mAbs and showed that Dectin-1 targeting efficiently induced CD4$^+$ T cell and antigen-specific antibody responses, while targeting DEC205 induced higher CD8$^+$ T cell responses [48]. Using similar strategies with anti-DCIR2 and anti-DEC205 to target DCIR2$^+$CD8α$^-$ and DEC205$^+$CD8α$^+$ DCs, respectively, Dudziak *et al.* and Soares *et al.* showed that DCIR2$^+$ DCs preferentially induce CD4$^+$ T cell proliferation and skewing towards Th2 responses, while CD8α$^+$ DCs induce mainly CD8$^+$ T cell proliferation and Th1 responses [45,49].

The expression of these cell surface markers has also been useful for isolating specific DC subsets for *in vitro* cultures and *in vivo* adoptive transfer studies. den Haan *et al.* [50] and Pooley *et al.* [51] showed that CD8α$^+$ DCs are superior to CD8α$^-$ DCs in cross-presenting cell-associated and soluble antigens, while CD8α$^+$ and CD8α$^-$ DCs can both equally cross-present immune complexes in *in vitro* cell cultures [52]. Our lab used anti-CD8α and anti-DCAL2 mAbs to isolate and adoptively transfer individual splenic DC subsets into mice and showed that DCIR2$^+$ DCs preferentially induced Th2 responses while DCAL2$^+$ DCs induced Th1 responses *in vivo* [43]. Together, these studies illustrated

that specific DC subsets are a major determinant of the outcome of an effector T cell response.

Another determinant that affects DC-mediated regulation of T cell responses is the lifespan of the DC. The immune system is kept in a delicate balance between the ability to rapidly mount effector T cells versus preventing the onset of autoimmunity by autoreactive T cells and immunopathology by over-reactive T cells. Controlling the proper length of time in which a DC survives is critical for maintaining this balance, as reflected by the numerous mechanisms in which DCs are induced to undergo death. Stimulating DCs with lymphotoxin A and TLR agonists directly induces only small amounts of the anti-apoptotic protein b cell lymphoma -2 (Bcl-2), but dramatically induces the upregulation of the pro-apoptotic protein, Bcl-2 interacting mediator (Bim; BCL2L11, Bcl-2 like protein 11) within 24 hours of stimulation [53]. This intrinsic mechanism limits the extent for which a fully matured DC can activate naive lymphocytes and thus controls the strength of the immune response. Activated cytotoxic T cells target DCs presenting cognate antigen for death, which also effectively limits the amplitude of the immune response once it has been initiated [54-56]. Therefore limiting DC lifespan while it is a highly potent and fully mature APC is important for the maintenance of peripheral tolerance and appropriate silencing of the immune responses after pathogen clearance.

The limited lifespan of a DC is important for regulation during both steady-state homeostasis and antigen encounter [57]. During steady-state, only about 5% of DCs are dividing at any given time [58]. Using *in vivo* BrdU uptake assays, Kamath and colleagues

estimated the half-life of individual DC subsets in steady-state to be between 1.5 – 2.9 days [59,60]. In these studies, DCIR2$^+$ subsets had the longest half-life of about 2.9 days, DCAL2$^+$ DCs about 2 days, and CD8α$^+$ DCs with the shortest half-life of about 1.5 days. A later study using parabiosis techniques revealed that total DC populations in the peripheral lymphoid organs underwent continual renewal from blood precursors and could go through only a limited number of divisions before being completely replaced; this study found that the half-life of the total DC pool is about 5-7 days during homeostasis [61]. DC maturation via TLR stimulation or protein antigen encounter does not profoundly increase the proliferation rate or lifespan of individual DCs; on the contrary, these stimuli appear to only enhance the rate of DC turnover [59,60], likely by decreasing the ratio of anti-apoptotic molecule Bcl-2 to the pro-apoptotic molecule Bim [53]. Thus, the control of the adaptive immune response and maintenance of peripheral tolerance after lymphocyte activation is governed by the regulation of DC-intrinsic factors such as DC subset and lifespan.

DCs regulate B cell responses

In addition to regulating T cell responses, DCs can also regulate B cell responses. The initial understanding of naive B cell activation and differentiation into antibody forming cells (AFCs) was that B cells required cell contact-dependent interaction with activated T cells that had already undergone cognate TCR and MHC-peptide complex signaling to become activated [62,63]. Specifically, T cell cytokine secretion [63,64] and providing CD40L signaling to CD40 expressed on B cells [32,65] was required for B cell

differentiation and antigen-induced isotype class-switching. While $CD4^+$ T cell help clearly plays a central role in inducing B cell differentiation into AFCs, other studies had reported that other cell types and signals also drive B cell maturation in the absence of T cell help (e.g. macrophage and DC-derived cytokines such as B cell activating factor/B lymphocyte stimulator (BAFF/BlyS) and a proliferation inducing ligand (APRIL) [66-69]. Thus, this implied that other accessory cell types may have direct or indirect roles in directing B cell differentiation, class-switching and production of monoclonal antibodies. Indeed, it was recognized early on that DCs were important accessory cells that indirectly supported B cell antibody production by activating $CD4^+$ T cells to provide help to B cells, but did not directly participate in the activation of resting B cells [70].

However, recent studies have shown that certain DC subsets can play a direct role in induction of B cell activation, antibody production and even undergo antigen exchange. Our lab and others have shown that B cells and DCs directly make cell-cell contact [71-77] and can activate naive B cells [71-75,78]. Several groups showed that antigen internalized by DCs as immune complexes or as soluble protein antigens can be presented and taken up by B cells that come in contact with antigen-bearing DCs [71-73]. This process of antigen presentation highlighted a previously uncharacterized mechanism in which B cells acquire antigen and become activated.

The regulation of B cells by DCs in the absence of T cell help is mediated by both cell contact-dependent and –independent mechanisms [68,72,76,79,80]. For example, the production of soluble factors BAFF and APRIL by DCs is involved in promoting B cell

survival and proliferation [66,81-83], class-switching [68] and antibody production [83]. DCs also provide signals for B cell antibody production and activation dependent upon cell-contact. For example, our lab and others showed that the separation of DCs and B cells using transwells to prevent cell-cell contact abrogated DC-mediated regulatory effects on proliferation [74] and class-switching [75,79] that were observed when DCs and B cells were in contact. In addition, adhesion molecules such as lymphocyte function-associated-1 (LFA-1) [77] and CD22 [74] have been shown to participate in DC-B cell interactions. DCs may also provide CD40 signaling to B cells without T cell help, as one study showed that DCs upregulate CD40L expression after stimulation with Poly I:C and CpG and exposure to influenza virus [84]. Together the current understanding of the activation of B cells should no longer place DCs in a linear, indirect position in which DCs only activate $CD4^+$ T cells that subsequently activate naive B cells (**Fig. 1.1A**). Rather, the updated model should place DCs and $CD4^+$ T cells participating in a multi-cell cluster with B cells in which both DCs and activated $CD4^+$ T cells can concomitantly engage and activate naive B cells (**Fig. 1.1B**).

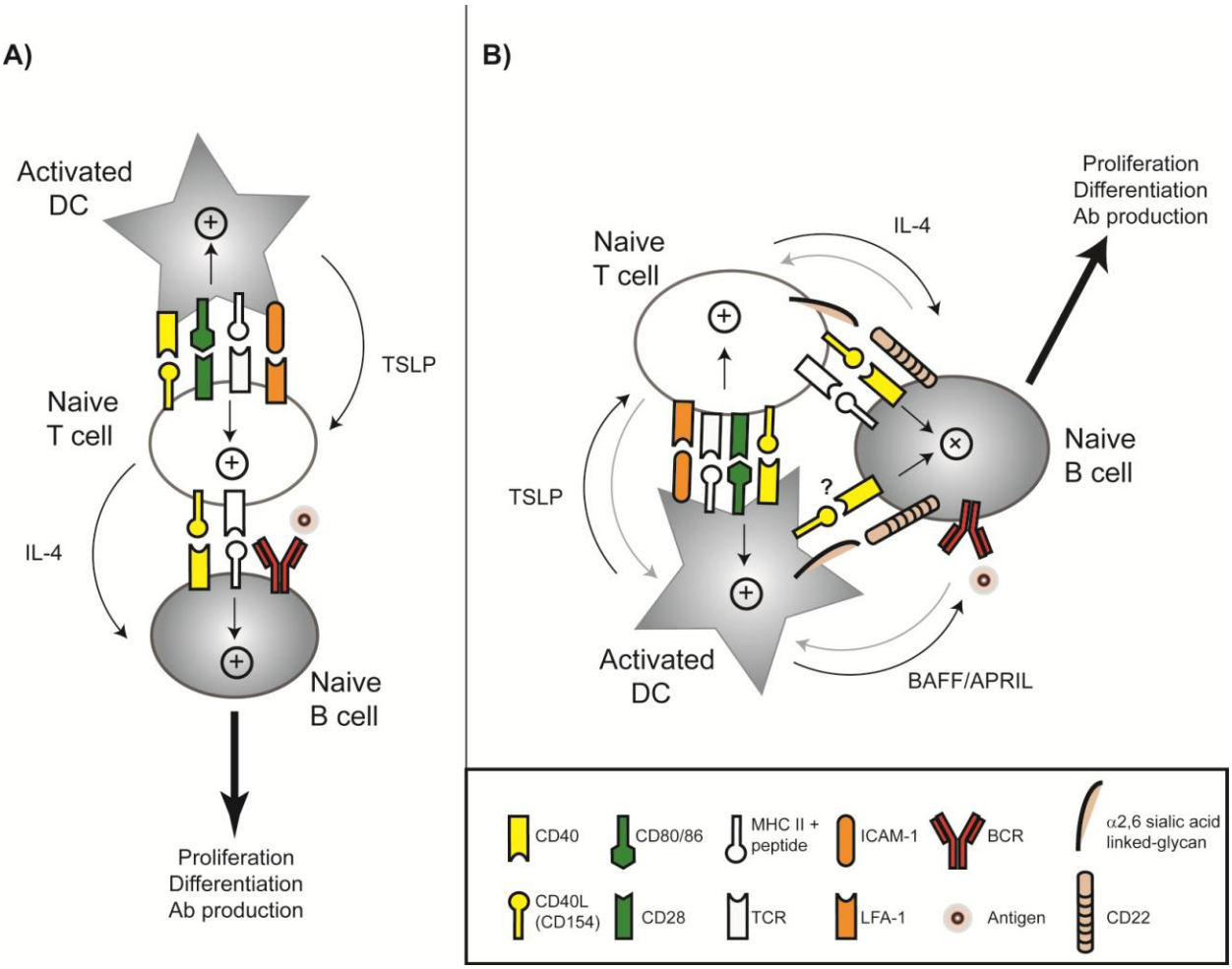

Figure 1.1. The activation of naive B cells involves a cooperative effort between DCs and T cells

A) The model of naive B cell activation is shown where DCs activate naive T cells which in turn activate naive B cells, leading to proliferation, differentiation and antibody production. Activated DCs provide multiple signals to T cells, including MHC II-peptide interacting with TCR (signal 1), CD80/CD86 interacting with CD28 (signal 2) as well as CD40-CD40L and ICAM1-LFA1 signals to naive T cells. This interaction leads to bi-directional activation, and activated T cells can go on to activate naive B cells. In this model, DCs do not directly interact with naive B cells. B) An updated model of the potential interactions that can occur between naive B cells, naive T cells and DCs: DCs can directly interact with naive B cells via CD22L-CD22, CD40L-CD40 and production of soluble BAFF/APRIL. Naive B cells could also receive signals from activated T at a

given time. Direct interactions between DCs and T cells, which have been well characterized, are also depicted. It is also important to note that bi-directional signaling occurs between each of these cell types (grey arrows).

CD22: A Siglec that regulates B cell responses via DC-dependent and –independent mechanisms

CD22 (Siglec-2) is a transmembrane glycoprotein, approximately 135 kDa in size that is part of the Siglec (Sialic acid-binding Ig-like Lectin) family [85]. The extracellular tail contains seven immunoglobulin (Ig)-like domains, and the most distal domains, 1 and 2, are required for binding to ligands [86,87]. The cytoplasmic tail consists of five conserved tyrosine motifs [88,89], which each serve as an important docking site to mediate intracellular protein interactions. CD22 is expressed in both the mouse and in humans, with orthologues found in all mammalian species examined [90].

CD22 expression was originally identified to be restricted to resting and activated cells of the B cell lineage [91-93]. Initial studies using anti-CD22 mAb identified some CD22 expression in early B cell precursors (e.g. TdT^+, pre B, surface IgM^+ and IgD^-) in the bone marrow [92]. In contrast, CD22 is expressed by the majority of peripheral mature B cells including B1 cells, and at the highest levels on follicular, mantle and marginal zone (MZ) B cells in the spleen [94,95]. However, our lab and others have identified expression of CD22 on other populations such as $CD8\alpha^-$ DCs [96] and eosinophils [97], thus implicating a role for CD22 in populations other than B cells.

Binding to CD22 and its regulation of B cell signaling pathways

Ig-like domains 1 and 2 of CD22 bind to α-2,6 sialic acid linkages [86] and several cell types express CD22 ligands including T cells, B cells, and DCs [74,98]. The enzyme β-galactosidase α2,6 sialyltransferase (ST6GAL-I) catalyzes addition of α-2,6 sialic acid linkages to Galβ1,4GlcNAc disaccharides on N- and O-glycans [99,100]. This enzyme is

responsible for addition of α2,6 sialic acids to glycans on cells such as T cells [101], and also catalyzes the addition of α-2,6 sialic acid linkages to CD22 on the surface of B cells [102]. Thus CD22 can function in 'trans' to mediate adhesion between B cells and other cell types [103-105], and also in 'cis' with itself and the B cell receptor (BCR) to modulate pathways involving signaling elements such as Lyn, Src homology 2 domain-containing phosphatase 1 (SHP-1) and growth factor-receptor bound protein 2 (Grb2) [106-108].

CD22 regulates B cell intracellular signaling pathways via recruitment of signaling molecules such as Src homology-2 domain-containing inositol polyphosphate-5'-phosphatase (SHIP), SHP-1 and Grb2, as well as direct binding and activation of an intracellular calcium pump called plasma membrane Ca^{2+} ATP-ase 4 (PMCA-4) [85,109] (**Fig. 1.2**). Phosphorylation of specific tyrosine residues within the intracellular tail leads to differential recruitment of specific signaling molecules [85]. Of the six total residues found in the cytoplasmic tail, three are part of the ITIM domains that mediate recruitment of phosphatases SHIP and SHP-1, one belongs to an ITIM-like domain, and the last is part of a Grb2-binding consensus sequence.

Tyrosine residue phosphorylation of CD22 is mediated by the Src family kinase, Lyn, which becomes activated downstream of BCR engagement [110,111]. Lyn-mediated phosphorylation of tyrosine residues on CD22 is also regulated by other signaling molecules such as CD40 [112], CD45 [113] and CD150/SLAM-associated protein (SAP) [114], thus illustrating a tightly-controlled and intricate network to regulate the function of CD22. Phosphorylation of at least two residues in the ITIM domains is required for recruitment of SHP-1 [115-117]. SHP-1 recruitment leads to reduced intracellular calcium

flux through mechanisms that may involve decreasing phosphorylation of molecules such as Vav-1 [118], CD19 [112] and SH2 domain-containing phosphoprotein of 65 kDa (SLP65)/B-cell linker protein (BLNK) [119]. In addition, SHP-1 recruitment is involved with CD22 binding and activation of PMCA-4 that functions to increase calcium efflux out of the cell, thus leading to reduced intracellular calcium-dependent signaling [120].

The events downstream of SHIP recruitment to CD22 are less clear, although it is known that Grb2 and Shc association with CD22 is required for the recruitment of SHIP to CD22 [121]. SHIP is known to reduce intracellular calcium flux, and thus may be involved in regulating calcium levels similar to SHP-1. This is consistent with the finding that CD22-deficient B cells had reduced SHIP recruitment, decreased calcium flux and decreased activation of the mitogen-activated protein kinase (MAPK) and c-Jun N-terminal kinase 2 (JNK2) [121]. Interestingly, activation of the MAPKs extracellular signal-regulated kinases, Erk1 and Erk 2, which depends on calcium signaling and is activated downstream of BCR ligation [122] was not enhanced in CD22-deficient B cells in this study, suggesting that CD22 may not affect these signaling pathways directly.

CD22 phosphorylation also leads to recruitment and interaction with other signaling molecules such as Grb2, spleen tyrosine kinase (Syk), phospholipase Cγ2 (PLC γ2), Shc phosphoinositide 3 – kinase (PI3K) and SH2D1A/SAP [85]. The downstream effects of these proteins recruited by CD22 are still unclear, but these molecules have generally been associated with cell activation signaling pathways and thus implicate CD22 in cell activation events. Indeed, a few groups have shown that CD22-deficient B cells have decreased responses to BCR engagement (reviewed in [123]). Thus CD22 is

likely to have functions involved with augmenting cell signaling and activation as well as dampening responses after BCR ligation.

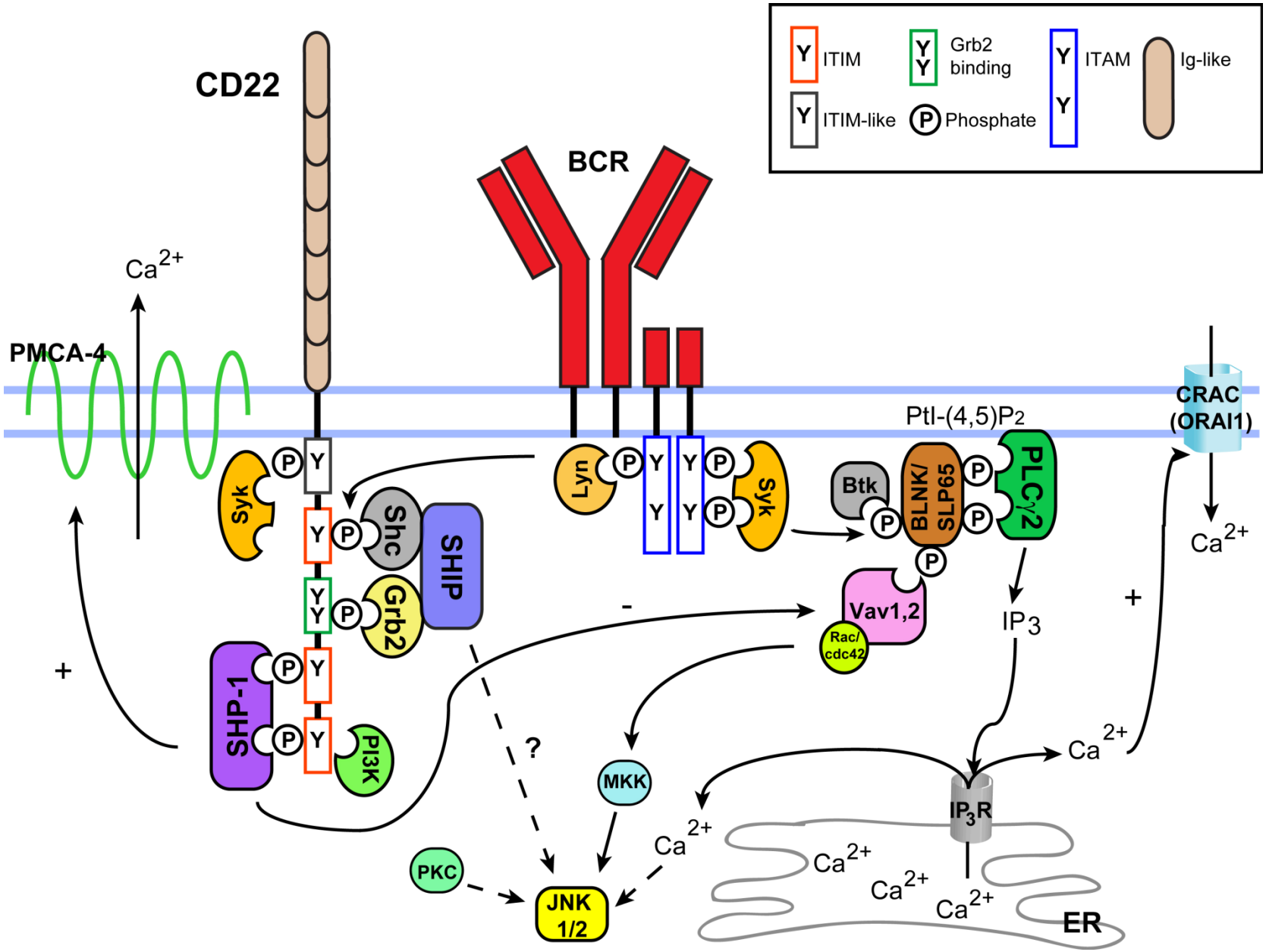
Y ITIM
Y Y Grb2 binding
Y ITAM
Ig-like
Y ITIM-like
P Phosphate
CD22
BCR
Ca2+
PMCA-4
CRAC (ORAI1)
PtI-(4,5)P2
Lyn
Syk
Btk
BLNK/ SLP65
PLCγ2
Shc
SHIP
Grb2
SHP-1
PI3K
Vav1,2
Rac/ cdc42
IP3
IP3R
MKK
PKC
JNK 1/2
ER
+
-
?

Figure 1.2. CD22 signaling in B cells

On the surface of B cells BCR ligation leads to activation of Lyn kinase, which phosphorylates various tyrosine-containing motifs on the intracellular tail of CD22. Phosphorylated tyrosine residues serve as scaffolds that allow recruitment of multiple molecules including Syk, PI3K, SHP-1 and the Grb2-Shc-SHIP complex. SHP-1 modulates the signaling pathways activated downstream of BCR ligation, including Ca^{2+} flux activated by Syk-Btk-BLNK/SLP65-PLCγ2 pathway. CD22 also interacts with PMCA-4 via SHP-1, which leads to increased Ca^{2+} efflux out of the cell. The recruitment of PI3K, Syk and SHIP may also lead to regulation of other signaling pathways, such as the activation of JNK MAPKs, but have not been well characterized. "+" represents activating signaling, and "-" represents inhibitory signaling.

CD22 regulates B cell responses: Studies using Cd22$^{-/-}$ mice

Much of the knowledge of how CD22 affects B cell responses after BCR activation was derived from studies using CD22-deficient mice. *Cd22*$^{-/-}$ mice have been developed by several labs including our own [95,118,124-126]. Although CD22 is expressed in early B cell precursors, B cell development is largely normal in *Cd22*$^{-/-}$ mice, with the exception of decreased MZ B cells in the spleen [74,127]. Follicular B cell subset numbers are unaffected in *Cd22*$^{-/-}$ mice. This finding may explain why *Cd22*$^{-/-}$ mice produce normal antibody responses to T cell-dependent (TD) protein antigens such as dinitrophenol-keyhole limpet hemocyanin (DNP-KLH) and 4-hydroxy-3-nitrophenylacetyl-ovalbumin (NP-OVA), but have diminished responses to T cell-independent (TI) antigens such as DNP-Ficoll [95,125]. One group reported no differences in TD or TI antibody responses [118] and a second group reported augmented TD-specific and autoantibody production [124] in *Cd22*$^{-/-}$ mice; these discrepancies may be due to differences in the generation of CD22-deficient mice. Studies from our lab using *Cd22*$^{-/-}$ mice also revealed that the decrease in TI-antigen specific antibodies more profoundly affected IgG subclasses rather than IgM [125], which suggested that CD22 regulates class-switching without affecting germinal center formation [95]. *Cd22*$^{-/-}$ B cells also exhibit increased apoptosis and dysregulated proliferation upon BCR ligation [95,124-126]. *Cd22*$^{-/-}$ B cells had increased turnover in response to anti-IgM stimulation [95,125,126] and decreased proliferation [118,125,126]. However, proliferation of *Cd22*$^{-/-}$ B cells was either augmented or similar to wildtype (WT) B cells in response to lipopolysaccharide (LPS), CD40 or CD38

+ IL-4 stimulation (reviewed in [123]). These observations suggested that CD22 regulation was specific to BCR-induced signaling pathways.

Given that DCs express ligands for CD22 as well as CD22 itself [96] (and see Chapter 3), it was plausible that DC-mediated regulation of B cells may utilize CD22 interactions. Indeed, our lab has shown that inhibition of BCR-induced B cell proliferation by unstimulated DCs required the expression of CD22 on B cells but not ST6GAL I on DCs [74]. This inhibition was cell contact-dependent and could be rescued with the addition of exogenous BAFF. Both unstimulated bone marrow-derived DCs (BMDCs) and splenic DCs were able to abrogate BCR-induced B cell proliferation. Thus there is a role for CD22 involvement in DC regulation of B cell responses.

West Nile Virus

WNV is a member of the *Flavivirus* family and is related to Dengue virus, yellow fever virus, and Japanese encephalitis virus. Since first being isolated in 1937 in Uganda [128], it has become a major global concern in the last two decades, mainly due to the speed in its transmission across continents. Spread via mainly avian-arthropod transmission, WNV emerged in the Western Hemisphere around 1999 and rapidly spread across North America over 4 years [129]. WNV is transmitted to humans as dead-end hosts through the bite of the mosquito. Over 30,000 human cases were reported to the Center for Disease Control from 1999-2010 in the United States (CDC, 2011), with a recent outbreak in 2012 of over 4,000 new cases and 41 deaths in just three months

(CDC, 2012). Thus developing prevention and therapeutic strategies for dealing with this emerging threat to global public health remains a high priority internationally.

The genome of WNV and other flaviviruses consists of a single-stranded, positive sense RNA containing 11 to 12 kilobases [128]. The flavivirus virion consists of an icosahedral nucleocapsid that envelops the genome, which itself is surrounded by a virion envelope consisting of membrane from the host cell lipid bilayer and integral envelope (E) proteins [128,130]. In mature virions, prM protein is cleaved into M protein that is incorporated into the mature virion. The flavivirus genome encodes seven nonstructural proteins that are responsible for the intracellular viral replication. The nonstructural proteins NS3 and NS4B have been identified to be immunodominant epitopes for $CD4^+$ and $CD8^+$ T cells, respectively [131,132].

The pathogenesis and lifecycle of WNV has been reviewed in detail elsewhere [130,133,134]. WNV is passed between avian and mosquito arthropod hosts. The bite of the mosquito is the major mode of transmission to humans and mammals, and once WNV has entered the host, it is thought that Langerhans cells (LCs) and other interstitial DCs are the first cells to take up the virus [135,136]. LCs carrying virus will traffic to draining lymph nodes (dLNs) where other cells can become activated, including T and B cells [137]. Following viremia, virus disseminates to peripheral tissues including the spleen, where it can eventually make its way into the central nervous system (CNS) [134]. Uncontrolled viral replication and death of neurons will lead to encephalitis, neuronal destruction and ultimately death of the host.

Protection against WNV requires both innate and adaptive immune responses

Components of both innate and adaptive immunity are critical to protection against WNV infection, and defects in early innate mechanisms may influence the late adaptive mechanisms for controlling virus (summarized in **Table 1.1**). Of the innate immune response, early Type I interferon (IFN) production is critical for the survival of the host. 100% of mice lacking either IFNα/β Receptor (*Ifnα/βR*$^{-/-}$) [138] or IFNβ production (*Ifnβ*$^{-/-}$) [139] succumb rapidly after infection to WNV with increased viremia and virus tropism in tissues such as the spleen, kidney and CNS. *Ifnα/βR*$^{-/-}$ mice succumb to WNV infection with particularly rapid kinetics, with a mean survival time (MST) of 3.8 days, thus highlighting the crucial requirement for type I IFN signaling in generating protective immunity to WNV.

A molecule known as interferon promoter stimulator-1 (IPS-1; MAVS, VISA, Cardiff) activates Type I IFN responses and other proinflammatory cytokines after WNV detection by the RNA helicases retinoic acid inducible gene-I (RIG-I) and melanoma differentiation antigen 5 (MDA5) of the RIG-I like Receptor (RLR) family[140]. IPS-1 is involved in regulation of Type I IFN signaling, and we found that IPS-1 deficient mice (*Ips-1*$^{-/-}$) are also highly susceptible to WNV infection with a MST of 7.3 days and display similar widespread and increased tissue viral tropism as in *Ifnα/βR*$^{-/-}$ mice [141]. Both *Ips-1*$^{-/-}$ and *Ifnβ*$^{-/-}$ mice have dysregulated T_{reg} numbers in the spleen after infection. Further, *Ips-1*$^{-/-}$ mice have significantly decreased numbers of T cells in the spleen after infection, thus indicating a role for RLR sensors of innate immunity in regulating adaptive immune responses. Studies using other mice with deficient innate

immune responses may also illustrate the importance of innate immune responses to adaptive immune responses during WNV infection. For example, mice lacking CD8α$^+$ DCs have decreased cytotoxic CD8$^+$ T cell responses to WNV [142], and only 50% of mice lacking the inducible nitric oxide synthase (iNOS/NOS2) to produce nitric oxide survive after WNV infection [143].

Among the components of the adaptive immune response, mice lacking either B cells (μMT) [144] or secretion of IgM (sIgM) [145] are highly susceptible to WNV infection, but succumb to infection generally later compared to mice with defects in the Type I IFN (with an MST of about nine days). Both lines of mice also display increased tissue virus burden similar to Type I IFN deficient mice, and it was determined that immune WNV-specific IgM is essential for survival [145]. Indeed, passive transfer of immune sera could partially rescue recombination activating gene-1 (RAG-1) deficient mice from succumbing to WNV infection [144], and thus highlights the importance of antibody responses for protection to WNV.

CD4$^+$ T cell [131,146] and CD8$^+$ T cell [147-149] deficient mice are also highly susceptible to WNV, and both lines of mice had a MST that was similar to mice with B cell defects. CD8$^+$ T cells have been reported to be protective during WNV infection by killing infected neurons [149], and trafficking of CD8$^+$ T cells to the CNS is thought to be required for prevention of encephalitis [147,148]. Indeed, mice lacking the chemokine receptor C-C motif receptor 5 (CCR5) have decreased T and natural killer (NK) cell infiltrates to the CNS and succumb to WNV infection with more frequency and rapid kinetics than WT mice [150]. Although CD4$^+$ T cells have also been shown to exhibit cytotoxic effects for

protection of WNV-infected cells [131], they may be more specialized for regulating WNV-specific antibody responses while $CD8^+$ T cells are more important in cytotoxicity of infected cells [146]. $CD4^+$ T cell deficient mice had decreased IgM and IgG responses when compared to WT mice [146], and mice lacking $CD8^+$ T cells or MHC I generated largely normal WNV-specific antibody responses [147,149]. Similar to mice with defects in Type I IFN, B cells or antibodies, T cell deficient mice were unable to control viral burden in the CNS after infection. However, in contrast to IFN$\alpha/\beta R^{-/-}$, *Ifnβ*$^{-/-}$ and *Ips-1*$^{-/-}$ mice, mice lacking $CD4^+$ or $CD8^+$ T cells were able to effectively prevent viremia and viral burden in the spleens and kidneys. Thus the functions mediated by the innate and adaptive immune responses are highly specialized in generating protective responses against WNV and require coordinated participation of both branches to prevent disease.

Table 1.1. Phenotype of selected genetically deficient mouse lines to WNV infection

				Virus burden compared to WT					Responses compared to WT		
Name	**Deficiency**	**% survival**	**MST (days)**	**Serum**	**Spleen**	**Kidney**	**Brain**	**Spinal Cord**	**Antibody**	**T cells**	**Refs**
IFNα/βR$^{-/-}$	Type I IFN signaling	0	3.8 ± 0.5	↑↑↑	↑	↑	↑	↑	ND	ND	[138]
Ifnβ$^{-/-}$	IFNβ production	5	10.2	↑	No diff	<1 log diff	↑	↑	No diff	↑ Spleen T_{reg}	[139]
Ips-1$^{-/-}$	RLR-mediated, Type I IFN signaling	0	7.3	↑	↑	↑	↑↑	↑	↑ IgM & IgG, ↓ neutralization	↓Spleen CD4, CD8, T_{reg}	[141]
Batf3$^{-/-}$	CD8α^{+} DCs	No defect	ND	ND	ND	ND	ND	ND	No diff	↓ CD8	[142]
Nos2 $^{-/-}$	NO production	50[a]	10	ND	ND	ND	ND	ND	ND	ND	[143]
μMT	B cells	0	~9	↑	↑	ND	↑	↑	None	ND	[144]
sIgM$^{-/-}$	No secreted IgM	0	9.8 ± 0.1	↑	↑	↑↑	↑	↑	↓ IgG, no IgM	ND	[145]
CD4-depleted	CD4^{+} T cells	0	21 ± 9	No diff	No diff	ND	↑	↑	↓IgM, ↓neutralization	Late ↓ CNS CD8	[146]
MHCII$^{-/-}$	CD4^{+} T cells	0	18 ± 11	No diff	No diff	ND	↑	↑	↓ IgM, ↓neutralization	Late ↓ CNS CD8	[146]
CD8$^{-/-}$	CD8^{+} T cells	16	10	No diff	↑ early, ↑↑ late	ND	↑	↑	ND	No CD8	[147]
MHCI$^{-/-}$	CD8^{+} T cells	12	12	No diff	↑ early, ↑↑ late	ND	↑	↑	ND	No CD8	[147]
Rag1$^{-/-}$	B & T cells	0	10	ND	ND	ND	ND	ND	None	None	[144]
Ccr5$^{-/-}$	CCR5	0	~11	ND	No diff	ND	↑	ND	ND	↓ CNS CD4, CD8	[150]
Lgp2$^{-/-}$	RLR-mediated signaling	12.5	ND	No diff	No diff	No diff	No diff	No diff	No diff	↓ Spleen CD8	[151]

Table 1.1. Phenotype of selected genetically deficient mouse lines to WNV infection

The names and cellular and molecular deficiency of specific genetic mouse lines are listed and their phenotypic characteristics to WNV infection compared to WT control mice are indicated. For viral burden in various tissues: ↑ = 1-3 log-fold increase; ↑ ↑ = 4-6 log-fold increase;

↑ ↑ ↑ = 7-10 log-fold increase; No diff = no differences compared to WT; ND = not determined in the study. Unless otherwise indicated, all data were obtained from experiments using a 10^2 PFU dose of pathogenic WNV.

[a] Study was performed with a 10^3 PFU dose of pathogenic WNV.

Questions to address

This dissertation examines how specific molecules influence the interface between innate and adaptive immunity during antigen encounter. In particular, it will focus on how CD22 is important for regulation of the adaptive immune response during encounter with the pathogen WNV and how it may be involved in DC-mediated regulation of adaptive immunity. In addition, this dissertation will address how the molecule Bim and control of lifespan affects DC regulation of B cells.

Chapter 2: Materials and Methods

Mice and WNV infection. *Cd22*$^{-/-}$ mice (Cd22^{tm1Eac}) [125] were generated and backcrossed to C57BL6/J mice for more than 10 generations. B cell-deficient μMT breeders (B6.129S2-*Ighm*^{tm1Cgn}/J) were kindly provided by Dr. David Rawlings (University of Washington). MD4 HEL-specific B cell receptor (BCR) transgenic (Tg) mice were a generous gift from Dr. Jason Cyster (University of California at San Francisco). NP-specific BCR Tg B1-8^{hi} mice were a generous gift from Dr. Michel Nussenzweig at (Rockerfeller University, New York). *Bim*$^{-/-}$ and C57BL/6 mice had previously been purchased from The Jackson Laboratory (Bell Harbor, ME, USA) and subsequently bred in-house. All mice were housed and maintained in a specific pathogen free (SPF) facility at the University of Washington. 6-10 week old, age and sex-matched female and male mice were injected under anesthesia in one or both hind footpads with 10 μl of virus diluted in a vehicle of Hank's buffered salt solution (HBSS) containing 1% fetal calf serum (FCS). All procedures were approved and conducted according to regulations of the Institutional Animal Care and Use Committee (IACUC) of the University of Washington (Seattle, WA, USA).

Virus. All virus stocks were maintained and characterized by the Virology Core within the University of Washington's Center for Flavivirus Immunity. The WNV isolate TX-2002 HC (WNV-TX) strain [152] was used at 10^3 plaque-forming units (PFU) dose, as determined by a plaque assay using baby hamster kidney (BHK) cells. In some experiments, a viral molecular clone generated from plaque-purified WNV-TX isolate

was used at the doses described above [153]. No differences in pathogenesis have been observed between the biological isolate and the infectious cloned viruses used in this study.

Viral Tissue Burden Quantification. Mice were sacrificed and perfused with 30 ml of Phosphate Buffered Solution (PBS), and tissues harvested into centrifuge tubes containing 1.4 mm PreCellys® ceramic beads (Cayman Chemical, Ann Arbor, MI, USA) and 500 µl PBS. All tissues were homogenized in a PreCellys®-24 homogenizer (Bertin Technologies, Paris, France) at 5000 RPM for 20 seconds, except brain tissues that went through two cycles of homogenization. Samples were spun down, and the supernatants were analyzed by a standard plaque assay using BHK cells. Serum viral titers were determined by real-time qPCR as previously described [141]. Briefly, peripheral blood samples were taken from infected mice at various timepoints, and viral RNA extracted using the QiaAMP Viral RNA extraction kit (Qiagen, Valencia, CA, USA). Sequences for primers and Taqman probes used were as previously published [154].

Quantification of WNV-specific antibody responses. To determine relative quantities of WNV-specific antibodies, a sandwich ELISA was performed as previously described using WNV envelope (E) protein purified from BL21 bacterial colonies [155]. 5 µg/ml WNV E protein was diluted in carbonate binding buffer (sodium carbonate in PBS, pH 7.2) and used to coat ELISA immunoassay plates (Nalge NUNC International, Rochester, NY, USA) at 4^{o}C overnight. Serum samples were inactivated for virus by exposure to ultraviolet light for 30 minutes, serially diluted three-fold starting at 1/20 in 0.1% milk

casein in PBS and incubated for at least one hour. Goat anti-mouse IgM, total IgG, IgG2b and IgG2c antibodies conjugated to horse radish peroxidase (HRP) (Southern Biotech, Birmingham, AL, USA) were added at dilutions of 1:2000 or 1:4000 as recommended by the manufacturer's protocol. Absorbance values were read at 450 nm and 570 nm wavelengths to correct for machine background on a Bio-Rad Micromanager Plate Reader (version 1.2). To determine relative quantities, a positive reading was determined to be a value above the cutoff value determined from the mean of negative control wells (naive and/or mock-infected mice) + standard deviation of the mean x standard deviation multiplier, f [156]. Negative control wells contained serial dilutions from at least three individual mice per experiment.

To determine neutralizing antibody titers, sera samples were analyzed in a Plaque Reduction Neutralization Titer (PRNT) assay as previously described [141]. Briefly, sera samples were diluted in Dulbecco's modified essential medium (DMEM) and complement inactivated by incubation at 56^{o}C for 30 minutes. Samples and 10^2 PFU virus suspended in DMEM were incubated for 1 hour at 37^{o}C prior to being plated onto BHK cells in 6-well plates and incubated for one hour before being overlaid with 2 ml of 0.5% agarose layer.

WNV epitope-specific peptides and MHC class I Tetramer. For *in vitro* restimulation, 1 µM of $CD8^+$ T cell specific NS4B 9-mer SSVWNATTA [132] or $CD4^+$ T cell specific $NS3_{2066-2080}$ 15-mer RRWCFDGPRTNTILE [131] peptide (Genemed Synthesis Inc., San Antonio, TX, USA) was added to $4x10^6$ cells splenocytes cultured in 96 well plates in the presence of

GolgiPlug containing Brefeldin A (BD Biosciences) at 37°C for 5 or 16 hours, respectively. Cells were then spun down and used for intracellular cytokine staining (ICS) as described below.

To generate a MHC class I tetramer, monomeric subunits were generated from NS4B 9-mer peptide at the Fred Hutchinson Immune Monitoring facility (Seattle, WA, USA). Monomers were subsequently tetramerized using streptavidin-PE (BD Biosciences, San Diego, CA, USA). All tetramer batches were titrated and tested prior to use.

Cell isolation. Spleen and lymph node tissues were harvested and resuspended in serum-free RPMI-1640 media (Thermo Scientific, Waltham, MA, USA) in the presence of Liberase collagenase mix (Roche, Pleasanton, CA, USA) and DNase I (Roche). Tissues were digested at 37°C for 45 minutes with mechanical disruption using a magnetic stir bar. Cells were then washed with FCS-containing RPMI and spleens lysed with 1x RBC Lysis Buffer (BioLegend, San Diego, CA, USA) prior to staining for flow cytometry.

For isolation of lymphocytes from the brain, tissues were harvested and finely chopped with scissors over a wire screen mesh in cold 5% FCS-containing PBS. Cells were washed twice with serum-free PBS before being resuspended in 30% Percoll (Sigma-Aldrich, St. Louis, MO, USA). A 70% Percoll layer was underlaid, and cells spun down for 20 minutes at room temperature. Lymphocytes were obtained from the 30-70% interface and washed with serum-containing RPMI-1640 prior to staining for flow cytometry.

Flow cytometry. At indicated timepoints p.i., popliteal dLNs or spleens were harvested from mice and made into a single cell suspension. The following rat-anti-mouse antibodies obtained from eBioscience (San Diego, CA, USA), Miltenyi Biotec (Auburn, CA, USA) or BD Biosciences were used: anti-DCIR2-biotin (eBioscience, clone 33D1) with Streptavidin-PE or Streptavidin PE Cy7 (eBioscience); anti-CD205/DEC205-PE (CedarLane Laboratories Limited, Burlington, Ontario, Canada or Miltenyi Biotec, clone NLDC-145); CD3ε-PerCP Cy5.5 (eBioscience, clone 145-2C11) or CD3ε-PE Cy7 (eBioscience, clone 145-2C11); CD45R/B220-eFluor450 (eBioscience, clone RA3-6B2) or CD45R/B220-PerCP (BD, clone RA3-6B2); CD11c-APC (eBioscience, clone N418); NK1.1-PerCP Cy5.5 (eBioscience, clone PK136); mPDCA1-PE (Miltenyi, clone JFO5-1C2.4.1); CD44-PE Cy7 (eBioscience clone IM7); CD8α-APC Cy7 (BD, clone 53-6.7); CD4-APC (BD, clone RM4-5); CD22-FITC or CD22-PE (BD, clone Cy34.1); I-A^b/I-E/MHC II-FITC (eBioscience, clone M5/114.15.2); CD40-PE (eBioscience, clone 1C10); CD69-PE Cy7 (eBioscience, clone H1.2F3); CD44-PE Cy7 (eBioscience, clone IM7); CD25-FITC (eBioscience, clone Bio3C7). Anti-DCAL2 antibody clones were generated in our lab and conjugated to APC fluorochromes [43].

To detect WNV-specific $CD8^+$ T cells, cells were first stained with surface markers and washed before staining with 1:100 – 1:250 dilution of MHC I-tetramer-PE at 4°C for 25 minutes. All samples were stained in PBS containing 2% FCS and 0.05% azide (FACS buffer) at 4°C, and fixed with PBS containing 4% paraformaldehyde before acquisition.

For ICS, cells were spun out of media containing WNV-specific peptide and Brefeldin A, and stained for surface markers, fixed with PBS containing 4% paraformaldehyde, then permeabilized and stained in FACS buffer containing 0.1% saponin with IFN-γ-Pacific Blue (eBioscience, clone XMG1.2) or IgG1 isotype control.

For staining for surface CD22 ligand (CD22L) expression, cells were stained using anti-mouse CD22 recombinant globulins (Rgs) generated in our lab [86]. Full-length (Rg 1-7) and truncated (Rg 3-7) fusion proteins were used at 300nM concentration using a protocol that was previously described [86].

All cells were acquired on a LSR II flow cytometer (Becton Dickinson, Franklin Lakes, NJ, USA) using FACSDiva software. All acquired data was analyzed using Flowjo software (Treestar Incorporated, Ashland, OR, USA).

Annexin V Staining. Splenocytes were harvested and processed as described, and cells were stained for surface markers, Annexin V-Pacific Blue (eBioscience) and Live/Dead-APC (Invitrogen) according to manufacturer's protocol (eBioscience). Cells were fixed in 1% paraformaldehyde and events immediately acquired on a flow cytometer.

Cell sorting of DC subsets. DCIR2$^+$ DCs were sorted on a Becton Dickinson Aria machine as previously described [43]. Briefly, single-cell suspensions of splenocytes from WT and *Cd22*$^{-/-}$ mice were positively selected using mouse anti-CD11c magnetic beads and LS magnetic columns (Miltenyi Biotech, Auburn, CA, USA). Selected cells were then incubated with monoclonal antibodies for 30 minutes on ice: B220-FITC, NK1.1-PE Cy7,

CD11c-PE, CD8α-APC Cy7/Alexa eFluor 780 (eBioscience) and anti-DCAL2-APC, Clone P2E7 [43]. DCIR2$^+$ DC subsets: B220$^-$NK1.1$^-$CD11c^{hi}DCAL2$^-$CD8α$^-$; DCAL2$^+$ DC subsets: B220$^-$NK1.1$^-$CD11c^{hi}DCAL2$^+$CD8α$^-$; CD8α$^+$ DC subsets: B220$^-$NK1.1$^-$CD11c^{hi}DCAL2$^+$CD8α$^+$. DCIR2$^+$ DC subsets were verified to express DCIR2 after sorting. Cells were washed twice and sorted. Cell purity was >96% after sorting.

Adoptive transfer experiments. For transfer of DCIR2$^+$ DCs, 1.4 x 10^6 cells of B220$^-$NK1.1$^-$CD11c^{hi}DCIR2$^+$DCAL2$^-$CD8α$^-$ DCs were sorted as described above, and washed twice with cold PBS before injected intravenously (i.v.) into age and sex-matched WT and *Cd22*$^{-/-}$ recipients. Recipient mice were infected 3 hours s.c. after transfer with 10^3 PFU WNV-TX, and harvested 7 days post-infection for flow cytometry analysis. For transfer of Ly5.1$^+$ splenocytes, female Ly5.1$^+$ (CD45.1$^+$) spleens from C57BL/6 mice were harvested and digested with collagenase as described. After red cell lysis, cells were washed and resuspended at 7.5 x 10^7 cells/ml in sterile cold PBS. 200µl of single-cell suspension was injected i.v. into tail veins of recipient WT or *Cd22*$^{-/-}$ mice (Ly5.2$^+$/ CD45.2$^+$). One day after transfer, the left hind footpad was injected s.c. with 10^3 PFU WNV-TX, while the right hind footpad was left uninjected (naive) or injected s.c. with 10µl of 1% FCS/HBSS vehicle (mock). 24 hours after infection, left and right popliteal dLNs were harvested and processed for flow cytometry.

In vivo BrdU incorporation. In vivo BrdU uptake by cell populations was performed using a commercially available BrdU kit according to the manufacturer's protocol (BD Biosciences). Briefly, 24 hours prior to harvest of tissues, infected mice were injected

with 100 μg/ml of BrdU resuspended in sterile PBS i.p. Tissues were harvested and digested with Liberase as described, and single cell suspensions were stained for various surface markers. Intracellular BrdU staining was performed the following day after fixation/permeabilization, and events immediately acquired on a flow cytometer.

RNA isolation and real-time quantitative PCR. Total mRNA was isolated from whole lymph nodes using Qiagen RNAeasy Mini Spin Columns according to the manufacturer's protocol (Valencia, CA, USA). Viral RNA was extracted from serum samples using QiaAMP Viral RNA Extraction Kit (Qiagen, Valencia, CA, USA). In brief, lymph nodes were homogenized and treated with RLT Lysis buffer to obtain lysates for RNA isolation. Whole blood samples were spun down in Vacutainer Serum Separator tubes (BD Biosciences), and serum samples were collected and stored at -80^{o}C until use. Isolated RNA was reverse-transcribed using Cloned AMV Reverse Transcriptase Kit (Invitrogen, Grand Island, NY, USA) to make cDNA for real-time qPCR analysis by Taqman (Applied Biosystems Incorporated, Foster City, CA, USA) or Sybr Green (Roche). Thermocycler conditions and primers for *Ifnβ* and *Gapdh* analysis using Sybr Green were previously described [157] and purchased from Invitrogen. Taqman primers for determination of chemokine and *18s* reference gene expression from whole lymph nodes were designed and purchased from Applied Biosystems Incorporated. The primers and thermocycler conditions for determination of viral RNA in the serum were performed as previously described [141,154].

For determination of BAFF and APRIL expression, WT and *Bim*$^{-/-}$ BMDCs cultured with various stimuli were harvested and total mRNA isolated using Qiagen RNAeasy Mini kit. Total mRNA was used directly in one-step real-time qPCR using MultiScribe reverse transcriptase and RNAse Inhibitor (Applied Biosystems Inc.) with Sybr Green Master Mix (Roche). Values for BAFF and APRIL were made relative to GAPDH expression values and normalized to WT media control samples. Primers and thermocycler conditions for real-time qPCR were previously described [68].

Type I IFN Bioassay. Serum samples were collected at indicated timepoints p.i. and complement inactivated by incubation at 56^{o}C for 30 minutes. Samples were analyzed using a Type I IFN bioassay with Encephalomyocarditis virus on BHK cells as previously described [141]. All samples were run in duplicate in 96-well plates.

Infection of sorted DC subsets and assays for cytokine expression. DCIR2^{+}, DCAL2^{+} and CD8α^{+} DCs were sorted as previously described. 1x10^{5} cells were plated in duplicate in a 96-well round bottom plate with 1.0 or 0.5 MOI of WNV-TX. After 24 hours, cells were spun down and supernatants collected for cytokine analysis. Cell viability was assessed by Trypan Blue and determined to be 100% viable for all wells.

A custom panel of Milliplex MAP Mouse Cytokine/Chemokine Magnetic Bead panel containing individual analytes was purchased from Millipore Corporation (Catalog # MCYTOMAG-70K, Billerica, MA, USA). 25µl of supernatants were used in individual wells for analysis according to manufacturer's protocol. In brief, supernatants were incubated on a rocking platform overnight and incubated with detection antibody

followed by Streptavidin-PE the following day prior to analysis on a Bio-Plex 200 array reader (Bio-Rad Laboratories, Hercules, CA, USA).

Generation of BMDCs and In vitro *Cultures.* BMDCs were generated from WT and *Bim*$^{-/-}$ mice as previously described [74]. After 7 days of differentiation with GM-CSF (20 ng/ml), cells were washed and re-plated in 10% FCS-containing RPMI media. To assess viability, 10% Trypan Blue (Sigma-Aldrich) suspended in PBS was used. To generate mature DCs, stimuli were added at indicated doses: LPS (Sigma-Aldrich); anti-CD40 (Clone 1C10, generated in Clark lab); CpG A (Sigma-Aldrich); TGFβ (R&D Biosystems Inc., Minneapolis, MN, USA); Type I IFN (Promega, Madison, WI, USA). Cells were treated for various timepoints with and without stimuli in RPMI media and washed before being co-cultured with B cells. For ICS of stimulated DCs, BMDCs were stimulated with various agonists for 18 hours, with the addition of Brefeldin A for the remaining 6 hours. Cells were spun down and washed prior to staining for surface markers followed by ICS staining with IL-6 –PE (eBioscience, clone MP5-20F3) or IgG1 isotype control.

B cell-DC Co-cultures. B cell-DC co-cultures were set up in 24-well plates as previously described [74]. B cells from C57BL/6 and MD4 mice were isolated using magnetic negative selection with EasySep Mouse B cell Enrichment Kits (StemCell Technologies, Vancouver, BC, Canada) and loaded with 5 μM of CFSE (Sigma-Aldrich) as previously described [74]. For cross-linking of the BCR, graded doses of anti-IgM Fab'2 fragments (Jackson Laboratories) were added. B cells were plated at $8x10^5$ cells/well and BMDCs plated at various ratios relative to B cell numbers.

Antigen-specific B1-8^{hi} B cells were isolated using EasySep Mouse B cell Enrichment kits with the addition of 1 µl of anti-κ light chain-biotinylated antibody (eBioscience). Purity was >90% for NP-binding B cells. Antigen specificity of B cells was verified by staining with NP-PE and assessed by flow cytometry. Day 7 differentiated BMDCs from WT and *Bim*$^{-/-}$ mice were harvested and washed from GM-CSF. Cells were pulsed with graded doses of NP (NP-OSu, Pierce Biochemicals, Rockford, IL, USA) conjugated to CGG (Sigma-Aldrich) or HEL (Sigma-Aldrich) in 2 ml round bottom tubes at 1x10^6 cells/ml overnight at 37^{o}C. Cells were then washed five times with media and pelleted before plating. Antigen-specific B cells were loaded with 5µM CFSE and plated at 1-2x10^5 cells/well in 96 well round-bottom plates with various ratios of BMDCs. After 72 hours cells were harvested and events acquired for CFSE dilution. In some experiments, 20ng/ml of recombinant BAFF (Pierce Biochemicals) was added to all wells.

Ethics Statement. All animal experiments were performed in accordance to NIH guidelines listed in the Guide for the Care and Use of Laboratory Animals, the Animal Welfare Act, and US federal law. All experiments were approved by the University of Washington Institutional Animal Care and Use (IACUC) committee, animal welfare assurance number A3464-01. The University of Washington Animal Care and Use Program is fully accredited by the Association for Assessment and Accreditation of Laboratory Animal Care International (AAALAC), accreditation number 000523, and registered with the USDA, certificate number 91-R-0001.

Chapter 3: CD22 is required for protection against West Nile Virus infection

Introduction

WNV is an emerging virus and a member of the *Flaviviridae* family. Protective immunity against WNV requires both innate and adaptive immune responses. Type I and type II interferon (IFN) production and signaling, as well as humoral and $CD4^+/CD8^+$ T effector responses [134] are required to protect against lethal WNV infection. B cell-deficient (μMT) mice are highly susceptible to WNV infection [144], and notably, mice that are unable to secrete IgM are also highly susceptible [145]. Passive transfer of immune sera protects μMT mice from rapidly succumbing to WNV infection [144,158], underscoring the importance of humoral immunity. In addition, adoptive transfer of purified B cells from immune mice partially rescues immunodeficient *Rag1*$^{-/-}$ mice, which lack functional B or T cells, from succumbing to WNV infection [144]. Together these findings highlight the importance of antibody and B cell effector responses for protection against encephalitic disease, and prompted us to further investigate the requirements for generating protective B cell responses to WNV.

CD22 (Siglec-2) is a cell surface glycoprotein that is approximately 135 kDa in size [88,89]. The proximal extracellular portion of CD22 binds to α-2,6 sialic acid linkages [86] and a number of cell types express CD22 ligands including T cells, B cells, and dendritic cells (DCs) [74,98]. In contrast, human and mouse CD22 has been reported to be restricted

to the B cell lineage [93,105,159]. *Cd22*$^{-/-}$ mice produce normal antibody responses to T cell-dependent protein antigens, but have diminished responses to T cell-independent antigens and reduced numbers of marginal zone B cells [74,127]. In addition, *Cd22*$^{-/-}$ B cells exhibit increased apoptosis and dysregulated proliferation upon BCR ligation [95,124-126]. Although CD22 regulates multiple B cell functions, the role of CD22 in protection against viral pathogens is unclear. For example, *Cd22*$^{-/-}$ mice infected with lymphocytic choriomeningitis virus [160], vesicular stomatitis virus [160] or *Staphylococcus aureus* [161] have no differences in survival compared to wild type (WT) mice.

Here we reveal that CD22 plays an essential role in protection against WNV infection. *Cd22*$^{-/-}$ mice were highly susceptible and succumbed to WNV infection, but surprisingly, this was not due to defects in antibody responses. Rather we found a defect in accumulation of antigen-specific CD8^{+} T cells in the spleen and the brain of *Cd22*$^{-/-}$ mice, which was due to impaired cell proliferation and cell migration to infected tissues. We conclude that CD22 regulates CD8^{+} T cell-mediated immune responses and cell migration after WNV infection.

Results

Cd22$^{-/-}$ mice have increased susceptibility to WNV-TX infection

To determine whether CD22 plays a role in protection against WNV infection, we assessed susceptibility of WT and *Cd22$^{-/-}$* mice to infection after subcutaneous (s.c.) inoculation with 10^3 plaque-forming units (PFU) of WNV-TX. 88% of *Cd22$^{-/-}$* mice succumbed to infection (mean survival time 9.5 days) compared to 15% of infected WT mice ($p<0.0001$) (**Fig. 3.1A**). Moreover, while symptoms began to resolve in WT mice by 7 days post-infection (p.i.), encephalitic disease and paralysis-like conditions were significantly enhanced in *Cd22$^{-/-}$* mice (**Fig. 3.1B**). Similar to the *Cd22$^{-/-}$* mice, WNV-TX was highly virulent in μMT mice (**Fig. 3.1A**), further demonstrating the importance of B cells in protection against WNV infection [144].

WNV-infected Cd22$^{-/-}$ mice have enhanced virus replication in peripheral and CNS compartments.

WNV infection in mammalian hosts is acquired through peripheral inoculation [134]. Infected cells migrate into the skin dLNs, where the virus infects and activates both myeloid and lymphoid cells; this is followed by viremia and viral entry into peripheral tissues such as the spleen, kidney and liver. 6-7 days after initial infection, virus is detected in the CNS, which can lead to encephalitis symptoms in the host. To define the role of CD22 in controlling WNV *in* vivo, we inoculated WT and *Cd22$^{-/-}$* mice s.c. with 10^3 PFU of WNV-TX and then monitored viral burden within peripheral and CNS tissues using a plaque assay on BHK cells. We observed similar kinetics and

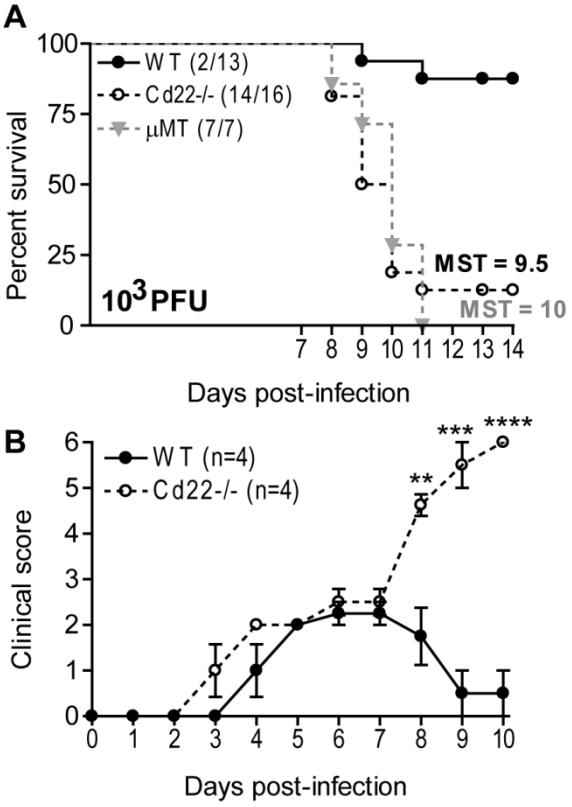

Figure 3.1. *Cd22*$^{-/-}$ mice are more susceptible to WNV infection compared to WT mice

WT and *Cd22*$^{-/-}$ mice were inoculated s.c. with 10^3 PFU of WNV-TX and monitored daily for A) survival and B) morbidity. A) *Cd22*$^{-/-}$ mice had a mean survival time (MST) of 9.5 days and µMT mice had a MST of 10 days. Statistics were performed using a log-rank test for significance comparing percent of surviving WT mice to *Cd22*$^{-/-}$ mice ($p<0.0001$). Survival curves list the numbers of individual mice that succumbed to infection/total number of mice. Data are pooled from three independent experiments. B) Clinical scores for mice inoculated s.c. with 10^3 PFU WNV-TX (infected) are represented, where 1 = ruffled fur, lethargy, hunched posture, no paresis; 2 = very mild to mild paresis; 3 = frank paresis involving at least one hind limb and/or conjunctivitis or mild paresis in two hind limbs; 4 = severe paresis while still retaining feeling and possibly limbic; 5 = true paralysis; 6 = moribund. Error bars represent variance of clinical scores. Statistics were performed using a Student's t-test, where **$p<0.01$, ***$p<0.001$, and ****$p<0.0001$. Data shows one representative of three independent experiments with four mice per group.

peak virus replication in the spleens of infected WT and *Cd22*$^{-/-}$ mice. Infected *Cd22*$^{-/-}$ mice exhibit normal tissue tropism (**Fig. 3.2A, 3.2B**). Infected *Cd22*$^{-/-}$ mice, unlike WT mice, exhibited increased virus in the serum on day 4 p.i. However, serum viral loads in the *Cd22*$^{-/-}$ mice returned to normal levels by day 7 p.i (**Fig. 3.2C**). This increase in the *Cd22*$^{-/-}$ mice in serum viral loads at day 4 preceded significantly higher viral loads on day 7 p.i. in the brain and spinal cord compared to infected WT mice (**Fig. 3.2D, 3.2E**). The detection of increased virus in the CNS coincided with the enhanced clinical scores on day 7 p.i. observed in infected *Cd22*$^{-/-}$ mice (**Fig. 3.1B**). These data demonstrate that CD22 is dispensable for controlling virus replication in the periphery (spleen and kidneys), but is essential in controlling viremia at early times during infection and virus replication in the CNS.

Cd22*$^{-/-}$ *mice have normal WNV-specific antibody responses

The enhanced viral burden in the serum and CNS compartments of infected *Cd22*$^{-/-}$ mice is consistent with previous observations in mice unable to secrete IgM [145], suggesting that CD22 may function to regulate antibody production during WNV infection. However, by-in-large serum levels of WNV-specific IgM and IgG were similar in infected WT and *Cd22*$^{-/-}$ mice as quantified by ELISA to WNV Envelope (E) protein (**Fig. 3.3A**). At day 4 p.i. in *Cd22*$^{-/-}$ mice, there was a significant increase in serum WNV-specific IgM antibodies, but at day 7 p.i. IgM antibody levels were similar to levels in WT mice. WT and *Cd22*$^{-/-}$ mice had similar WNV-specific serum IgG2b and IgG2c levels

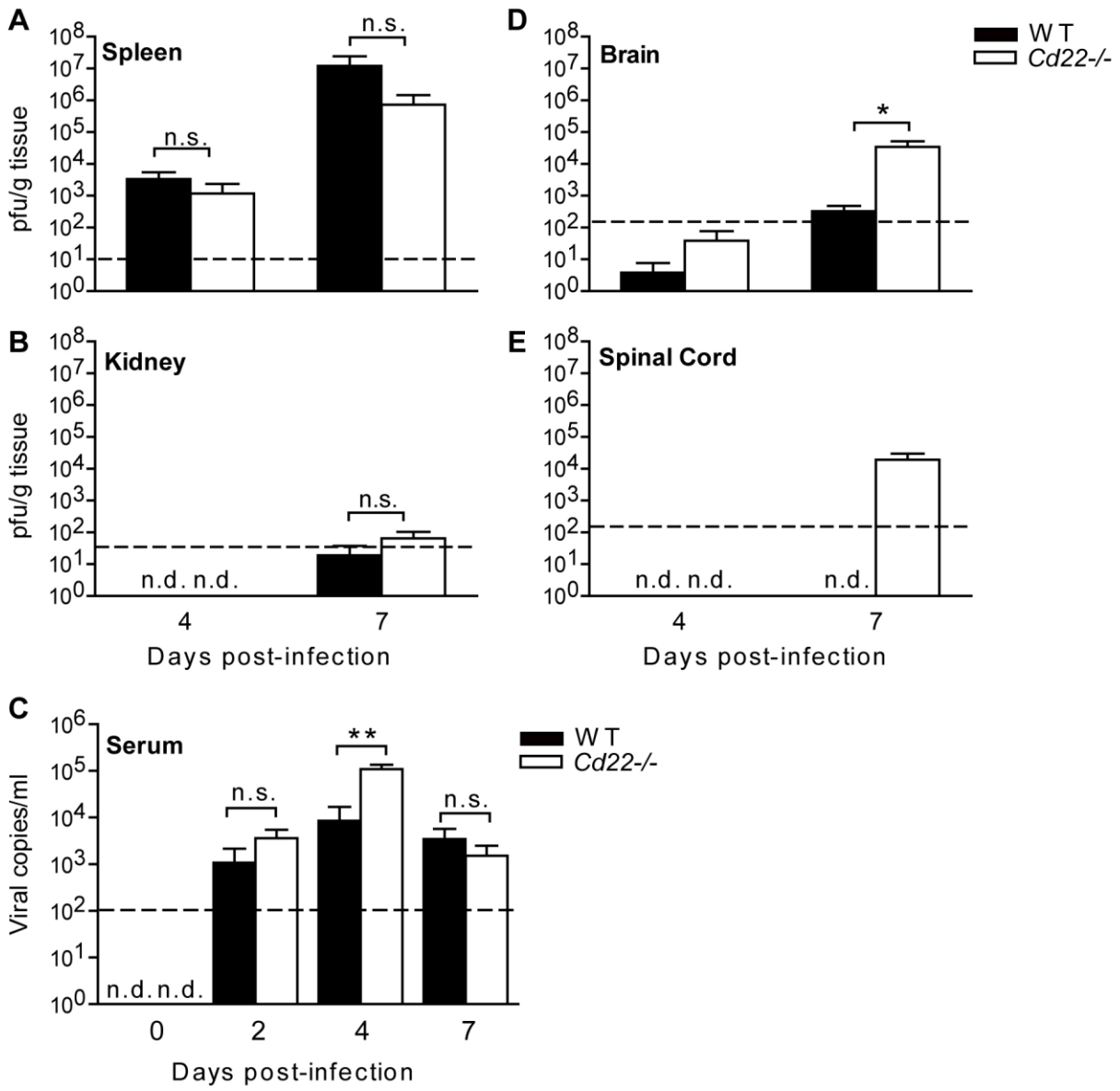

Figure 3.2. Increased viral titers in the CNS and serum of WNV-infected *Cd22*$^{-/-}$ mice

Viral titers were determined using A, B, D, E) a standard plaque assay or C) quantification using real-time qPCR from various tissues. Mice were inoculated as described and tissues harvested at indicated days p.i. Graphs show PFU of virus plaqued per gram of tissue or copies of viral RNA per ml of serum. Dotted lines show limit of detection of plaque assays. Statistics were performed using a Mann-Whitney U test of the median where *$p<0.05$, **$p<0.01$ and n.s. = not significant; n.d. = not detected. Data shows samples pooled from three independent experiments with 2-4 mice per timepoint.

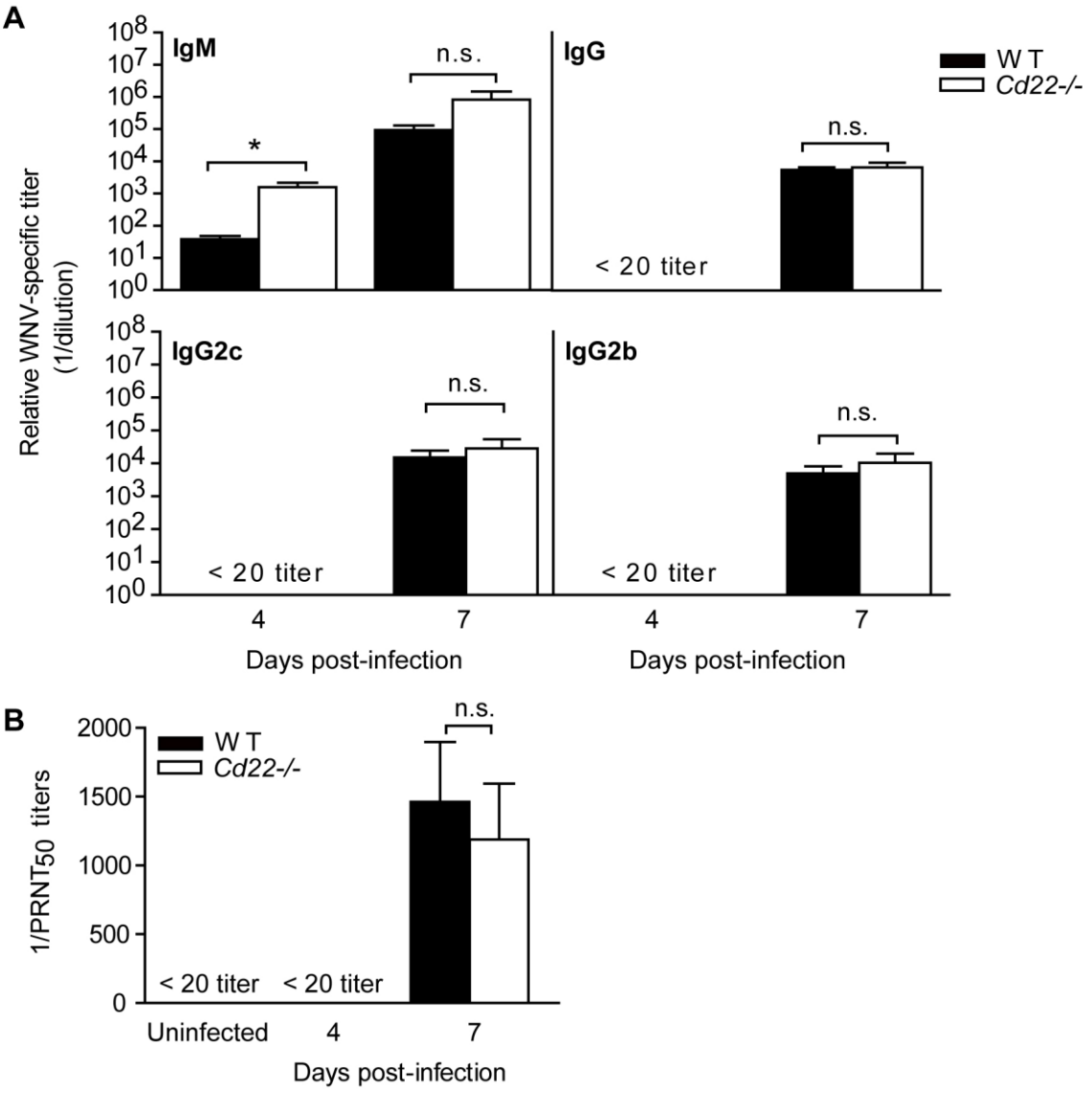

Figure 3.3. Normal virus-specific antibody responses in WNV-infected *Cd22*$^{-/-}$ mice

A) WNV E-protein specific sandwich ELISAs were performed on serial dilutions of serum samples from mice that was naive/mock-infected with vehicle as negative controls or infected in the footpads with 10^3 PFU WNV-TX. Each symbols shows relative titers of antigen-specific antibody from an individual mouse represented as 1/dilution as described in Materials and Methods. Data shows samples of mice from three independent infections, where n $\geq$ 9 individual mice for IgM and total IgG and n = 5-9 for IgG subclasses. B) A standard PRNT assay

was performed on serial dilutions of serum samples, and shows relative titers of antibody with 50% virus neutralizing capacity expressed as values of $1/PRNT_{50}$. Data shows one out of three independent infections with at least four mice per group per timepoint. Statistics was performed using a Student's t-test where *$p<0.05$ and n.s. = not significant.

(**Fig. 3.3A**), and furthermore, had similar neutralizing antibody titers at day 7 p.i. (**Fig. 3.3B**). Thus, humoral immunity is not defective in WNV-infected *Cd22*$^{-/-}$ mice.

Cd22*$^{-/-}$ *mice have decreased CD8*$^{+}$ *T cell responses to WNV

During WNV infection, CD4^{+} or CD8^{+} T cells are essential in controlling viral titers in the CNS at late times after infection [146,147]. Thus, we examined WNV-specific T cell responses in the absence of CD22. Using a MHC class I tetramer specific for the immunodominant peptide for NS4B [132], we found that on day 5 p.i., WNV-specific CD8^{+} T cells had expanded to similar levels in the spleens of infected WT and *Cd22*$^{-/-}$ mice (**Fig. 3.4A**). However by day 7 p.i., there were 2.5-fold fewer WNV-specific CD8^{+} T cells in infected *Cd22*$^{-/-}$ mice. Furthermore, upon restimulation with the NS4B peptide, infected *Cd22*$^{-/-}$ mice had ~3-fold fewer IFNγ-secreting CD8^{+} T cells at day 7 p.i. (**Fig. 3.4B**).

We next examined whether the decreased WNV-specific CD8^{+} T cells in infected *Cd22*$^{-/-}$ mice was due to either increased cell death or dysregulated cell proliferation. Using Annexin V staining to detect dying cells, we found no differences in frequency of early apoptotic WNV-specific CD8^{+} T cells in the spleens of infected WT and *Cd22*$^{-/-}$ on either day 5 or 7 p.i. (**Fig. 3.5A, 3.5B**). In contrast, using BrdU incorporation as a measure of T cell proliferation *in vivo*, we found that at the earliest timepoint when WNV-specific CD8^{+} T cells could be clearly detected by MHC I tetramer staining (day 5 p.i.), the frequency of dividing tetramer^{+} CD8^{+} T cells at the peak of cell division (day 5 p.i.) was reduced in infected *Cd22*$^{-/-}$ mice compared to WT mice (**Fig. 3.4C**). In contrast,

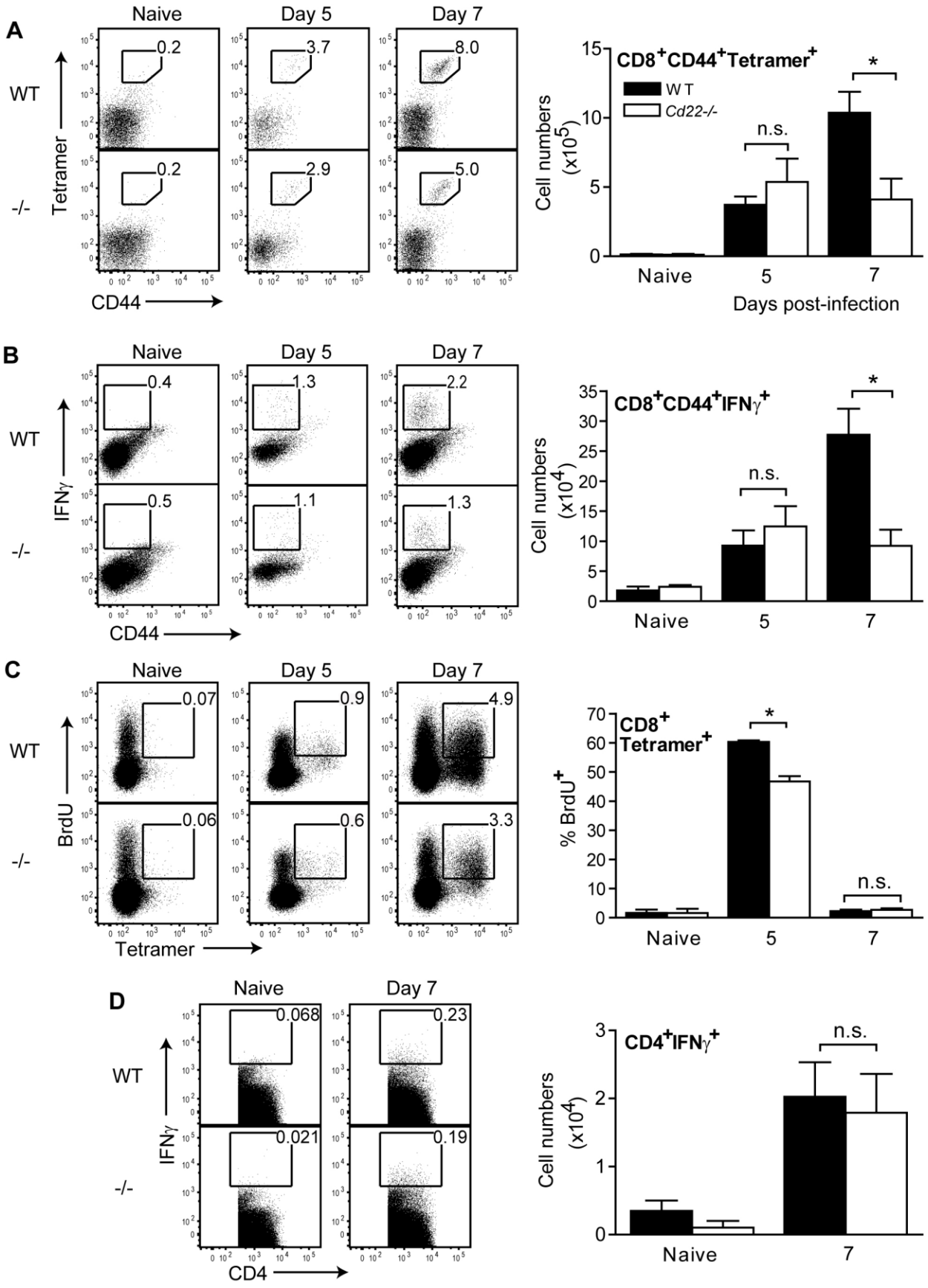
A
Naive
Day 5
Day 7
WT
-/-
Tetramer
CD44
0.2
3.7
8.0
0.2
2.9
5.0
CD8+CD44+Tetramer+
WT
Cd22-/-
Cell numbers (x10^5)
n.s.
*
Naive
5
7
Days post-infection
B
IFNγ
0.4
1.3
2.2
0.5
1.1
1.3
CD8+CD44+IFNγ+
Cell numbers (x10^4)
C
BrdU
0.07
0.9
4.9
0.06
0.6
3.3
CD8+ Tetramer+
% BrdU+
D
0.068
0.23
0.021
0.19
CD4
CD4+IFNγ+

Figure 3.4. Impaired WNV-specific CD8$^+$ T cell responses in the spleens of infected *Cd22*$^{-/-}$ mice

Mice were inoculated as described. A, B) spleens harvested at indicated days p.i. and total splenocytes were stained with the activation marker CD44 and A) MHC I tetramer or B) restimulated *ex vivo* WNV NS4B 9-mer peptide prior to ICS. C) WT and *Cd22*$^{-/-}$ mice were inoculated s.c. with 10^3 PFU WNV-TX and i.p. with BrdU as described. Splenocytes were stained for CD8$^+$ T cell markers and tetramer prior to ICS to detect BrdU incorporation, and data expressed as the frequency of CD8$^+$Tetramer$^+$ cells that are BrdU$^+$. D) Total splenocytes were restimulated *ex vivo* with WNV NS3 15-mer peptide prior to ICS. Representative flow plots were gated on A-C) CD8$^+$ T cells (B220$^-$NK1.1$^-$CD3$^+$CD4$^-$CD8$^+$) and D) CD4$^+$ T cells (B220$^-$NK1.1$^-$CD3$^+$CD4$^+$CD8$^-$) and numbers indicate gated populations as a proportion of total CD8$^+$ or CD4$^+$ populations. Data shows one representative of three independent experiments with at least three mice per group per timepoint. Statistics were performed using a Student's t-test where *$p<0.05$ and n.s. = not significant.

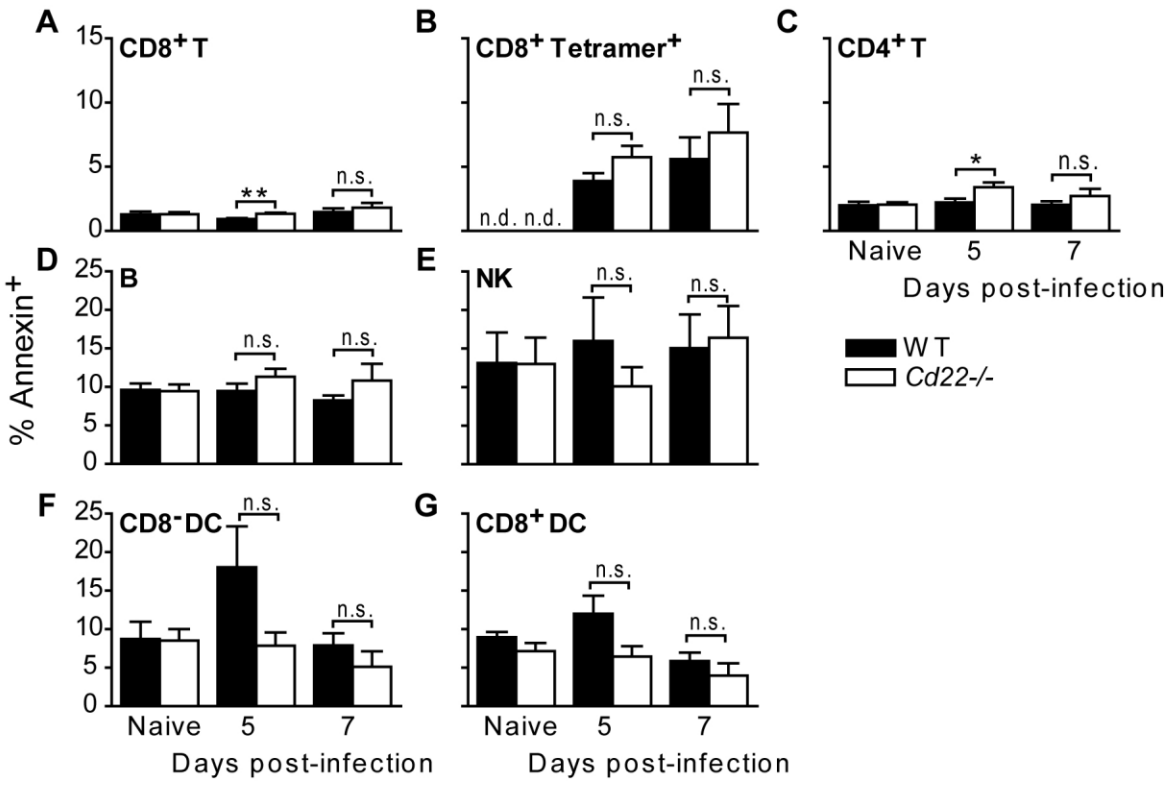

Figure 3.5. Annexin V staining of splenocyte populations

Splenocytes were isolated at various timepoints from WT and *Cd22*$^{-/-}$ mice, and stained with surface markers, Annexin V and Live/Dead stain as described in Materials and Methods. Cells were gated on A) total CD8$^+$ T cells; B) CD8$^+$Tetramer$^+$; C) total CD4$^+$ T cells; D) B cells; E) NK cells; F) total CD8$^-$ DCs; G) CD8$^+$ DCs. Bar graphs show the frequency of Annexin$^+$Live/Dead$^-$ cells. Data are from three independent experiments with 3-4 mice per timepoint per group. Statistics were performed using a Student's t-test where *$p<0.05$, **$p<0.01$ and n.s.= not significant; n.d. = not detected.

there were no significant differences between WT and *Cd22*$^{-/-}$ mice in the numbers of splenic WNV-specific IFNγ-secreting CD4^{+} T cells (**Fig. 3.4D**) or in the frequency of splenic BrdU^{+} B cells, CD4^{+} cells or total CD8^{+} T cells (**Fig. 3.6A-3.6C**). These results demonstrate that the lower number of WNV-specific CD8^{+} T cells in the spleens of infected *Cd22*$^{-/-}$ mice is due in part to reduced CD8^{+} T cell proliferation rather than to an increased frequency of cell death and that CD22 regulates CD8^{+} T cell proliferation during WNV infection.

WNV-infected Cd22*$^{-/-}$ *mice have decreased expansion of CD8*$^{+}$ *T cells, DCs and NK cells

CD22 interacts with ligands on antigen-presenting cell populations such as DCs [74] that in turn are responsible for priming and regulating antiviral T cell responses. Thus, we enumerated both DC and lymphocyte numbers in the footpad dLNs and spleens of infected WT and *Cd22*$^{-/-}$ mice to determine how CD22 affects cell expansion and recruitment after WNV infection. One day p.i., total cells numbers in the dLNs were expanded to similar levels in infected WT and *Cd22*$^{-/-}$ mice (**Fig. 3.7A**); there were no significant differences in either DC or lymphocyte populations (**Fig. 3.7B, 3.7C**). However, there were nearly two-fold fewer NK cells in the dLNs of infected *Cd22*$^{-/-}$ mice compared to WT mice (**Fig. 3.7B**).

Splenic non-plasmacytoid DCs can be divided broadly into CD8α^{+} and CD8α^{-} populations [162], and CD8α^{-} DCs can be further subdivided into two subsets based on

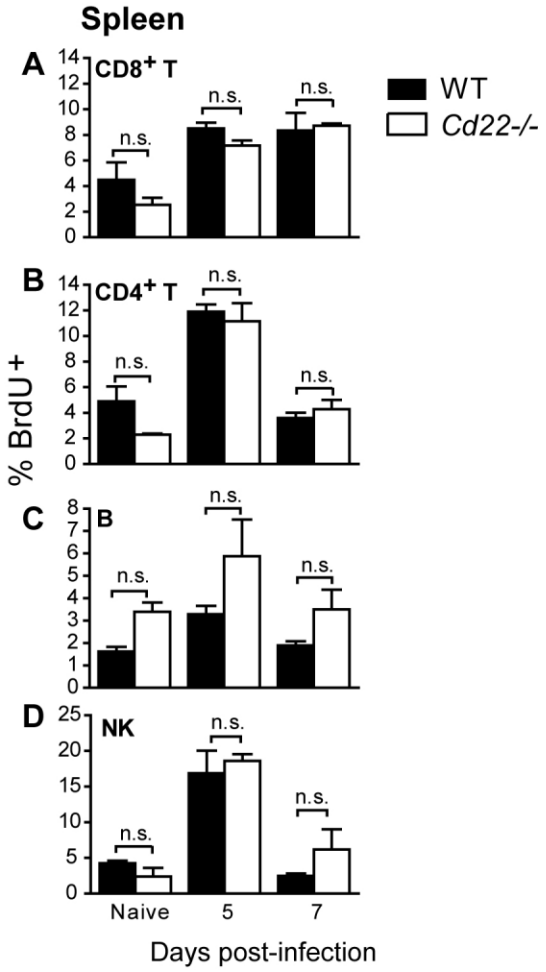

Figure 3.6. BrdU incorporation in splenic lymphocyte populations

WT and *Cd22*$^{-/-}$ mice were inoculated s.c. with 10^3 PFU as described. 24 hours prior to tissue harvest at indicated timepoints, mice were given one dose of 1mg BrdU by i.p. injection. Spleens were harvested as described, and surface stained for A) $CD8^+$ T cells, B) $CD4^+$T cells, C) B cells and D) NK cells prior to ICS to detect BrdU incorporation. Data shows one representative of three independent experiments with at least three mice per group. Statistics were performed using a Student's t-test where n.s. = not significant.

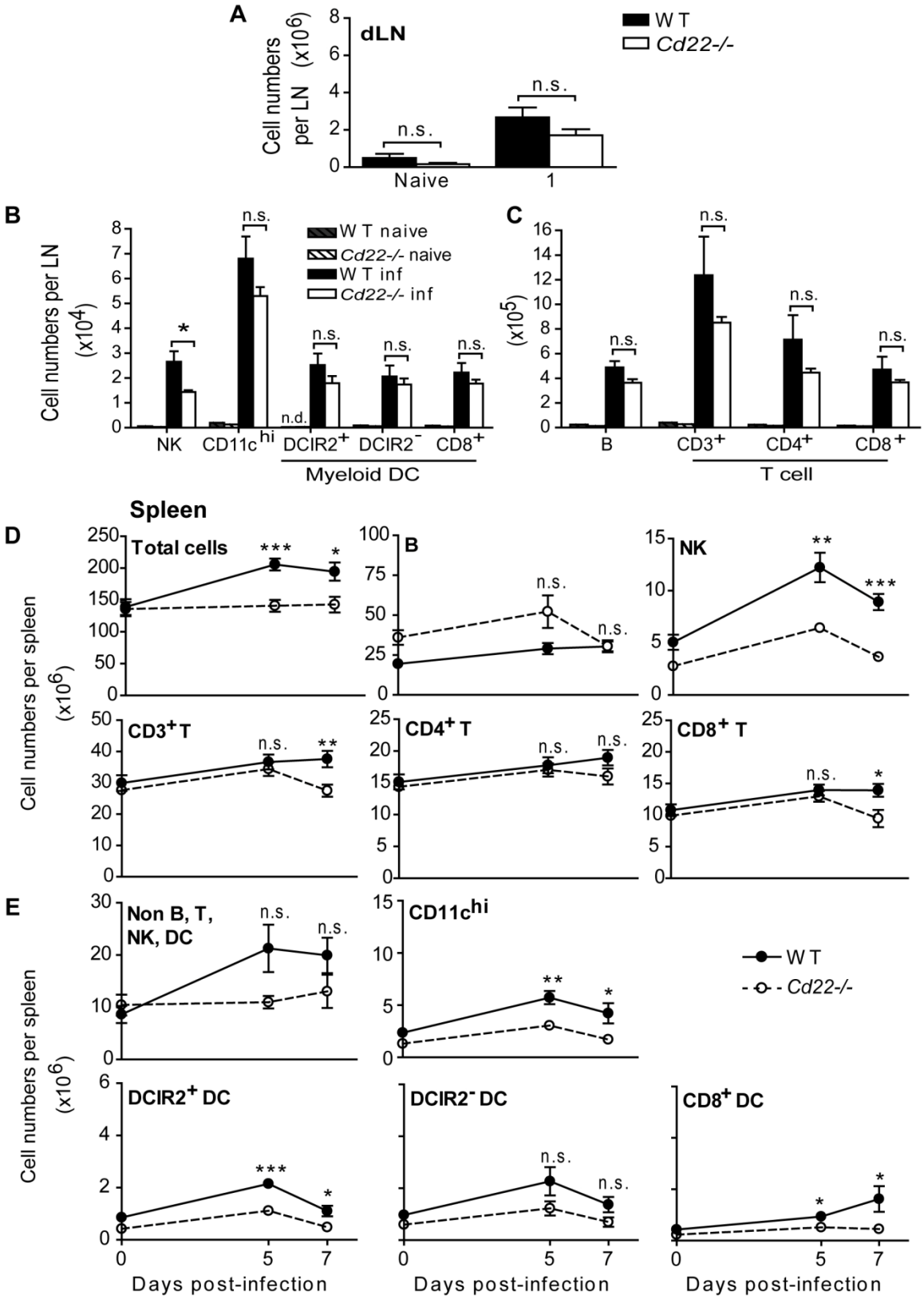
A
dLN
Cell numbers per LN (x10^6)
WT
Cd22-/-
n.s.
Naive
1
B
Cell numbers per LN (x10^4)
WT naive
Cd22-/- naive
WT inf
Cd22-/- inf
NK
CD11c^hi
DCIR2^+
DCIR2^-
CD8^+
n.d.
Myeloid DC
C
(x10^5)
B
CD3^+
CD4^+
CD8^+
T cell
Spleen
D
Total cells
B
NK
CD3^+ T
CD4^+ T
CD8^+ T
Cell numbers per spleen (x10^6)
E
Non B, T, NK, DC
CD11c^hi
DCIR2^+ DC
DCIR2^- DC
CD8^+ DC
Days post-infection

Figure 3.7. CD8$^+$ T cells, NK cells and DC populations are decreased in the dLNs and spleens of WNV-infected *Cd22*$^{-/-}$ mice

A, B, C) Pooled popliteal dLNs and D, E) spleens were harvested from naive or mice infected with 10^3 PFU WNV-TX at indicated days p.i. Total cells were stained for the following populations: NK (CD19- B220-CD3-NK1.1$^+$); CD11c^{hi} (CD19-B220-NK1.1-CD3-CD11c^{hi}); DCIR2$^+$ DCs (CD19-B220-NK1.1-CD3-CD11c^{hi}CD8-DCIR2$^+$); DCIR2- DCs (CD19-B220-NK1.1-CD3-CD11c^{hi}CD8-DCIR2-); CD8$^+$ DCs (CD19-B220-NK1.1-CD3-CD11c^{hi}CD8$^+$DCIR2-); B (CD19$^+$B220$^+$CD3-NK1.1-); CD3$^+$ T (CD19-B220-NK1.1-CD3$^+$); CD4$^+$ T (CD19-B220-NK1.1-CD3$^+$CD4$^+$CD8-); CD8$^+$ T (CD19-B220-NK1.1-CD3$^+$CD4-CD8$^+$); Non B, T, NK, DC (B220-CD3-NK1.1-CD11c$^{lo/-}$). Cell numbers are shown A, B, C) per dLN 1 day post-infection or D, E) per spleen at indicated timepoints. Statistics was performed using a Student's t-test where *$p<0.05$, **$p<0.01$, ***$p<0.001$ and n.s. = not significant; n.d. = not detected. Data shows one representative of 3 independent experiments with three mice per group per timepoint (dLNs) or mice from three independent experiments where $n \geq 9$ per group per timepoint (spleen).

their expression of either DCIR2 (Dendritic Cell ImmunoReceptor 2/33D1) or DCAL2 (Dendritic Cell Associated C-type lectin 2, Myeloid inhibitory C-type lectin, Clec12a)-expressing subsets [43]. The DCIR2$^+$ and DCAL2$^+$ (DCIR2$^-$) DC subsets differ in how they regulate T cell immune responses [43]. Interestingly, little or no DCIR2$^+$ DCs were detectable in the dLNs of uninfected WT or *Cd22*$^{-/-}$ mice, but their numbers increased significantly in dLNs in both genotypes as early as 1 day post WNV infection (**Fig. 3.7B**).

The numbers of total splenocytes in infected WT mice expanded 1.3-fold compared to uninfected mice by 5 and 7 days p.i, yet total cell numbers remained relatively unchanged in the spleens of infected *Cd22*$^{-/-}$ mice (**Fig. 3.7D**). Compared to WT mice, WNV-infected *Cd22*$^{-/-}$ mice had no significant differences in the numbers of splenic B cells, but did have fewer total CD3$^+$ T cells at day 7 p.i. (**Fig. 3.7D**). This decrease in splenic T cell numbers could be attributed mainly to CD8$^+$ T cells, which were 1.5-fold lower in *Cd22*$^{-/-}$ mice compared to WT mice at day 7 p.i. While splenic NK cells and DC subsets all expanded after infection of WT mice, they remained relatively unchanged in *Cd22*$^{-/-}$ mice (**Fig. 3.7D, 3.7E**). Specifically, there were significant increases in DCIR2$^+$ and CD8$^+$ DCs in WT mice after infection but not in *Cd22*$^{-/-}$ mice (**Fig. 3.7E**). Non-lymphoid, non-DC populations, which include cells such as monocytes and macrophages also did not expand in *Cd22*$^{-/-}$ mice (**Fig. 3.7E**). Taken together, these data show that CD22 regulates changes in NK, CD8$^+$ T and DC cell numbers in the spleen in WNV-infected mice, resulting in an inability of these populations to expand, be recruited or be retained in the spleens of *Cd22*$^{-/-}$ mice after infection.

Based on these findings we examined BrdU uptake by NK and DC populations to assess whether there was a defect in splenocyte expansion after infection in *Cd22*$^{-/-}$ mice. Surprisingly, the frequency of BrdU^{+} NK cells and DC subsets in the spleen were similar between infected WT and *Cd22*$^{-/-}$ mice (**Fig. 3.6D** and data not shown). Annexin V staining revealed no significant differences in early apoptotic death in NK or DC populations in the spleen (**Fig. 3.5E-3.5G**). Thus, lower numbers of splenic NK cells and DC subsets in WNV-infected *Cd22*$^{-/-}$ mice were not simply due to reduced proliferation or increased cell death, raising the possibility that the reduced numbers were due to a defect in cell migration.

The splenic defect in WNV-specific CD8^{+} T cell responses in *Cd22*$^{-/-}$ mice also correlated with decreased cellular infiltrates into the brains of infected *Cd22*$^{-/-}$ mice 7 days p.i. (**Fig. 3.8**). A decrease was evident in CD4^{+} T cells, CD8^{+} T cells and WNV-specific CD8^{+} T cells (**Fig 3.8B-3.8D**), but not in NK cells (**Fig. 3.8E**). The numbers of infiltrating non-lymphoid populations, which likely include infiltrating macrophages and resident microglial cells, were also not significantly different between infected WT and *Cd22*$^{-/-}$ mice (**Fig. 3.8F**). Thus, the CD22-dependent defect in migration of cells into the CNS predominantly affects T cells. It has been established that infiltrating T cells are important for controlling virus replication in the CNS, and ultimately survival of the host from succumbing to encephalitic disease [163,164]. Thus, the diminished number of WNV-specific CD8^{+} T cells in the spleens of *Cd22*$^{-/-}$ mice along with the decreased CD8^{+}

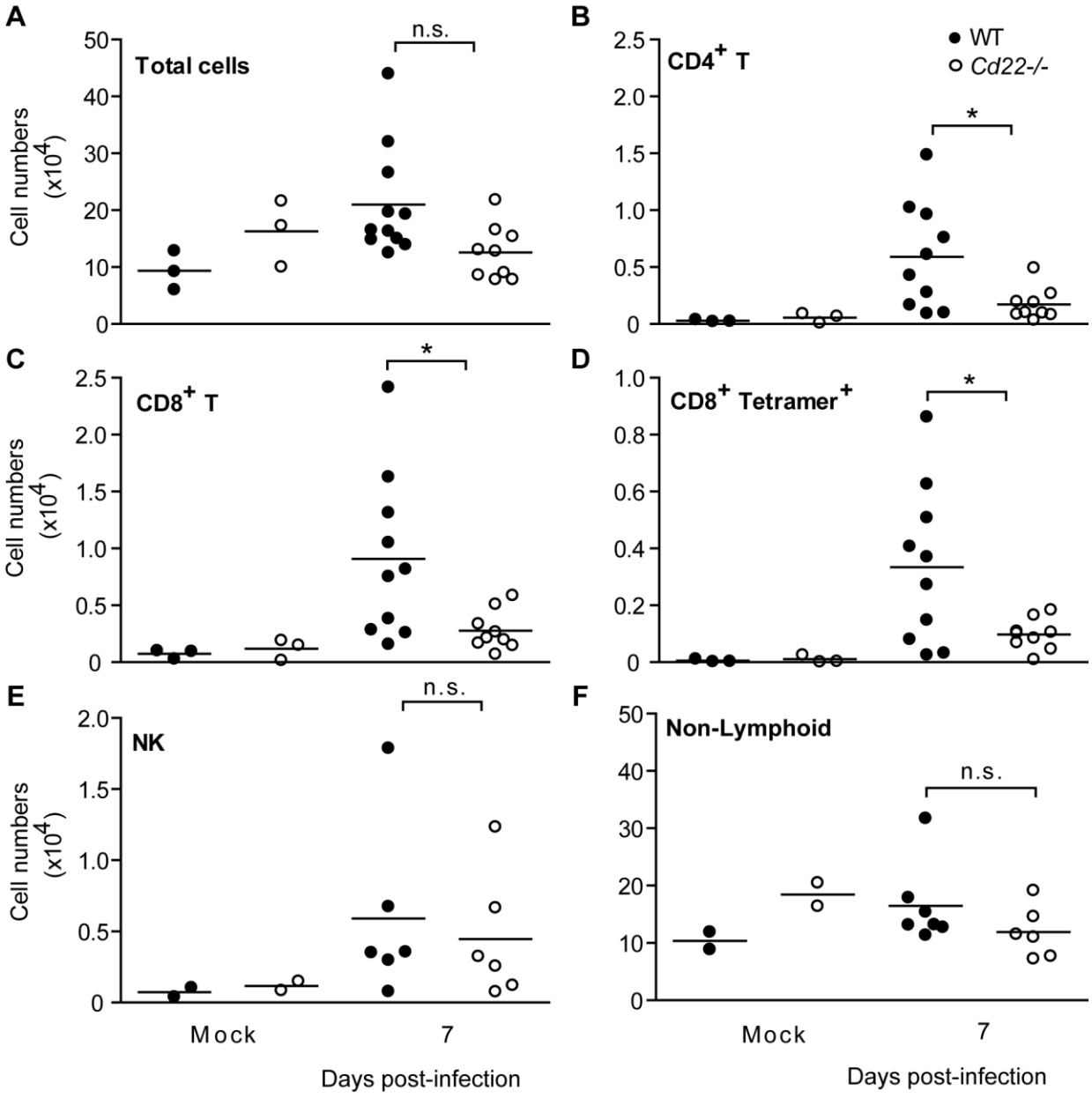

Figure 3.8. Decreased T cell infiltrates into the brain of WNV-infected *Cd22*$^{-/-}$ mice

Mice were inoculated s.c. with WNV and perfused with PBS on day 7 p.i. Brains were harvested, and lymphocytes were isolated as described. Cell numbers were enumerated after flow cytometry analysis for: A) total leukocytes; B) total CD4$^+$ T cells; C) total CD8$^+$ T cells; D) CD8$^+$ Tetramer$^+$ T cells; E) total NK cells; and F) Non-lymphoid cells (CD19$^-$CD3$^-$NK1.1$^-$). Symbols

indicate individual mice from at least three independent experiments. Statistics were performed using a Student's t-test where *$p<0.05$ and n.s. = not significant.

T cell infiltrates and inability to control viral replication in the brain likely accounts for *Cd22*$^{-/-}$ mice succumbing to disease after WNV infection.

Cd22*$^{-/-}$ *mice have a defect in cell recruitment

The overall normal rates of cell proliferation and cell death in infected *Cd22*$^{-/-}$ mice suggested that decreased CD8^{+} T cells and certain subsets of DCs in infected tissues of *Cd22*$^{-/-}$ mice may be due to defective cell migration. Subcutaneous infection of the footpad with WNV predictably induces entry of leukocytes from circulation into dLNs [165], which thus has the potential to provide a reliable assay to examine leukocyte migration into a site of infection. To directly test this possibility, we adoptively transferred congenically marked WT Ly5.1^{+} splenocytes into Ly5.2^{+} WT and *Cd22*$^{-/-}$ recipients by intravenous (i.v.) injection and subsequently infected them with WNV. We then harvested individual dLNs of hind footpads that had been inoculated with WNV, with vehicle alone or left injected, and as an indicator of cell migration [166,167] quantified the numbers of Ly5.1^{+} subsets 24 hours p.i. (**Fig. 3.9**). Both lymphocytes and DCs migrated into the dLNs of WNV-infected WT and *Cd22*$^{-/-}$ mice. The infected dLNs from *Cd22*$^{-/-}$ mice had significantly fewer Ly5.1^{+} NK cells, CD3^{+} T cells, CD4^{+} T cells, and CD8^{+} T cells than WT mice (**Fig. 3.9A-3.9D**). There was no significant difference in the number of migrating Ly5.1^{+} CD11c^{+} DCs in the dLNs of *Cd22*$^{-/-}$ mice compared to WT mice (**Fig. 3.9E**) and no differences in the number of B cells that had entered into dLNs (**Fig. 3.9F**). Thus, CD22 regulates the migration of NK cells and T cells into dLNs and probably other sites after WNV infection.

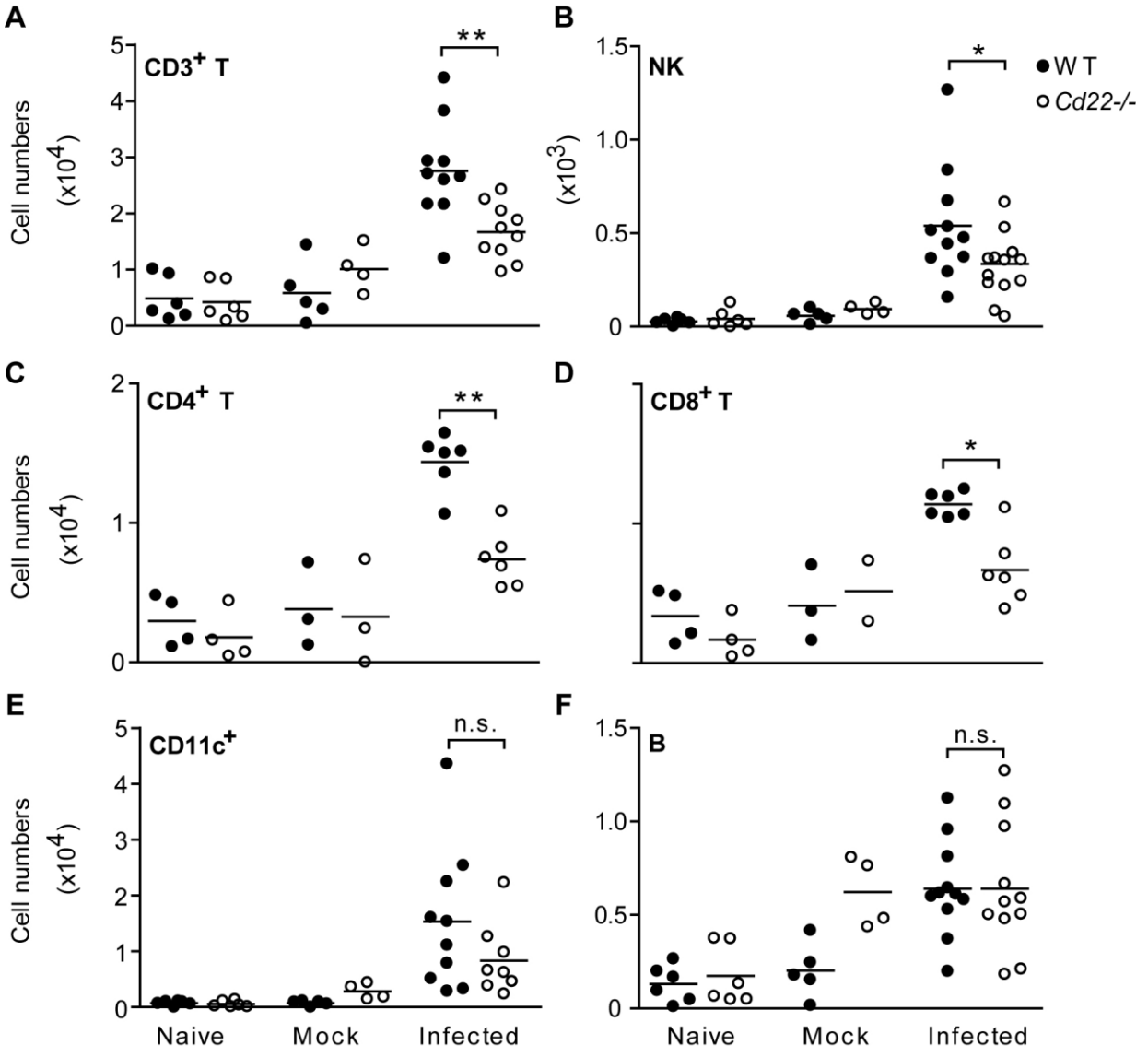

Figure 3.9. Impaired recruitment of T cells and NK cells into infected dLNs in *Cd22*$^{-/-}$ mice

Ly5.1^{+} total splenocytes from WT C57BL/6 mice were adoptively transferred by i.v. injection into Ly5.2^{+} WT or *Cd22*$^{-/-}$ mice. The next day, individual footpads of recipient mice were left uninjected (naive), injected with 10ul of 1% FCS-containing HBSS vehicle (mock) or injected with 10^{3} PFU WNV-TX (infected). 24 hours p.i., individual dLNs were harvested and processed separately with liberase digestion before staining for the following populations: A) CD3^{+} T cells; B) NK cells; C) total CD4^{+} T cells; D) total CD8^{+} T cells; E) CD11c^{+} DCs; and F) B cells. Symbols

represent individual dLNs from mice from three independent experiments. Statistics were performed using a Mann-Whitney U test of the median where *$p<0.05$, **$p<0.01$ and n.s. = not significant.

We hypothesized that dysregulation of chemokine production within the dLNs of infected *Cd22*$^{-/-}$ mice may lead to impaired migration of cells from the circulation. CCR5 and its ligands CCL3, CCL4 and CCL5 have been implicated in the pathogenesis of WNV infection and are important for recruitment of T cells into the CNS for protection from encephalitis [168]. Thus, we isolated dLNs early after infection to determine whether expression of chemokine genes was altered in *Cd22*$^{-/-}$ mice (**Fig. 3.10**). Compared to expression in dLNs from WT mice, the dLNs from *Cd22*$^{-/-}$ mice had decreased mRNA expression of *Ccl3* and *Ccl5* 6 hrs after WNV infection (**Fig. 3.10A-3.10C**). However, this difference was no longer present at 12 hrs p.i. Expression of *Ccl3* and *Ccl4* were induced 5 to 35-fold, respectively, in WT dLNs at 6 and 12 hours p.i. (**Fig. 3.10A, 3.10B**), while *Ccl5* levels did not increase significantly (**Fig. 3.10C**). This defect of chemokine gene expression in the *Cd22*$^{-/-}$ dLNs was restricted to *Ccl3* and *Ccl5*; there was no difference between WT and *Cd22*$^{-/-}$ mice in induction of *Ccl4* expression or in expression of other cytokine genes such as *Ifna, Ifnß, Ifnγ, Tnfa, Cxcl10, Cxcl11 and Ccl2* (**Fig. 3.10D** and data not shown). Serum levels of type I IFN also were not different between infected WT and *Cd22*$^{-/-}$ mice (**Fig. 3.10E**). These data show that the expression of CCR5 ligands was selectively altered in the dLNs of WNV-infected *Cd22*$^{-/-}$ mice even though the numbers of T cells and DCs, populations that can produce CCR5 agonists [16], were similar between infected WT and *Cd22*$^{-/-}$ mice (**Fig. 3.7B, 3.7C**).

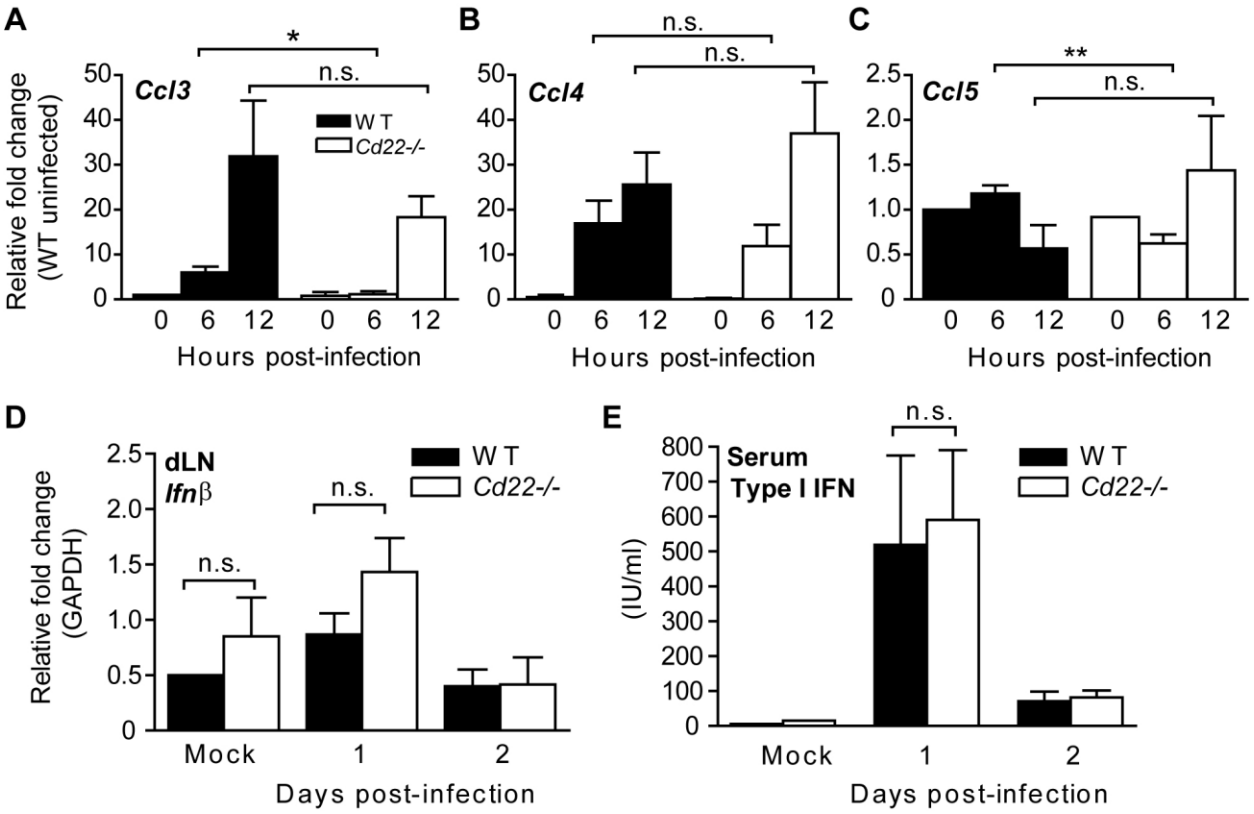

Figure 3.10. CD22 expression regulates production of specific chemokines early in the WNV-infected dLNs

A-D) Mice were inoculated and dLNs were harvested at indicated timepoints p.i. A, B, C) Expression for a gene of interest was made relative to *18s* expression and normalized to WT uninfected controls. D) Expression of *Ifnβ* was made relative to *Gapdh* expression. Data show one representative of three independent experiments with two mice per group per timepoint. E) Mice were inoculated and serum samples taken at indicated timepoints. Total sera was assessed for Type I IFN production using a standard Type I IFN bioassay and quantified as International Units (IU) per ml of serum. Data show one representative of two independent experiments with three mice per group per timepoint. Statistics were performed using a Student's t-test and *$p<0.05$, **$p<0.01$ and n.s. = not significant.

DCIR2$^+$ CD8α$^-$ DCs express CD22

Antiviral effector CD8$^+$ T cell responses are primed and maintained by accessory cells including DCs [169]. Given the profound CD8$^+$ T cell defect in infected *Cd22$^{-/-}$* mice, we next investigated the possibility that dysregulation of DCs in WNV-infected *Cd22$^{-/-}$* mice might contribute to the decreased WNV-specific CD8 T cell activation and expansion. Previously, Edwards *et al.* reported that CD22 is expressed at low levels on CD8α$^-$ DCs in the spleen but not on CD8α$^+$ DCs [96]. We re-examined the expression of CD22 on splenic DC subsets and found that CD22 was expressed as expected on B cells (**Fig. 3.11A**), but was also present on the subset of CD8α$^-$ DCs expressing DCIR2 (**Fig. 3.11B**). CD22 was not detected on CD8α$^-$DCAL2$^+$ DCs, CD8α$^+$ (DEC205$^+$) DCs or plasmacytoid DCs (**Fig. 3.11A, 3.11B**). As in the spleen, the DCIR2$^+$ DCs are the only DC subset that expresses CD22 in the infected dLNs (**Fig. 3.11C**).

Given that both DCIR2$^+$ DCs and CD8$^+$ T cells were reduced in the spleens of WNV-infected *Cd22$^{-/-}$* mice, we directly evaluated the role of CD22$^+$ DCIR2$^+$ DCs on splenic CD8$^+$ T cell levels in WNV-infected mice. We adoptively transferred purified DCIR2$^+$ DCs from WT or *Cd22$^{-/-}$* mice into naive *Cd22$^{-/-}$* recipients, and then examined total splenocyte and CD8$^+$ T cell numbers 7 days post WNV infection. Infected *Cd22$^{-/-}$* mice had fewer total splenocytes (**Fig. 3.11D**) and CD8$^+$ T cells (**Fig. 3.11E**) than WT mice. Infected *Cd22$^{-/-}$* mice that received WT DCIR2$^+$ DCs had splenocyte levels restored to normal and that were significantly higher than *Cd22$^{-/-}$* mice that received no DCs (**Fig. 3.11D**). CD8$^+$ T cell numbers were also increased in *Cd22$^{-/-}$* mice after transfer of WT

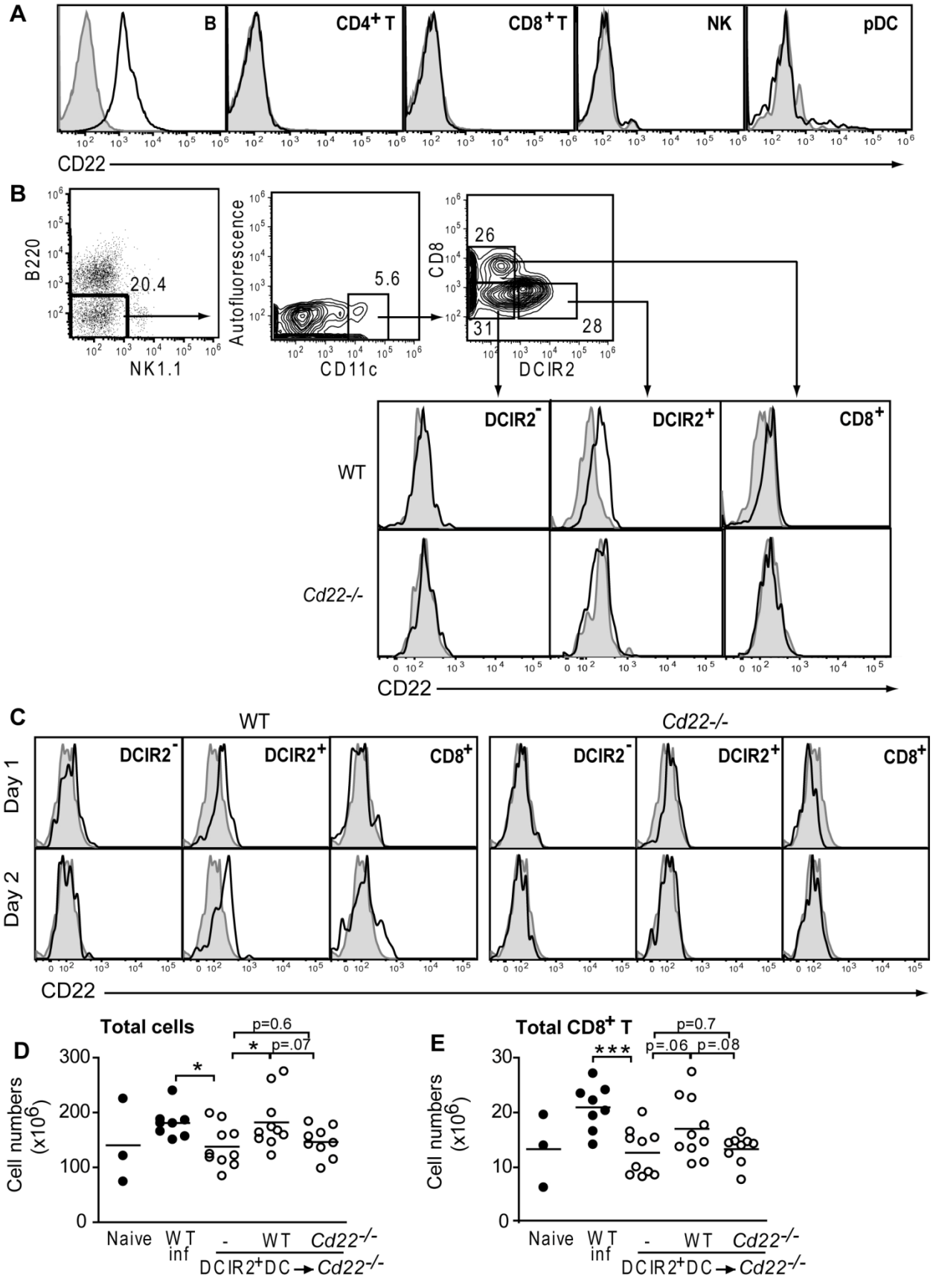
A
B
CD4+ T
CD8+ T
NK
pDC
CD22
B
B220
20.4
NK1.1
Autofluorescence
5.6
CD11c
CD8
26
31
28
DCIR2
DCIR2-
DCIR2+
CD8+
WT
Cd22-/-
CD22
C
WT
Cd22-/-
Day 1
Day 2
D
Total cells
p=0.6
* p=.07
Cell numbers (x10^6)
Naive
WT inf
WT
Cd22-/-
DCIR2+DC → Cd22-/-
E
Total CD8+ T
p=0.7
p=.06 p=.08
***

Figure 3.11. DCIR2$^+$ DCs express CD22

Flow cytometry analysis of CD22 expression on splenic populations in WT C57BL/6 and *Cd22*$^{-/-}$ mice. A) Spleen cells were isolated from naive WT C57BL/6 mice, and the following cell subsets were assessed for CD22 expression by staining with anti-CD22 mAb along with mAbs to the surface markers indicated: A) B cells, CD4$^+$ T cells, CD8$^+$ T cells, NK cells and plasmacytoid DCs (B220$^+$CD3$^-$NK1.1$^-$CD11c^{int}mPDCA1$^+$). B,C) CD22 is expressed on a subset of splenic DCs. Dot and contour flow plots show after gating on live populations through forward and side scatter the gating scheme of the DC subsets. B220$^-$NK1.1$^-$CD11c^{hi} populations were subdivided into DCIR2$^+$, DCIR2$^-$ (DCAL2$^+$) and CD8α$^+$ DCs and analyzed for expression of CD22. Histogram plots show staining of DC subsets in the B) spleens of naive WT and *Cd22*$^{-/-}$ mice and C) dLNs of infected WT and *Cd22*$^{-/-}$ mice using anti-CD22 antibody (bold) and isotype control antibody (shaded). Data show one representative of four independent experiments with three to four mice per group per timepoint. D, E) Sorted DCIR2$^+$ DCs from WT and *Cd22*$^{-/-}$ mice were adoptively transferred into naive *Cd22*$^{-/-}$ recipient groups i.v. *Cd22*$^{-/-}$ mice that received no DCs (-), WT DCs or *Cd22*$^{-/-}$ DCs were inoculated with 10^3 PFU WNV-TX and spleens harvested 7 days p.i. D) Total cell numbers or E) total CD8$^+$ T cell numbers were enumerated after flow cytometry analysis. Symbols show individual mice pooled from three independent experiments. Statistics were performed using a Student's t-test with some p-values reported and *$p<0.05$, ***$p<0.001$ and n.s. = not significant.

DCIR2$^+$ DCs but this increase was not significant (**Fig. 3.11E**). In contrast, adoptive transfer of CD22$^-$ DCIR2$^+$ DCs into WNV-infected *Cd22*$^{-/-}$ mice had little or no effect on splenocyte or CD8$^+$ T cell expansion. Thus, DCIR2$^+$ DCs may contribute to splenocyte and CD8$^+$ T cell expansion after WNV infection through a CD22-dependent process.

These data suggested that CD22$^-$ DCIR2$^+$ DCs were lacking a function that CD22$^+$ DCIR2$^+$ DCs retain. To evaluate how CD22 might regulate DCIR2$^+$ DCs, we compared cytokine and chemokine production by WT and *Cd22*$^{-/-}$ DCIR2$^+$ DC subsets. We isolated splenic DCIR2$^+$, CD8α$^+$ and DCAL2$^+$ DC subsets from WT and *Cd22*$^{-/-}$ mice based on their expression of CD11c, CD8α and DCAL2 [43], and then assessed cytokine and chemokine production 24 hours after *in vitro* infection with WNV by Milliplex assay. Of the 13 DC-associated cytokines and chemokines assessed (IFNγ, IL-1α, IL-1β, IL-6, IL-12p40, IL-12p70, IL-15, CCL2/MCP-1, CXCL10/IP-10, CCL3/MIP-1α, CCL4/MIP-1β, CCL5/RANTES, and TNFα), DCIR2$^+$ DCs predominantly produced the chemokine ligands that bind to CCR5 (C-C Chemokine Receptor type 5) [170]: CCL3 (MIP-1α), CCL4 (MIP-1β) and CCL5 (RANTES) (**Fig. 3.12**). DCIR2$^+$ DCs produced all three chemokines independent of viral stimulation (**Fig. 3.12A-3.12C**). In contrast, while the DCAL2$^+$ and CD8α$^+$ DC subsets made CCL5 they did not produce CCL3 or CCL4. There were no significant differences between WT and *Cd22*$^{-/-}$ DCs in their production of CCL3, CCL4 or CCL5 *in vitro*.

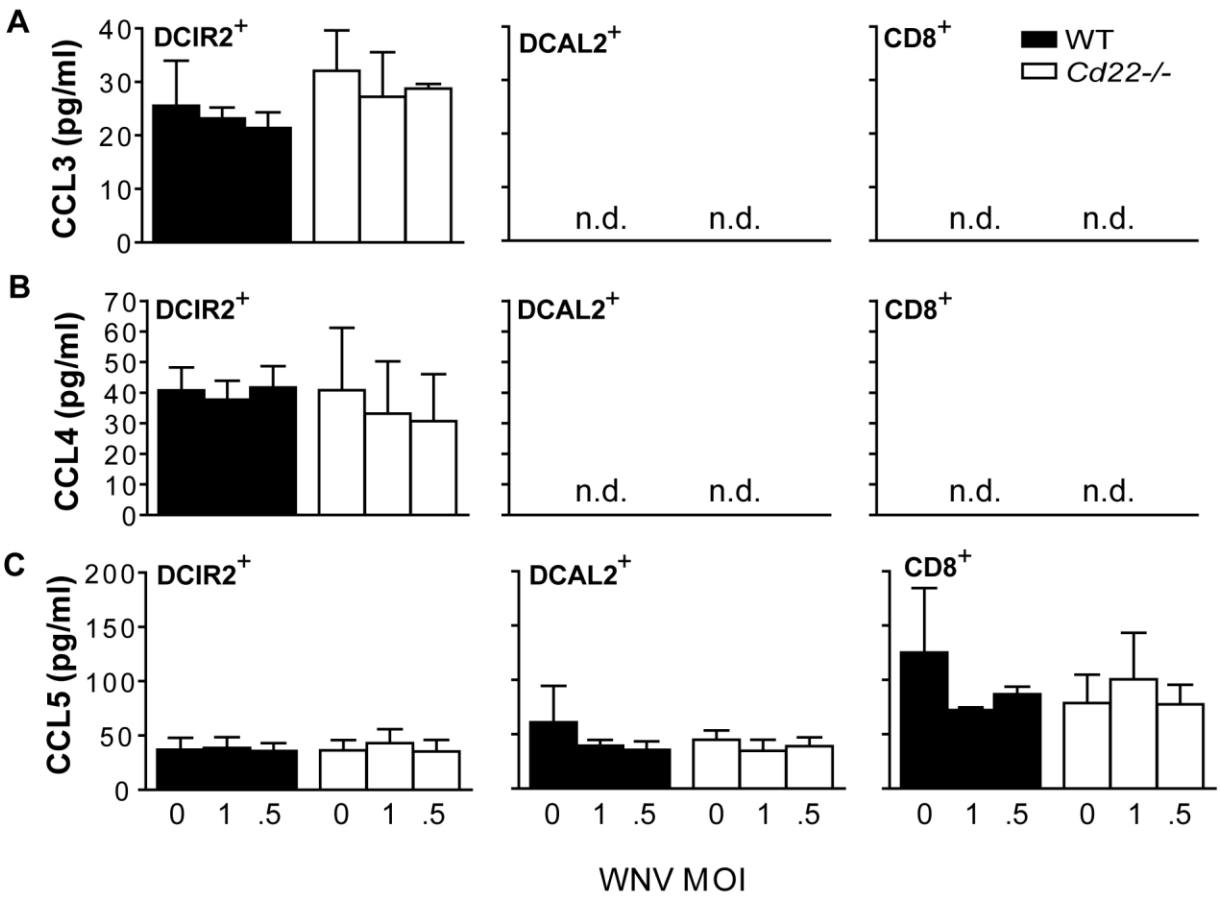

Figure 3.12. DCIR2⁺ DCs produce chemokines that bind to CCR5

DCIR2⁺, DCAL2⁺ and CD8α⁺ DCs from the spleens of WT and *Cd22*$^{-/-}$ mice were sorted as previously described. Cells were cultured in duplicate wells at 1.0 and 0.5 MOI WNV-TX *in vitro*, and supernatants collected after 24 hours and analyzed by Milliplex multiplex assay. Quantities of A) CCL3 (MIP-1α), B) CCL4 (MIP-1β) and C) CCL5 (RANTES) production by three DC subsets are graphed. Data shows quantification of chemokine production from cells obtained from three independent sorts, and n.d. = not detected.

NK cells express a ligand for CD22

We observed a decrease in the numbers of NK cells in the dLNs as early as 24 hours p.i. (**Fig. 3.7B**) that correlated with a reduced number of NK cells migrating into the dLN (**Fig. 3.9B**), but not in the brain (**Fig. 3.8E**). As NK cells also express CCR5, which is required for their trafficking to the brain during WNV infection [150], we hypothesized that the loss of CD22-CD22 ligand (CD22L) interactions may affect NK cell migration into or retention in infected tissues. To test whether NK cells can interact with CD22, we stained NK cells from the dLNs infected of WT and *Cd22*$^{-/-}$ mice with recombinant globulin (Rg) proteins that expressed either the full-length extracellular tail of mouse CD22 containing the sialic acid recognition domains (Rg 1-7) or a truncated tail lacking the sialylated CD22L binding domains (Rg 3-7) [86]. No binding was detected on B cells, T cells or NK cells when using Rg 3-7 (**Fig. 3.13A**), while binding was clearly evident using Rg 1-7 in WT mice (**Fig. 3.13B**), thus affirming the specificity of the fusion protein. In addition, the majority of activated and unactivated T and B cells all expressed CD22L from infected dLNs at similar levels, which was also the case in naive dLNs from WT mice (data not shown). In contrast, only about 18% of the total NK cell population expressed CD22L and with a lower MFI compared to T and B cells (**Fig 3.13B**). Therefore, NK cells express ligands for CD22, albeit at a lower level than T and B cells.

The loss of CD22 did not affect CD22L expression, as B, T and NK cells all bound to Rg 1-7 in *Cd22*$^{-/-}$ mice (**Fig. 3.13C**). Similar to WT mice, about 16% of total NK cells in

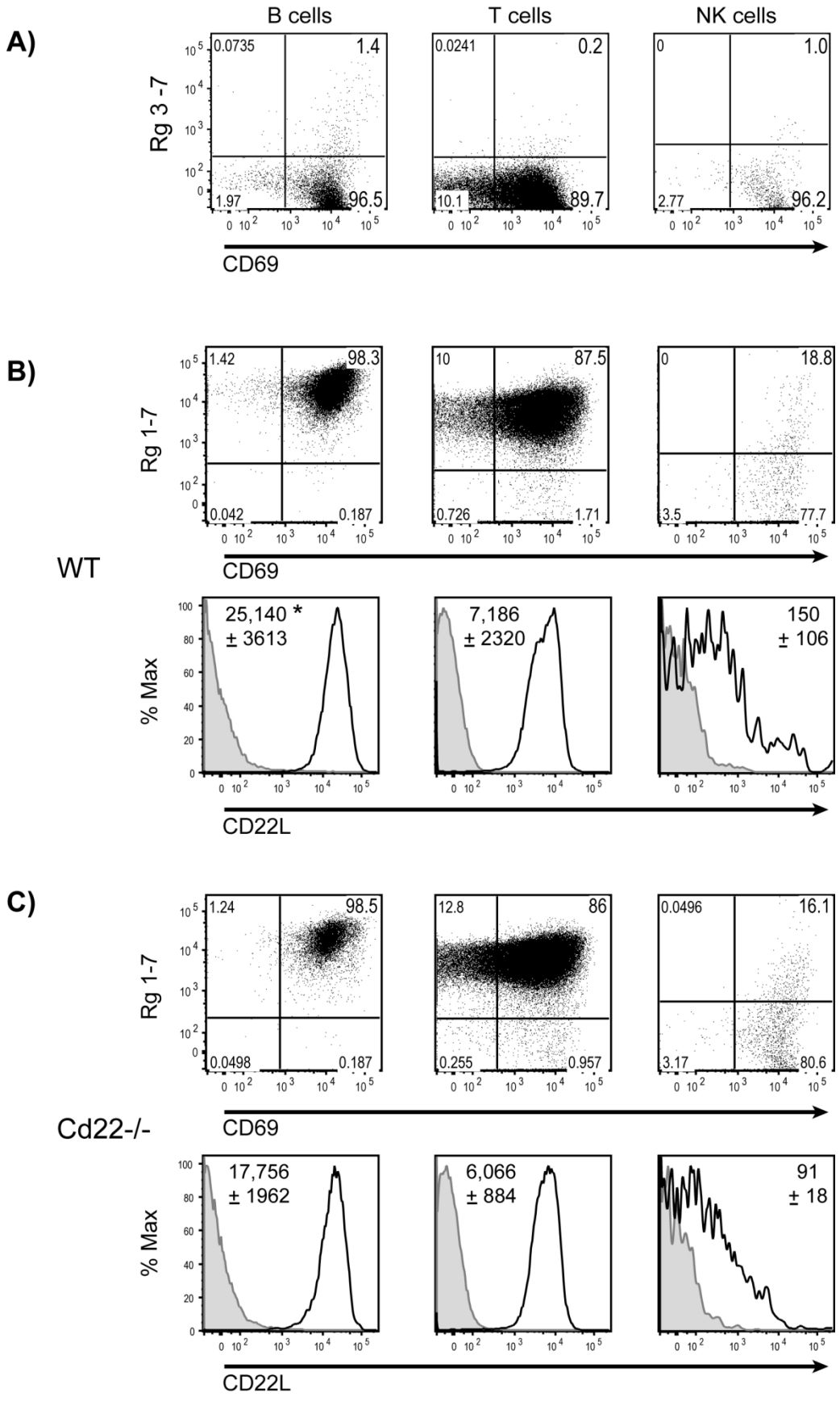
A)
B cells
T cells
NK cells
Rg 3 -7
0.0735
1.4
1.97
96.5
0.0241
0.2
10.1
89.7
0
1.0
2.77
96.2
CD69
B)
WT
Rg 1-7
1.42
98.3
0.042
0.187
10
87.5
0.726
1.71
0
18.8
3.5
77.7
CD69
% Max
25,140 *
± 3613
7,186
± 2320
150
± 106
CD22L
C)
Cd22-/-
Rg 1-7
1.24
98.5
0.0498
0.187
12.8
86
0.255
0.957
0.0496
16.1
3.17
80.6
CD69
% Max
17,756
± 1962
6,066
± 884
91
± 18
CD22L

Figure 3.13. NK cells express CD22L

WT and *Cd22*$^{-/-}$ mice were inoculated with WNV in the hind footpad as described, and infected dLNs were harvested. Cells were then stained for surface markers and gated for B cells, T cells and NK cells with murine CD22 fusion protein. Flow plots show expression of A) Rg 3-7 on WT mice or Rg 1-7 on B) WT and C) *Cd22*$^{-/-}$ mice versus CD69 expression. B, C) Histograms show staining of B, T or NK cells with Rg 3-7 (shaded) or Rg 1-7 (bold). The average geometric MFI of CD22L expression and standard deviation is shown. Numbers show the gate frequencies in the dot plots. All plots are representative of staining on 3-4 infected mice per group. Statistics are performed to compare average geometric MFI of WT versus *Cd22*$^{-/-}$ cells using Student's t-test where *$p<0.05$.

Cd22$^{-/-}$ mice expressed CD22L at a similar MFI to WT NK cells. The expression of CD22L in *Cd22*$^{-/-}$ lymphocytes was similar to that of WT lymphocytes, with the exception of B cells. There was a slight reduction in the binding to Rg 1-7 in infected *Cd22*$^{-/-}$ B cells compared to WT B cells. Nonetheless, the majority of B cells in *Cd22*$^{-/-}$ mice express CD22L similar to that of WT B cells. We conclude that NK cells are able to bind to CD22, but at a lower level compared to that of B and T cells.

Discussion

We have shown a direct role for CD22 in the generation of protective immune responses against WNV and have identified that CD22 is expressed on and may regulate a subset of splenic DCIR2^{+} CD8α^{-} DCs. CD22 contributes to adaptive immunity by more than simply regulating B cell-mediated antibody responses: it regulates the proliferation of WNV-specific CD8^{+} T cells, as well as cell migration into infected sites such as the brain and dLNs.

Although CD22 has been reported to be required for normal T cell-independent antibody responses [95,125], we detected no defects in WNV-specific antibody responses in infected *Cd22*$^{-/-}$ mice (**Fig. 3.3**). After WNV infection both μMT mice and mice unable to secrete IgM have significantly elevated viral loads in the spleen and kidneys [144,145]. This was not the case in WNV-infected *Cd22*$^{-/-}$ mice (**Fig. 3.2**). Furthermore, *Cd22*$^{-/-}$ mice had normal numbers of B cells in both the dLNs and spleen both before and after WNV infection (**Fig. 3.7**), and *Cd22*$^{-/-}$ B cells also migrated into dLNs at the same levels as WT

B cells (**Fig. 3.9F**). Thus, unlike the B cell-deficient and IgM-deficient mice, the increased susceptibility in *Cd22*$^{-/-}$ mice does not appear to be due to a defect in humoral immunity.

A significant and perhaps most surprising result was that infected *Cd22*$^{-/-}$ mice have fewer WNV-specific CD8^{+} T cells in both the spleen and the brain; in contrast, CD4^{+} T cells were lower in the brain but not in the spleen (**Fig. 3.4, 3.7, 3.8**). Previous studies have established that CD8^{+} T cells entering into the CNS play a vital role in protective immunity to WNV by lysing infected neurons to control viral replication [148,171] and prevent encephalitis [149,164,172]. CD4^{+} T cells support WNV-specific antibody responses and CD8^{+} T cell migration [131,146]. *Cd22*$^{-/-}$ mice have increased viral entry into the CNS (**Fig. 3.2D, 3.2E**) and increased severity of encephalitic symptoms (**Fig. 3.1B**) but have normal WNV-specific antibodies (**Fig. 3.3**); thus, the pathological characteristics of *Cd22*$^{-/-}$ mice most closely resemble those of CD8^{+} T cell-deficient mice [147]. Therefore, the increased susceptibility of *Cd22*$^{-/-}$ mice after WNV infection is most likely to be due to defective CD8^{+} T cell responses.

Infected *Cd22*$^{-/-}$ mice have significantly decreased T cell migration into the brain (**Fig. 3.8**) and decreased T cell-, NK cell-, but not B cell-trafficking into dLNs (**Fig. 3.9**), suggesting CD22 regulates migration of specific cell types during WNV infection. CD22 is known to control the migration of certain B cells [95], but unlike in this study, the effects of CD22 on migration were B cell intrinsic. For example, *Cd22*$^{-/-}$ and mice with mutated CD22 ligand binding domains have reduced numbers of long-lived B cells and recirculating B cells in the bone marrow *in vivo* [87,95]. However, T cells express surface

glycans that contain α2,6-sialic linkages that can bind to CD22 [105,173,174]. Furthermore, NK cells can bind CD22 (**Fig. 3.13**). Thus, T cells and NK cells could be regulated via direct binding to CD22 in trans. In addition, mice lacking the ST6Gal I glycosyltransferase, which adds CD22 ligand α2,6-sialic acid linkages to N-glycans, have a reduction in virus-specific $CD8^+$ but not $CD4^+$ T cells in the spleen after influenza infection [175]. Thus, it is possible that lack of binding to CD22 by T cells and NK cells in *Cd22*$^{-/-}$ mice leads to defective entry into or reduced retention of these cells within sites of WNV infection. The fact that both $CD8^+$ T cell proliferation (**Fig. 3.4C**), and migration (**Fig. 3.9D**) are reduced in infected *Cd22*$^{-/-}$ mice suggests that the decreased numbers of WNV-specific $CD8^+$ T cells in the spleens and brains of *Cd22*$^{-/-}$ mice is due to defects in both proliferation and in cell recruitment into infected tissues.

CD22 may also affect cell recruitment into infected tissues through regulation of chemokine production *in vivo*, as we observed an early reduction in expression of *Ccl3* and *Ccl5* but not *Ccl4* in the dLNs of infected *Cd22*$^{-/-}$ mice (**Fig. 3.10A-3.10C**). CCR5 and its ligands play an important role in the recruitment of T cells to sites of inflammation [176,177], and CCR5 is especially significant in the context of WNV infection [168]. Murine CCR5 is required for T and NK cell entry into the WNV-infected CNS [150], and loss of function mutations in human CCR5 expression has been correlated with increased presentation of neurological symptoms after WNV infection [178]. Thus, defective production of CCR5 agonists in the infected dLNs of *Cd22*$^{-/-}$ mice may account for fewer T and NK cell entering the dLNs and other sites of infection.

DCIR2$^+$ DCs may play essential roles in governing immune responses during WNV infection. This distinct subset of DCIR2$^+$ splenic DCs expresses CD22 (**Fig. 3.11**), and while not present in dLNs of uninfected mice, these DCs are detectable in the dLNs within 24 hours after infection (**Fig. 3.7B**) and thus are in a position to encounter and rapidly respond to WNV and help initiate adaptive immune responses. Adoptive transfer of CD22$^+$ DC1R2$^+$ DCs but not CD22$^-$ DCIR2$^+$ DCs restored splenocyte and CD8$^+$ T cell expansion to normal levels in infected *Cd22*$^{-/-}$ mice (**Fig. 3.11D, 3.11E**). Thus, DCIR2$^+$ DCs may regulate splenic cell expansion during WNV infection via a CD22-dependent mechanism.

Using mAbs to target DCIR2 and DEC205 on DCIR2$^+$ CD8α$^-$ and CD8α$^+$ DCs, respectively, our lab and others showed that DCIR2$^+$ DCs preferentially induce CD4$^+$ T cell proliferation and skewing towards Th2 responses and extrafollicular Ab responses, while CD8α$^+$ DCs induce CD8$^+$ T cell proliferation and Th1 responses [43,45,49,179]. These studies suggest that CD22$^+$DCIR2$^+$ DCs regulate a characteristic set of adaptive immune responses. However, *Cd22*$^{-/-}$ mice had normal WNV-specific CD4$^+$ T cell expansion in the spleen (**Fig. 3.4D**), implying that DCIR2$^+$ DC activation of CD4$^+$ T cells does not depend on CD22 during WNV infection. Also, the normal BrdU uptake by lymphocyte populations other than splenic WNV-specific CD8$^+$ T cells in infected WT and *Cd22*$^{-/-}$ mice (**Fig. 3.4C, 3.6**) suggests that rescue of spleen cell expansion by DCIR2$^+$ DCs was not simply due to effects on cell proliferation.

Although it remains unclear what cell types account for the dysregulated *Ccl3* and *Ccl5* expression in the dLNs of *Cd22*$^{-/-}$ mice, CD22^{+} DCIR2^{+} DCs are a likely candidate for affecting expression of these chemokines at infected sites and thereby affecting the recruitment or retention of CCR5^{+} T cells and NK cells since, unlike CD8α^{+} DCs and DCIR2^{-} CD8α^{-} DCs, they can produce all three of the major ligands for CCR5: CCL3, CCL4, and CCL5 (**Fig. 3.12**). In addition, DCs themselves also express CCR5 [16]; dysregulation of chemokine production by *Cd22*$^{-/-}$ DCIR2^{+} DCs thus could exert autocrine or paracrine effects on DCIR2^{-} or CD8α^{+} DCs. These effects may be responsible for decreased DC numbers in the spleen (**Fig. 3.7E**). Just how DCIR2^{+} DCs regulate cell numbers and immunity during WNV infection requires further study.

Our data support a working model that during acute WNV infection CD22 functions to promote CD8^{+} T cell expansion and leukocyte migration to sites of infection. This model is supported by the fact that absence of CD22 disrupts early chemokine production, which in turn affects the migration of specific CCR5^{+} cells to sites of viral replication. A reduced capacity to proliferate combined with dysregulated chemokine production may in turn impair CD8^{+} T cell entry into the CNS to control viral replication, accounting for the increased susceptibility of infected *Cd22*$^{-/-}$ mice.

In summary, we have shown that CD22 is important for protection against a viral pathogen, WNV, and that this protection does not operate through regulation of antigen-specific antibody responses. Rather, CD22 regulates antiviral T cell responses and cell migration. Furthermore, CD22 is expressed on DCIR2^{+} DCs that can affect cell

expansion *in vivo*. Further studies are needed to define how CD22 regulates DCIR2$^+$ DC functions and whether CD22$^+$DCIR2$^+$ DCs play a similar role in protective immune responses to other pathogens. Nevertheless, this study has provided new insights into how CD22 functions in the protection against WNV.

We have identified CD22 as a crucial factor in the initiation of CD8$^+$ T cell responses and in DCIR2$^+$ DC regulation of splenocyte expansion during WNV infection. Thus CD22 represents an important factor for the regulation of antigen-specific adaptive immune responses. We now turn our attention to another example, the pro-apoptotic molecule called Bim, and its role in regulation of B cell responses. In contrast to CD22, Bim is ubiquitously expressed on all cell types and directly controls the lifespan of a cell. Interestingly the lengthening or termination of a cell's lifespan is a highly effective way to initiate or conclude a cellular response, and is required to control numerous biological processes. Thus we will discuss how lifespan is utilized to regulate DC regulation of adaptive immune responses.

Chapter 4: The lifespan of DC affects DC-mediated regulation of B cell responses

Introduction

The generation of peripheral tolerance and appropriate dampening of the immune response after resolution of infection depends on the ability of the cell to undergo programmed apoptosis. Apoptosis in DCs and other APCs is important for protecting the host from continual effector cell activation and to limit pathogen-eradicating responses from causing extensive damage to uninfected tissues [180]. Three key studies used different strategies to manipulate the survival of DCs to study the effects of lifespan in DC-mediated regulation of T cell responses. Hou and van Parijs utilized Bcl-x_L and Bcl-2-deficient mice to obtain BMDCs with decreased survival and Bcl-2 overexpression transgenic mice with prolonged survival to show that increasing the survival of DCs enhances T cell proliferation using OVA antigen [53]. Chen and colleagues utilized DCs with prolonged survival by targeting the baculoviral caspase inhibitor, p35 to DCs to generate DC-p35 transgenic mice [181] as well as generating BMDCs from Bim-deficient mice [182]. DCs from DC-p35 transgenic mice induced increased T cell proliferation, and this study showed that prolonging survival in DCs alone induced spontaneous autoantibody production [181]. Later, the same group showed that Bim-deficient BMDCs produced higher amounts of Il-12p70 in response to TLR

stimulation, and adoptive transfer of Bim-deficient BMDCs into naive C57BL/6 mice led to increased T cell proliferation and autoantibody production *in vivo* [182]. Studies from our lab have also supported this model showing that Bim-deficient DCs have increased production of selective pro-inflammatory cytokines that may contribute to dysregulation of lymphocyte responses [183] (and see Results). Therefore, relative survival of DCs can have a profound influence in the regulation of adaptive immune responses.

Bim is a pro-apoptotic protein that is a part of the evolutionarily conserved Bcl-2 family [184]. Bcl-2 family members express from one to four conserved Bcl-2 homology (BH) domains, and Bim is a member of a diverse group of pro-apoptotic proteins called the BH3-only proteins (BOPs) that include Bad, Bid, Noxa and Puma. [185-187] When apoptosis is triggered, Bim binds directly to and displaces anti-apoptotic proteins Bcl-2, B cell lymphoma extra large (Bcl-x_L) and myeloid cell leukemia differentiation protein-1 (Mcl-1) that normally sequester the pro-apoptotic proteins, Bcl-2 associated X protein (Bax) and Bcl-2 antagonist/killer (Bak), thus freeing Bax/Bak to induce cytochrome c release from the mitochondria and cell death. Bouillet and colleagues generated *Bim*$^{-/-}$ mice and showed that Bim was crucial for normal embryonic and leukocyte development, maintaining homeostasis and prevention of systemic autoimmunity [188], thus illustrating the importance of lifespan in regulation of immune responses.

As DCs are critical regulatory cells of T and B lymphocytes, we hypothesized that Bim function in control of DC lifespan imparts regulation of B cells. We show that the homeostasis of DC subsets is dysregulated in *Bim*$^{-/-}$ mice, and Bim-deficient BMDCs

inhibits BCR-induced B cell proliferation. LPS-induced maturation could not reverse *Bim*$^{-/-}$ inhibition of BCR-induced B cell proliferation, indicating an intrinsic defect of Bim-deficient BMDCs to provide signals to support B cell activation. However, addition of exogenous BAFF could rescue B cell proliferation in the presence of *Bim*$^{-/-}$ BMDCs. The production of IL-6 was increased in *Bim*$^{-/-}$ DCs with and without LPS stimulation, but not on a per-cell basis, suggesting the dysregulation of cytokine production was due to prolonged survival and not through a cell-intrinsic mechanism. These studies reveal that prolonging the lifespan in DCs affects regulation of B cell responses, and may be a major contributing factor during the activation of naive B cells.

Results

Bim$^{-/-}$ DCs survive longer in culture compared to WT DCs

To determine how Bim influences DC lifespan, we first assessed whether *Bim$^{-/-}$* DCs survive longer compared to WT DCs. GM-CSF derived BMDCs from WT and *Bim$^{-/-}$* mice were washed from GM-CSF after 7 days of differentiation and cultured in media alone. Using trypan blue exclusion to assess survival, WT DCs dropped from 90 to ~50% cell viability within 24 hours and remained at a similar viability 48 hours after removal of GM-CSF (**Fig. 4.1**). In contrast, *Bim$^{-/-}$* DCs remained ~75% viable after 24 hours in culture, and did not further decline in viability up to 48 hours after GM-CSF removal. These results verified prolonged survival of *Bim$^{-/-}$* DCs compared to WT DCs in accordance to previous reports by Chen *et al.* [182]

Bim$^{-/-}$ BMDCs inhibit BCR-induced B cell proliferation regardless of maturation status

Our lab previously showed that immature WT BMDCs inhibit anti-IgM induced B cell proliferation while LPS-matured DCs did not [74]. To test whether *Bim$^{-/-}$* DCs were different in regulating BCR-induced B cell proliferation, we co-cultured WT and *Bim$^{-/-}$* BMDCs with CFSE-loaded splenic B cells from WT mice with anti-IgM Fab'2 fragments (**Fig. 4.2**). WT splenic B cells alone proliferated in a dose-dependent manner to anti-IgM stimulus. The addition of unstimulated WT or *Bim$^{-/-}$* BMDCs reduced proliferation by about 30% in B cell co-cultures at all doses of anti-IgM (**Fig. 4.2A**). In contrast, WT BMDCs matured with LPS for 24 hours no longer inhibited BCR- induced B cell proliferation (**Fig. 4.2B**). However, LPS maturation of *Bim$^{-/-}$* BMDCs had no effect on

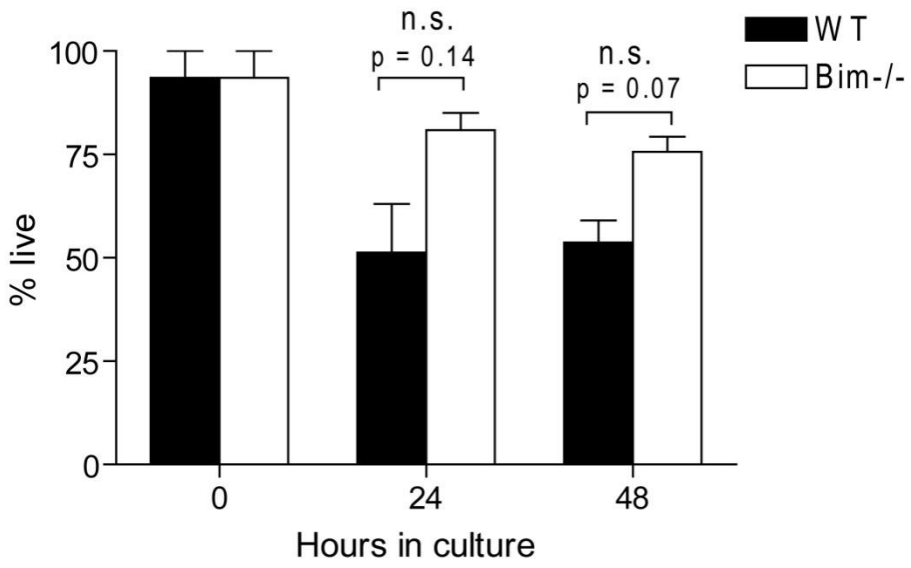

Figure 4.1. *Bim*$^{-/-}$ DCs survive longer in culture compared to WT DCs

GM-CSF-derived BMDCs after 7 days of differentiation from WT and *Bim*$^{-/-}$ mice were washed and replated in 10% FCS-containing media. At indicated timepoints, cells were assessed for viability using Trypan Blue exclusion and the frequency of live cells graphed. Data shows two independent experiments. Statistics were performed using a Student's t-test where n.s. = not significant.

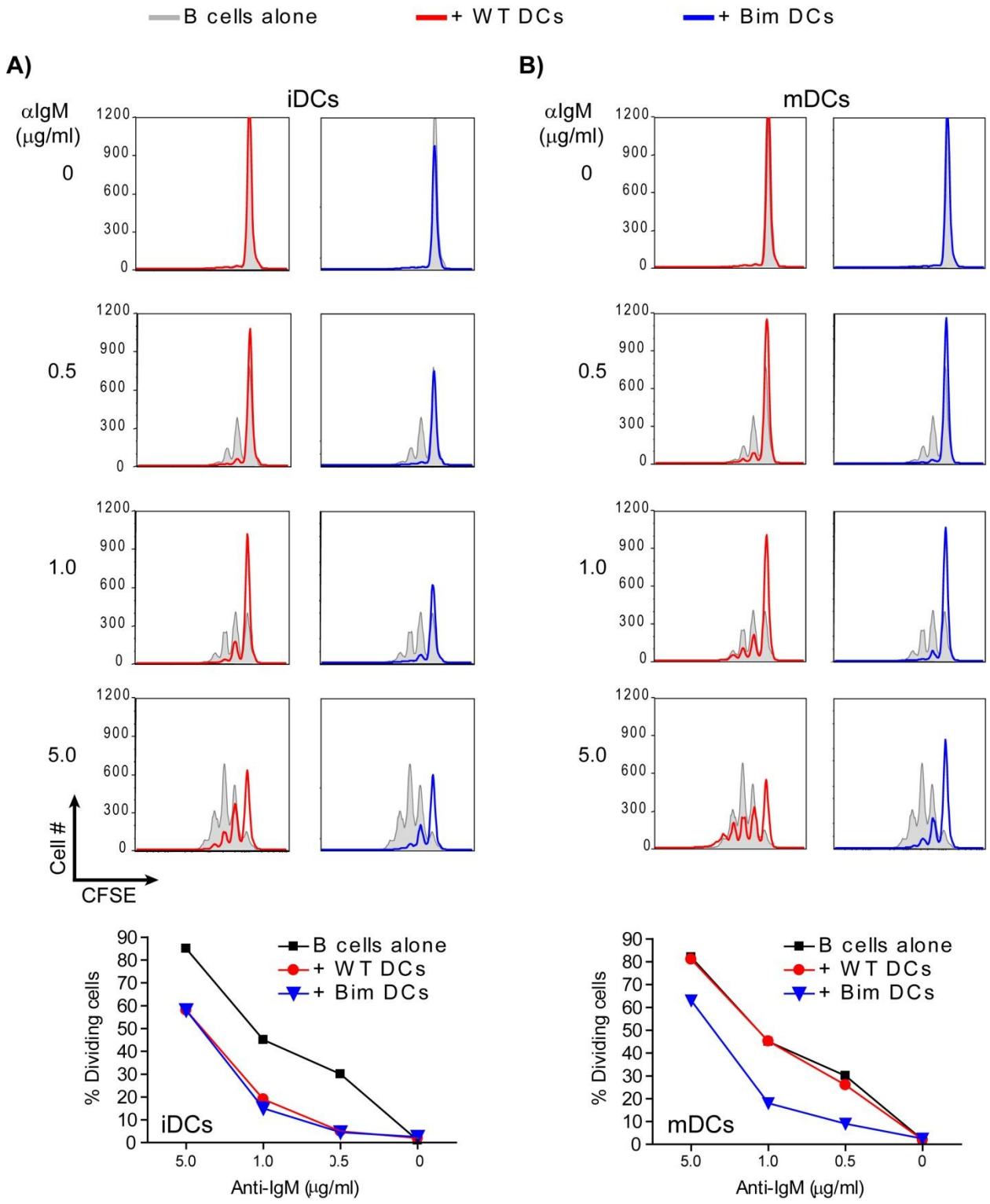
B cells alone
+ WT DCs
+ Bim DCs
A)
B)
iDCs
mDCs
αIgM (μg/ml)
0
0.5
1.0
5.0
1200
900
600
300
0
Cell #
CFSE
% Dividing cells
Anti-IgM (μg/ml)
5.0
1.0
0.5
0

Figure 4.2. *Bim*$^{-/-}$ BMDCs inhibit anti-IgM induced B cell proliferation regardless of maturation status

WT and *Bim*$^{-/-}$ BMDCs were generated as described. A) iDCs or B) mDCs matured with 1µg/ml LPS for 24 hours were washed and co-cultured with purified CFSE-labeled splenic B cells from WT mice with indicated doses of anti-IgM Fab'2 fragments for 72 hours. Histograms show CFSE dilution of B cells alone or co-cultured with BMDCs at a ratio of 4 B cells: 1 DC per well. The frequency of proliferating B cells cultured alone with anti-IgM, with WT DCs or Bim DCs in individual wells is indicated in the graphs. Data show one representative out of five independent experiments with similar results.

inhibition of BCR-induced B cell proliferation. These data show that *Bim*$^{-/-}$ BMDCs inhibit BCR-induced B cell proliferation, regardless of DC maturation status.

It was possible that inability of *Bim*$^{-/-}$ BMDCs to support B cell proliferation may be due to a defect in antigen presentation. To test this, we loaded BMDCs with protein antigens NP-conjugated chicken gamma globulin (NP-CGG) and hen egg lysozyme (HEL) and cultured them with purified transgenic B cells with antigen-specific receptors to NP (B1-8) [189] and HEL (MD4) [190], respectively (**Fig. 4.3A**). Transgenic B cells did not proliferate in the absence of BMDCs, even with high doses of antigen (**Fig. 4.3B, 4.3C**). At the highest dose of antigen and a 1:1 ratio of B cells: DCs, *Bim*$^{-/-}$ BMDCs induced less antigen-specific proliferation of B1-8^{hi} and MD4 B cells compared to WT BMDCs. Even though the differences were not statistically significant, there was a clear trend that WT DCs induced more proliferation of transgenic B cells compared to *Bim*$^{-/-}$ DCs. This suggested that *Bim*$^{-/-}$ BMDCs had defective antigen presentation to B cells.

***Bim*$^{-/-}$ DCs are dysregulated in production of specific cytokines and upregulation of activation markers**

We and others showed that LPS-matured *Bim*$^{-/-}$ BMDCs had increased production of TNFα and IL-12 compared to WT BMDCs, but not IL-23 [182,183]. We hypothesized that *Bim*$^{-/-}$ BMDCs may be dysregulated in cytokines associated with promoting B cell proliferation. IL-6 is important in inducing B cell differentiation into IgG-producing cells rather than proliferation [191]. We measured the production of cytokines in WT and *Bim*$^{-/-}$ BMDCs with or without stimulation with 1µg/ml LPS and

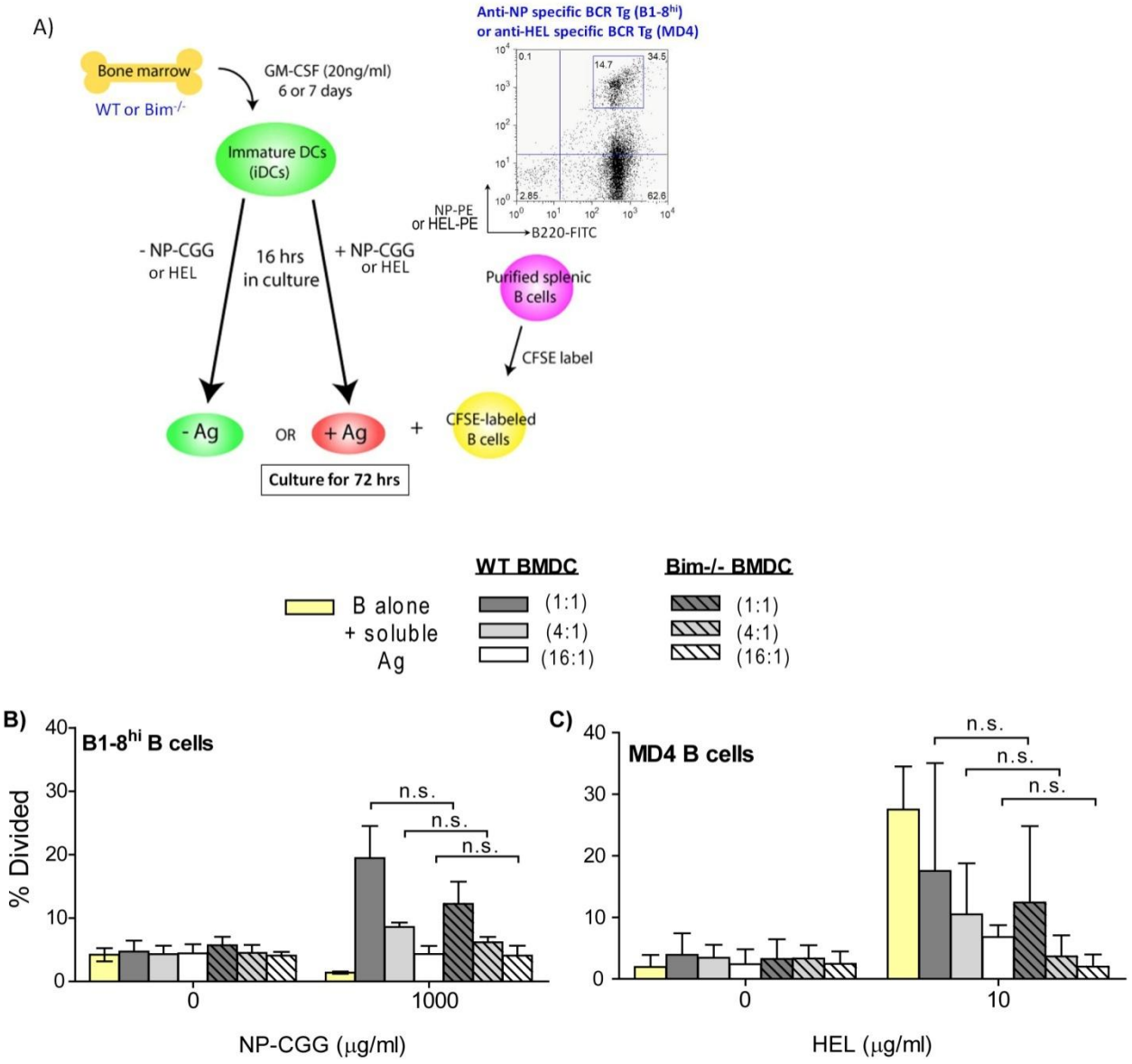

Figure 4.3. ***Bim*$^{-/-}$ BMDCs induce less antigen-specific B cell proliferation**

A) The experimental setup for *in vitro* co-cultures with transgenic B cells is shown. GM-CSF derived BMDCs were pulsed overnight with or without soluble NP-CGG or HEL. BMDCs were subsequently washed five times and co-cultured with CFSE-loaded transgenic B cells with antigen-specific BCRs to B) NP-CGG or C) HEL. The ratio of the number of B cells: DCs are shown in parentheses. After 72 hours, B cell proliferation was assessed and graphed. Data are from one representative of at least two independent experiments with similar results.

collected supernatants at 0, 24 and 48 hours to assess production of IL-6 by ELISA. *Bim*$^{-/-}$ BMDCs produced increased amounts of IL-6 compared to WT BMDCs with or without LPS maturation (**Fig 4.4A**). There was also increased production of the immunomodulatory cytokine IL-10 by *Bim*$^{-/-}$ splenic DCs stimulated with TLR agonists CpG and LPS, anti-CD40 mAb and NP-CGG antigen (**Fig 4.4B**). The increase in cytokine production was likely dependent on the survival of the DC cultures, as intracellular cytokine staining showed similar frequencies of IL-6 producing DCs from WT and *Bim*$^{-/-}$ BMDC cultures (**Fig 4.4C**). Thus the increased production of IL-6 and IL-10 by *Bim*$^{-/-}$ DCs may be inhibiting proliferation of B cells, and these increases in cytokine production are possibly due to the prolonged viability of the cells in culture.

We also examined the upregulation of costimulatory molecules in WT and *Bim*$^{-/-}$ splenic DCs after maturation stimuli to assess the immunogenicity of *Bim*$^{-/-}$ DCs. WT and *Bim*$^{-/-}$ splenic DCs expressed similar mean fluorescence intensity (MFI) of MHC II and CD40 in viable cells *ex situ*, 12 hours and 24 hours with and without stimulation (**Fig. 4.5A-4.5D**). However, *Bim*$^{-/-}$ DCs had increased expression of CD86 even in the absence of stimulation at 12 and 24 hours after isolation from the spleen (**Fig. 4.5E, 4.5F**). These differences were likely not due to the lifespan of the DC, as cell viabilities were similar between WT and *Bim*$^{-/-}$ DCs (data not shown), and the MFI was assessed only on viable cells. Although CD86 has not been reported to be involved in DC-B cell interactions, this suggests there are defects in *Bim*$^{-/-}$ DCs in expression of molecules

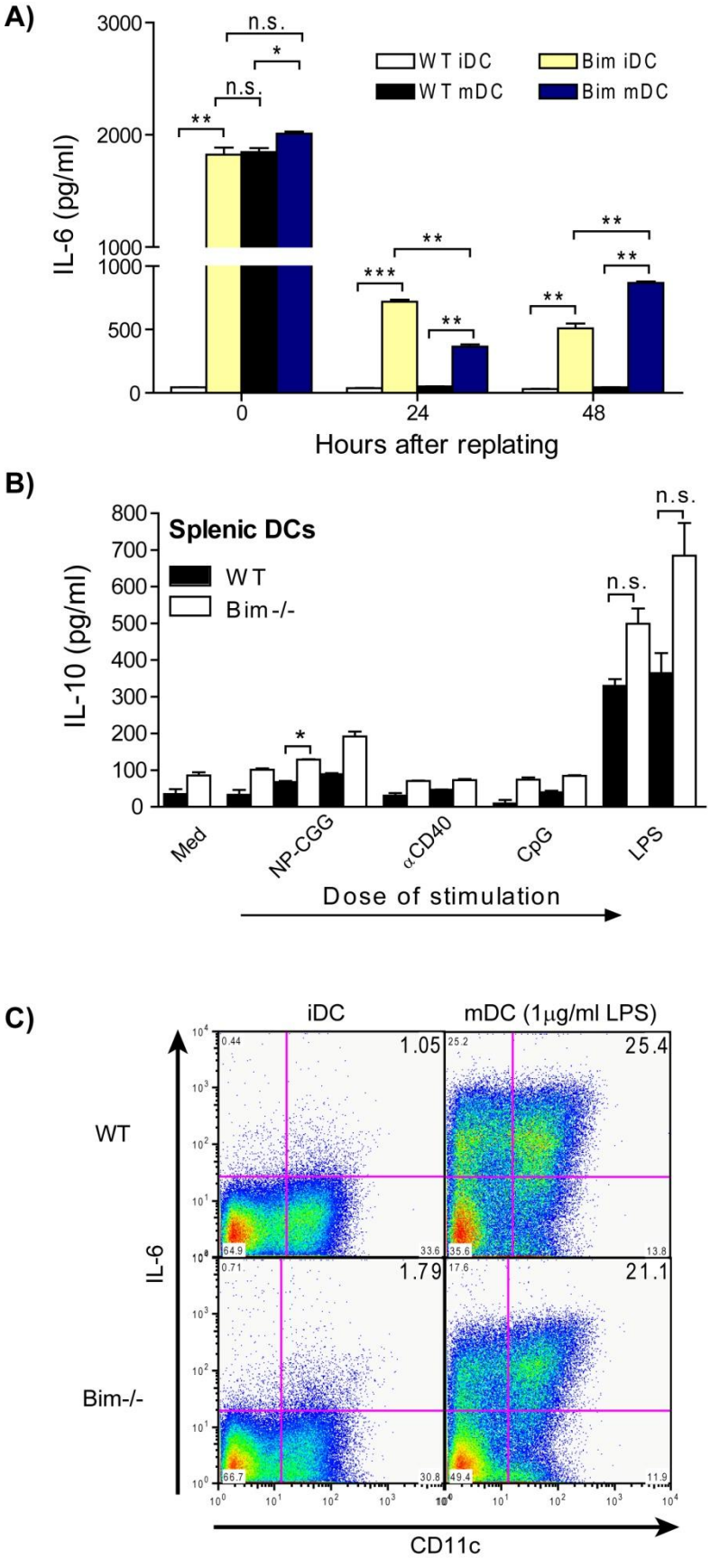
A)
IL-6 (pg/ml)
3000
2000
1000
500
0
n.s.
*
n.s.
**
WT iDC
Bim iDC
WT mDC
Bim mDC
**
***
**
**
**
**
0
24
48
Hours after replating
B)
IL-10 (pg/ml)
800
700
600
500
400
300
200
100
0
Splenic DCs
WT
Bim-/-
n.s.
n.s.
*
Med
NP-CGG
αCD40
CpG
LPS
Dose of stimulation
C)
iDC
mDC (1μg/ml LPS)
WT
Bim-/-
IL-6
1.05
25.4
1.79
21.1
0.44
64.9
33.6
25.2
35.6
13.8
0.71
66.7
30.8
17.6
49.4
11.9
CD11c

Figure 4.4. *Bim*$^{-/-}$ DCs secrete increased IL-6 and IL-10 compared to WT DCs

A) WT and *Bim*$^{-/-}$ BMDCs were generated in GM-CSF as described and were cultured with (mDCs) or without (iDCs) 1ug/ml LPS for 24 hours. After 24 hours, cells were washed from LPS and supernatants collected at indicated timepoints and assessed for IL-6. Data show one of at least three independent experiments. B) Splenic DCs were isolated from WT and *Bim*$^{-/-}$ mice and cultured for 24 hours with or without stimulation with graded doses of soluble NP-CGG, anti-CD40 mAb, CpG or LPS. Supernatants were collected and assessed for IL-10 production. Data are representative of at least two independent experiments. C) WT and *Bim*$^{-/-}$ BMDCs were generated in GM-CSF as described and were cultured with (mDCs) or without (iDCs) 1µg/ml LPS for 24 hours. Cells were stained for IL-6 by ICS. Gate frequencies for CD11c^{+}IL-6^{+} are shown. Data show representative plots from at least two independent experiments with similar results. Statistics are performed using a Student's t-test where *$p<0.05$, **$p<0.01$ and ***$p<0.001$.

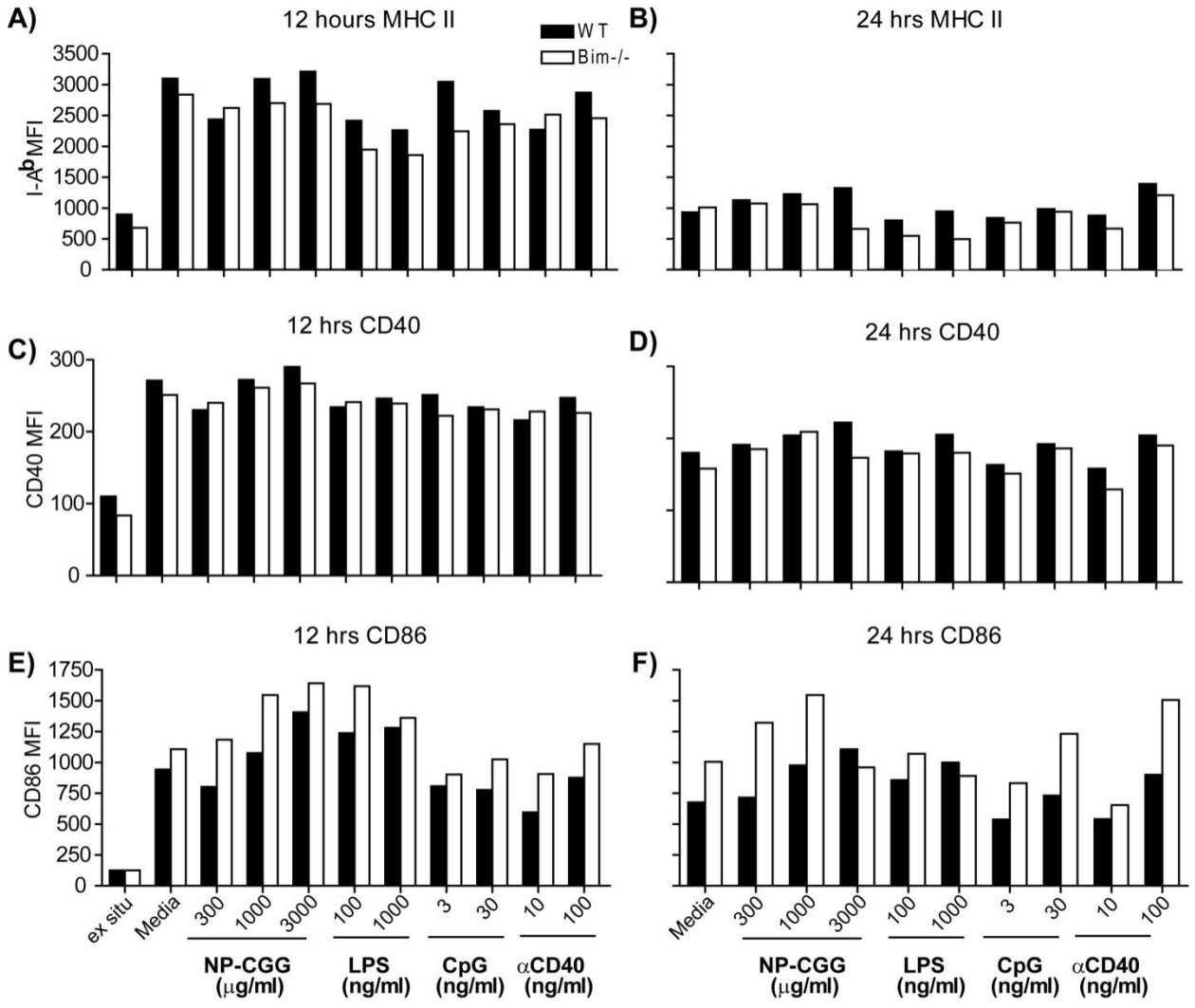

Figure 4.5. Splenic *Bim*$^{-/-}$ DCs have increased CD86 expression in culture

DCs were isolated from the spleens of WT and *Bim*$^{-/-}$ mice and processed as described. Cells were stained for surface expression of A-B) MHC-II (I-A^{b}), C-D) CD40 and E-F) CD86 at 12 and 24 hours after culture with and without indicated stimuli. The geometric MFI is shown for each condition.

involved with lymphocyte activation. Together, this data suggests lifespan-dependent and -independent defects in *Bim*$^{-/-}$ DCs in supporting B cell activation via dysregulation of cytokine production and expression of surface molecules.

Exogenous BAFF rescues the inability of Bim*$^{-/-}$ *BMDCs in inducing antigen-specific B cell proliferation

BAFF and APRIL are B cell pro-survival cytokines produced by DCs and other accessory cells [192]. We hypothesized that BAFF production may be dysregulated in *Bim*$^{-/-}$ DCs. We examined changes in gene expression of BAFF and APRIL by WT and *Bim*$^{-/-}$ BMDCs. At 6 hours after stimulation with LPS, there was surprisingly little gene induction of BAFF in *Bim*$^{-/-}$ BMDCs compared to WT BMDCs, as well as in unstimulated *Bim*$^{-/-}$ BMDCs (**Fig. 4.6A**). In contrast, there was increased gene induction of BAFF by *Bim*$^{-/-}$ BMDCs stimulated by Type I IFN. There was no difference in BAFF expression between WT and *Bim*$^{-/-}$ BMDCs stimulated with TGFβ. In addition, there was no clear difference in APRIL expression between WT and *Bim*$^{-/-}$ BMDCs with the exception of stimulation with Type I IFN; there was increased APRIL expression in *Bim*$^{-/-}$ BMDCs after stimulation with Type I IFN (**Fig. 4.6B**).

Surprisingly, by 12 hours in culture, *Bim*$^{-/-}$ BMDCs had decreased expression of both BAFF and APRIL compared to WT BMDCs at all stimuli used, with the exception of *Bim*$^{-/-}$ DCs in media, which had dramatically elevated expression of BAFF and APRIL (**Fig. 4.6C, 4.6D**). This drop in gene expression was not due to the death of the *Bim*$^{-/-}$

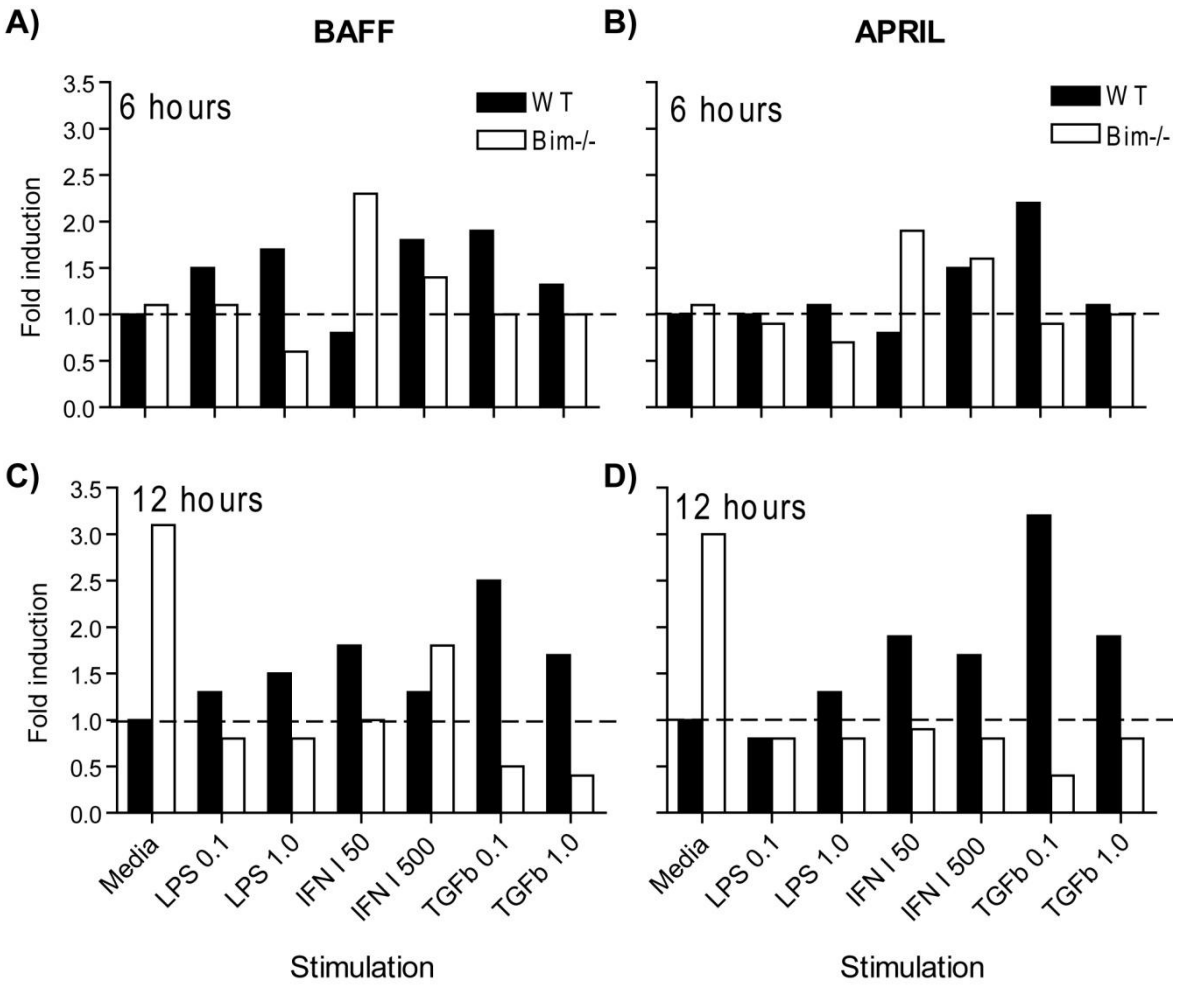
A)
BAFF
6 hours
WT
Bim-/-
Fold induction
B)
APRIL
6 hours
WT
Bim-/-
C)
12 hours
Fold induction
Media
LPS 0.1
LPS 1.0
IFN I 50
IFN I 500
TGFb 0.1
TGFb 1.0
Stimulation
D)
12 hours
Media
LPS 0.1
LPS 1.0
IFN I 50
IFN I 500
TGFb 0.1
TGFb 1.0
Stimulation

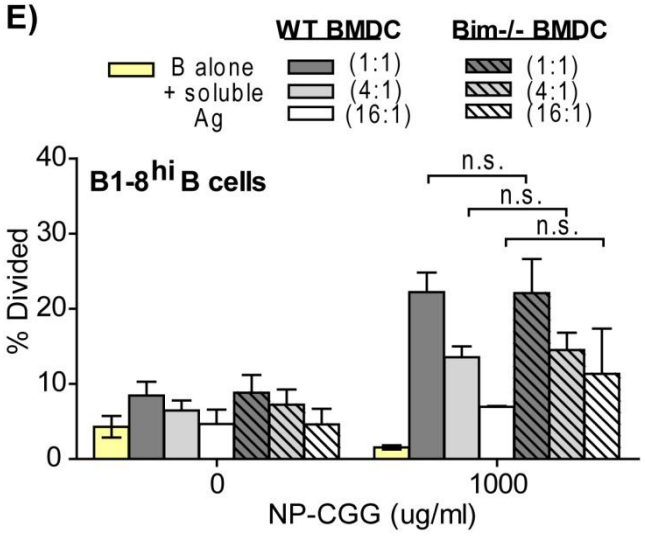
E)
WT BMDC
Bim-/- BMDC
B alone
+ soluble
Ag
(1:1)
(4:1)
(16:1)
B1-8hi B cells
% Divided
n.s.
n.s.
n.s.
NP-CGG (ug/ml)

Figure 4.6. *Bim*$^{-/-}$ DCs are dysregulated in BAFF and APRIL production

WT and *Bim*$^{-/-}$ BMDCs were generated as described and cultured with and without doses of LPS (0.1 and 1.0 µg/ml), Type I IFN (50 and 500 IU/ml) and TGFβ (0.1 and 1.0 µg/ml) for 6 and 12 hours. Relative fold induction of expression of A, C) BAFF and B, D) APRIL was normalized to WT media alone controls. E) Antigen-pulsed WT and *Bim*$^{-/-}$ BMDCs were co-cultured with CFSE-loaded B1-8^{hi} B cells at various B cell: DC ratios as previously described. 20ng/ml of recombinant BAFF was added to all the wells and cultured for 72 hours and frequency of divided cells graphed. Data show one representative experiment out of three independent experiments with similar results.

BMDCs in culture (data not shown). These cell-intrinsic defects in the expression of B cell pro-survival cytokines may be attributed to inability of mature *Bim*$^{-/-}$ BMDCs in promoting B cell proliferation. Indeed, the addition of exogenous BAFF to B1-8^{hi} B cells co-cultured with *Bim*$^{-/-}$ BMDCs rescued antigen-specific B cell proliferation to levels that were similar to those from WT BMDCs (**Fig. 4.6E**). The addition of exogenous BAFF did not increase proliferation in B1-8^{hi} B cells cultured alone with soluble antigen or with antigen-pulsed WT DCs (**Fig. 4.3B, 4.6E**), and thus only enhances B cell proliferation in the presence of DCs. Therefore, a defect in BAFF production may contribute to the defect of *Bim*$^{-/-}$ BMDCs in inducing antigen-specific B cell proliferation.

Bim*$^{-/-}$ *mice have increased numbers of CD8α*$^{+}$*DEC205*$^{+}$ *DCs in the spleen

Bim$^{-/-}$ mice develop spontaneous splenomegaly comprised of increased cell numbers of multiple leukocyte populations, including T cells, B cells and DCs [182,188]. As specific DC subsets have been shown to have differential functions in the regulation of T cells and different DC subsets have different half-lives *in vivo* (see Introduction), it is possible that Bim deficiency would affect specific DC subsets more profoundly than others, and thus impact DC-mediated regulation of specific adaptive immune responses. We therefore enumerated the numbers of splenic DC populations in *Bim*$^{-/-}$ mice. As expected, there were generally increased cell numbers of plasmacytoid, CD8α^{+}DEC205^{+} and DCIR2^{+} DCs in the spleens of *Bim*$^{-/-}$ mice (**Fig. 4.7A**). However, there was a statistically significant increase specifically in the CD8α^{+}DEC205^{+} DC subset (**Fig. 4.7B**). The frequencies of pDCs, CD8α^{+}DEC205^{+} and DCIR2^{+} DCs were not increased in *Bim*$^{-/-}$

mice (**Fig. 4.7C**), and in fact the frequencies of pDCs and DCIR2$^+$ DCs were actually decreased in the spleens of *Bim*$^{-/-}$ mice. Indeed, the half-life of the CD8α$^+$DEC205$^+$ subset in steady-state is the shortest compared to other DC subsets *in vivo* [59,60]. Therefore, the deficiency in Bim may most profoundly affect the functions of CD8α$^+$ DC-mediated regulation.

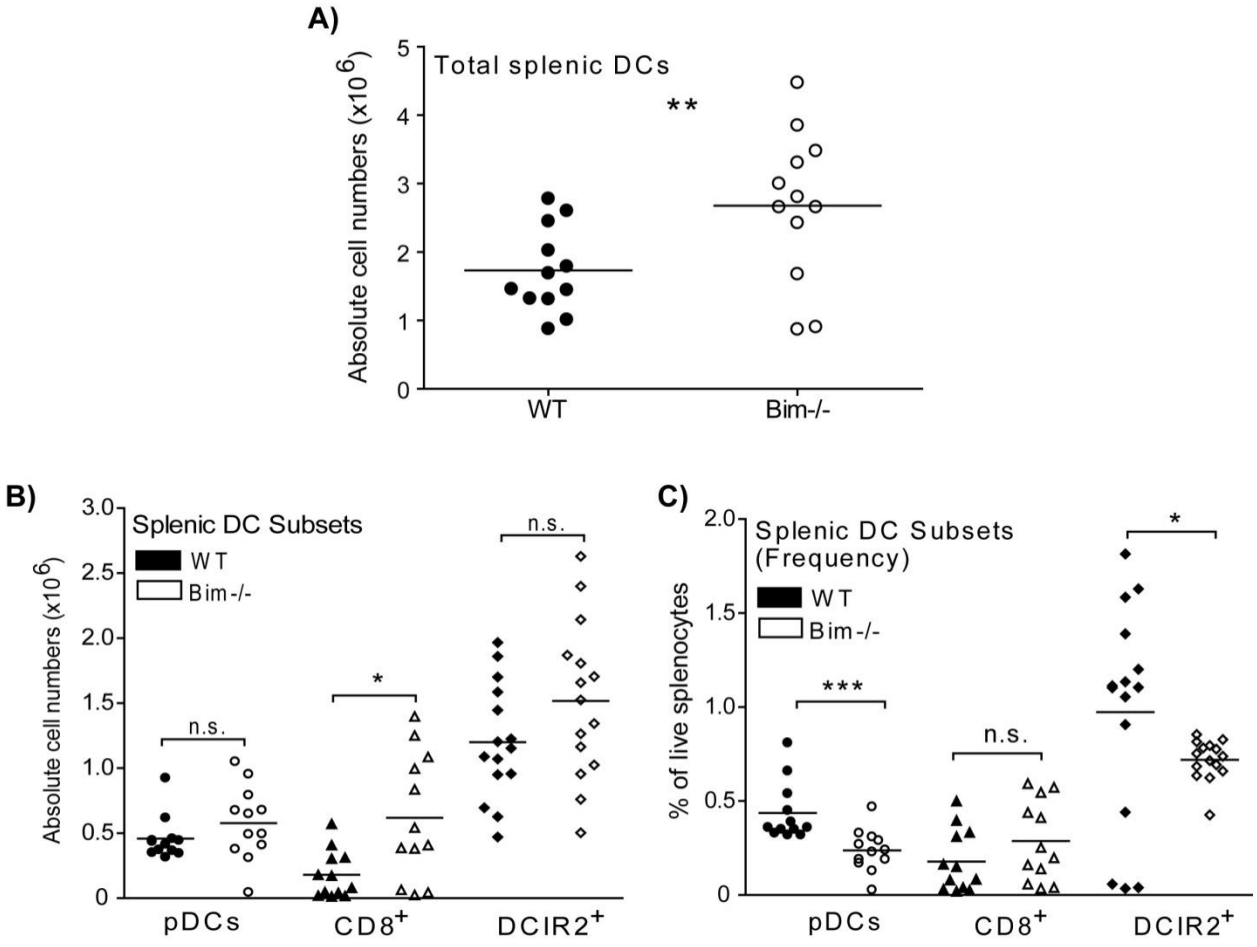

Figure 4.7. CD8α⁺DEC205⁺ DCs are increased in the spleens of *Bim*$^{-/-}$ mice

A) Total splenocytes were processed from WT and *Bim*$^{-/-}$ mice as described and cell numbers were enumerated. Statistics were performed using a Student's t-test where **p<0.01. B, C) Cells were stained for pDCs (CD11c^{lo}B220^{+}mPDCA-1^{+}), CD8α^{+} DCs (CD11c^{hi}B220^{-}CD8α^{+}DEC205^{+}DCIR2^{-}) and DCIR2^{+} (CD11c^{hi}B220^{-}CD8α^{-}DEC205^{-}DCIR2^{+}) subsets and B) absolute cell numbers and C) frequency of live splenocytes graphed. Each symbol represents an individual mouse. Data show mice from four independent experiments with at least three mice per group. Statistics were performed using a Mann-Whitney test for the median where *<0.05, ***p<0.001 and n.s. = not significant.

Discussion

Our observations reveal that loss of Bim in DCs causes dysregulation or defective BCR-induced B cell proliferation. Previously our lab showed that maturing WT BMDCs could overcome the suppressive effect that iDCs exert on B cell proliferation [74], which is consistent with the dogma that steady-state DCs exert a tolerogenic function on lymphocytes until they become matured through antigen uptake or stimulation such as a TLR agonist [193]. It is therefore surprising that mature *Bim*$^{-/-}$ DCs remained immunosuppressive to B cell proliferation (**Fig. 4.2, 4.3**), and suggests that Bim has a profound effect on the function of DC-mediated regulation of B cells.

It is unlikely that the inability of *Bim*$^{-/-}$ DCs to induce B cell proliferation is due to a defect to respond to maturation stimuli. Indeed, we showed that *Bim*$^{-/-}$ mDCs upregulated expression of CD86 as early as 12 hours after stimulation (**Fig. 4.5E**), and by 24 hours *ex vivo* expressed higher CD86 expression compared to WT even in the absence of maturation stimuli (**Fig. 4.5F**). In addition, *Bim*$^{-/-}$ DCs are highly capable of responding to maturation stimuli by producing cytokines such as IL-6 in response to LPS (**Fig. 4.4A, 4.4C**). Finally, analysis by ICS revealed that the absence of Bim expression in DCs does not alter the ability to produce cytokine, and the frequency of IL-6 producers was similar between WT and *Bim*$^{-/-}$ cultures (**Fig. 4.4C**). The increased IL-6 detected in the supernatants of *Bim*$^{-/-}$ DC cultures was most likely due to enhanced cell survival. Thus, prolonged lifespan of the DC or loss of Bim-dependent signaling may lead to the cell-intrinsic defects found in *Bim*$^{-/-}$ cells.

It is possible that Bim controls signaling pathways that directly regulate antigen presentation and production of B cell proliferation cytokines. Indeed, caspases, which are key players in the Fas-mediated apoptosis pathway have non-apoptotic functions such as T cell differentiation, activation of NF-κB signaling and cleavage of pro-IL-1 into bioactive IL-1 (reviewed in [194]). In a similar fashion, Bcl-2 family members Bcl-2, Bcl-x_L and Mcl-1 are all able to bind to the inositol triphosphosphate calcium receptor (InsP(3)R, IP_3R) to regulate intracellular calcium homeostasis as an anti-apoptosis mechanism [195].

Pro-apoptotic Bax and Bak have been shown to sequester anti-apoptotic members from interacting with IP_3R and thus indirectly regulate intracellular calcium flux [196]. Bim may also indirectly regulate other signaling pathways by sequestering anti-apoptotic Bcl-2 family members. Indeed, Ludwinski *et al.* reported that Bim expression was required for the activation of autoreactive T cells, as *Bim*$^{-/-}$ mice were resistant to experimentally autoimmune encephalomyelitis (EAE) [197]. *Bim*$^{-/-}$ T cells had decreased calcium-dependent activation of nuclear factor of activated T cells (NFAT) signaling and Bim may be similar to Bax and Bak in the ability to indirectly regulate calcium homeostasis by sequestering Bcl-2 from interacting with IP_3R. It would be intriguing to further investigate whether Bim and other members of the Bcl-2 family may have direct or indirect influence in other non-apoptotic signaling pathways.

BAFF and APRIL expression was decreased in *Bim*$^{-/-}$ DCs after *in vitro* stimulation, and the addition of recombinant BAFF modulates the inhibitory effects

Bim$^{-/-}$ DCs exerted on antigen-induced B cell proliferation (**Fig. 4.6E**). BAFF and APRIL are members of the tumor necrosis factor (TNF) family that have been well accepted as key players in regulating B cell development, differentiation, antibody class switching and survival [69,198-200]. BAFF especially has been at the forefront of interest in the field of autoimmunity, as BAFF inhibitors have been shown to be effective in ameliorating disease severity in murine models of systemic lupus erythematosus (SLE), arthritis, type I diabetes and multiple sclerosis. Several clinical human therapies aimed at blocking BAFF, APRIL and its receptors are currently being developed for the treatment of lupus and other B cell-associated diseases [201,202]. Also BAFF overexpressing [203,204] and deficient [205] transgenic mice have been developed and phenotypically exhibit clear B cell-associated autoimmune symptoms and severe defects in B cell development, respectively, highlighting the crucial role BAFF and other members have in regulating B cells.

DCs are major contributors to BAFF production and BAFF-mediated regulation of B cells *in vivo*. Using bone marrow chimeric mice, Gorelik *et al.* showed that while stromal cells were the major producers of BAFF and were required for full reconstitution of B cell subsets in the spleen, macrophage and DC-derived BAFF were also important contributors to BAFF-dependent B cell activation and antibody responses in the periphery [206]. In addition, pDC-derived IFNα is a potent inducer of BAFF production [207,208]. Therefore the dysregulation of BAFF and APRIL in *Bim*$^{-/-}$ DCs may reflect a previously undiscovered link between Bim signaling pathways or DC

lifespan to the regulation of B cell function. It will be interesting to determine how Bim signaling pathways may be connected to cytokine response of DCs and other cells.

Prolonging the lifespan of DCs can enhance generation of murine and human tumor-specific cytotoxic T cells. [209-212] However, prolonging lifespan also increases DC immunogenicity and can lead to excessive T cell proliferation [53,182] and development of autoimmunity [181,182]. Strategies for designing DC-based vaccines and therapies must take into consideration the enhancement of DC priming of immune responses by maximizing the viability of the APC, while simultaneously ensuring the safety of the therapy by preventing prolonged activation of immune responses that could lead to excessive inflammation and autoimmunity. Further understanding the function of Bim and other pro- and anti-apoptotic factors and how they maintain this delicate balance will be crucial to the future success of developing DC-mediated therapies.

Chapter 5: Conclusions and Final Remarks

CD22 and Bim are two molecules that influence the generation of adaptive immune responses, but function in very different ways to affect the priming of T and B cell responses. CD22 is important for protection against WNV infection, induces the generation of antiviral $CD8^+$ T cells, dictates DC-mediated expansion of splenocytes and may play a role in regulating cell chemotaxis into inflamed tissues. Bim affects the lifespan of DCs but also controls cell-intrinsic properties that direct B cell activation, including the production of B cell pro-survival cytokines BAFF and APRIL and pro-differentiation cytokine IL-6. Thus both CD22 and Bim regulate priming of adaptive immune responses. Further understanding of how these molecules function in regulating adaptive immunity would provide valuable insight for therapies aimed at enhancing protective immunity for various diseases.

The contribution of CD22 to cell migration has already been suggested, as *Cd22*$^{-/-}$ mice have decreased numbers of mature re-circulating B cells in the bone marrow [87,95,213]. There has been some contention though that decreased re-circulation was due to increased turnover of *Cd22*$^{-/-}$ B cells in the periphery rather than an inability to home to the bone marrow [87]. However, there were also decreased numbers of re-circulating B cells in *St6gal1*$^{-/-}$ mice that lack the ligands for CD22 [213]. Although *St6gal1*$^{-/-}$ B cells are somewhat impaired in proliferation and Ca^{2+} flux in response to various stimuli [214], it is possible the defects in B cell migration may be due to the effects of CD22-CD22 ligand interactions rather than to decreased survival alone. Indeed, CD22 was first

characterized as an adhesion molecule [104,105], and ligands for CD22 are broadly expressed across various cell types and tissues including on bone marrow sinusoidal endothelial cells that would be involved in B cell retention within the bone marrow [87]. Thus the loss of CD22 may result in reduced entry or retention of various CD22 ligand-expressing populations in peripheral lymphoid tissues, and may account for reduced numbers of myeloid and lymphocyte populations in the dLNs, spleens and brains of WNV-infected *Cd22*$^{-/-}$ mice (**Fig. 3.7-3.9**).

There was also an early reduction of NK cells in the dLNs and spleens, but not in the brains of WNV-infected *Cd22*$^{-/-}$ mice. NK cells do not express CD22 (**Fig. 3.11**), and for now the function of NK cells during WNV infection remains unclear. It is thus difficult to surmise the significance of this early reduction of NK cells for the survival of *Cd22*$^{-/-}$ mice and why the absence of CD22 affects NK cell numbers in infected tissues. Although NK cells can lyse WNV-infected cells, the lysis of infected astrocytes in the brain was solely carried out by cytotoxic T cells [215,216]. Therefore it is likely that NK cells have functions other than killing of infected neuronal cells to prevent WNV encephalitis. Indeed Zhang *et al.* showed that pre-treating Vero cells with supernatants of WNV-activated human NK cells protects them from infection by WNV *in vitro*, and that NK cell-derived IFNγ was involved in mediating protection [217]. In addition, the NK activating receptor NKp44 is able to bind WNV E protein, which suggests that NK cells may be functioning more as an innate immune responder that recognizes and can be directly activated by WNV to limit spread of infection in the periphery [218]. As NK cells

are able to bind to CD22 (**Fig. 3.13**) and have decreased migration into infected dLNs of *Cd22*$^{-/-}$ mice (**Fig. 3.9**), it is possible that CD22 directs migration or retention of NK cells into inflamed tissues via ligands expressed on NK cells themselves.

However, results from this study also suggest that CD22 may directly regulate production of chemokines. During WNV infection, T cells, macrophages and NK cells require CCR5 expression to migrate to the infected CNS [150,165]. Decreased induction of CCR5-binding chemokines in the infected dLN of *Cd22*$^{-/-}$ mice (**Fig. 3.10**) points to direct regulation of chemokine production by CD22, which may also control chemokine levels in other tissues such as the brain. A potential dysregulation of chemokine gradients within inflamed tissues may explain impaired recruitment of CCR5^{+} populations to the brain and dLNs in *Cd22*$^{-/-}$ mice during WNV infection (**Fig. 3.7**). Therefore, further research is necessary to elucidate the contribution of CD22 to cell chemotaxis during infection with viral pathogens, which may lead to discovery of CD22 regulation of cell migration in other contexts.

This study also brought to light the function of CD22 on DCs. While the regulation of BCR signaling in B cells by CD22 is well characterized, it remains unknown how CD22 may regulate signaling in other populations. This study showed that CD22 is expressed specifically on DCIR2^{+} DCs, and WNV-specific splenocyte expansion required expression of CD22 on this subset (**Fig. 3.11**). A better understanding of how CD22 may regulate the functions of DCIR2^{+} DCs would be of great value to current studies that target DCIR2^{+} DCs to enhance T cell [43,45,49] and B cell responses [179,219,220]. As CD22 is now found to be expressed on other non-B cell

populations such as eosinophils [97], it is likely that CD22 also functions to regulate innate immunity.

CD22 may directly regulate signaling pathways in activated DCs. Lyn kinase signaling has been shown modulate DC differentiation from bone marrow precursors, as well as induce maturation and IL-12 production with TLR and other stimuli to promote Th1 responses [221,222]. In addition, Lyn kinase activity can modulate activation of MAPKs, PI3K-Akt/PKB and NFκB signaling cascades and recruit SHP-1 and SHIP, the latter which is required for Lyn-dependent DC-mediated induction of IFNγ by NK cells [222]. As CD22 recruitment of adaptor molecules also depends on Lyn-dependent phosphorylation, and CD22 regulates multiple pathways activated by Lyn including MAPKs and PI3K in B cells, it is possible that CD22 may affect similar pathways in DCs. CD22 regulation of Lyn-dependent signaling cascades may therefore affect Th1 and NK cell responses, and one could hypothesize that altered WNV-specific lymphocyte and NK cell responses in *Cd22*$^{-/-}$ mice may be partly due to loss of CD22 regulation of DC signaling. Therefore, CD22 is likely an important factor in regulation of DC signaling pathways, and would thus have a more significant role in generation of adaptive T cell immune responses than previously described.

The involvement of CD22 in regulating WNV-specific antiviral T cell responses suggests that CD22 may play an important role in other diseases. It is possible that CD22 may be important for immunity to other types of viral or microbial pathogens, although it has already been demonstrated that CD22 was not required for survival

against LCMV [160], VSV [160] or *Staphylococcus aureus* [161]. As CD22 affected the migration of lymphocytes into the CNS (**Fig. 3.8**), protection from other encephalitic infections may also depend on the function of CD22. For example, other members of the neuroinvasive flavivirus family such as Japanese encephalitic virus and Dengue virus, which also depend on the function of antiviral $CD8^+$ T cells [223,224], may require CD22 function.

The influence of CD22 on $CD8^+$ T cell responses may also be significant in autoimmune diseases and cancer. Anti-CD22 mAbs such as Epratuzumab have already been developed to treat systematic lupus erythematosus (SLE) [225] and certain cancers such as acute lymphoblastic leukemia [226,227]. It is possible that anti-CD22 mAb strategies can be useful in other diseases caused by immunopathological $CD8^+$ T cells. For example, infiltrating $CD8^+$ T cells have been attributed to neuronal damage in the CNS and can exacerbate clinical severity of murine EAE and human multiple sclerosis (MS) [228]. Therefore, inhibiting CD22 may actually ameliorate symptoms associated with $CD8^+$ T cells in MS and EAE. In contrast, suppressing $CD8^+$ T cell responses via blocking CD22 may be counterproductive in treatment of cancers designed to enhance antitumor CTLs. Therefore, the applicability of targeting CD22 via use of mAb strategies must carefully weigh overall effects of blocking or ligating CD22, especially since results from our study suggest that CD22 can directly influence DC-mediated initiating of T cell expansion.

In addition to the importance of CD22 in regulating adaptive immune responses and potentially determining the function of DCs in regulating these responses, this

dissertation has also shown that the lifespan of the DC affects the regulation of adaptive immune responses. Results from this study have identified that lifespan of the DC is an important determinant in B cell responses as well as T cell responses. DCs from *Bim*$^{-/-}$ mice have prolonged survival, and *Bim*$^{-/-}$ DCs induce excessive T cell proliferation and activation [182]. This however was not the case in regulation of B cells, as *Bim*$^{-/-}$ DC failed to fully induce B cell proliferation even after LPS maturation (**Fig. 4.2**). This suggests that the factors that influence DC-mediated regulation of T cells may have completely different and distinct effects on DC-mediated regulation of B cells.

It is possible that DC-mediated regulation of B cell responses is more sensitive to the effects of the specific molecule or signaling pathways being targeted to extend DC longevity compared to DC-dependent regulation of T cells. Multiple groups have employed various strategies to generate DCs with increased lifespan, such as the overexpression of anti-apoptotic proteins of the Bcl-2 family, genetic knockouts of the decoy receptor osteoprotegrin (OPG) and Bim, and targeted expression of a baculovirus inhibitor of caspase [53,181-183,229]. DCs from all of these mice induced increased T cell activation and proliferation, but had a number of different B cell phenotypes. For example, both *Bim*$^{-/-}$ and *Opg*$^{-/-}$ BMDCs induce increased proliferation of T cells [182,229], yet *Opg*$^{-/-}$ mice had decreased production of TD antigen-specific IgG3 [229], a phenotype that was not observed in *Bim*$^{-/-}$ mice [182] (and data not shown). Another group generated mice with transgenic DCs induced with the p35 baculovirus inhibitor of caspase, and

although these DCs also have increased lifespan and induce increased T cell proliferation, they induce elevated autoantibody production *in vivo* [181] .

The mechanisms that account for the differences of the B cell responses from our studies are unclear, but it may have to do with how these molecules influence production of cytokines that affect B cell activation. Both *Bim*$^{-/-}$ and *Opg*$^{-/-}$ BMDCs produced higher levels of IL-12p40 and TNFα compared to WT BMDCs, and while *Opg*$^{-/-}$ BMDCs produced normal levels of IL-6 [183], *Bim*$^{-/-}$ BMDCs produced significantly higher levels of IL-6 compared to WT BMDCs (**Fig. 4.4A**). Although there may be multiple molecules that can directly affect the longevity of DCs, the outcome of DC-mediated regulation of B cell responses is likely to depend heavily on the molecular components being targeted and not simply due to the length of DC lifespan alone.

Another factor that may influence DC-mediated regulation of B cells is the subset of DC in which lifespan is being altered. This study showed that CD8α$^+$DEC205$^+$ DCs are specifically increased in cell number in the spleens of *Bim*$^{-/-}$ mice (**Fig. 4.7**). The relative half-life of CD8α$^+$DEC205$^+$ DCs in steady state is the shortest among the three DC subsets in the spleen (see Chapter 1), and so the CD8α$^+$ DC subset may be most profoundly affected by the loss of Bim. While the function of CD8α$^+$DEC205$^+$ DCs in regulating B cell responses is still unclear, one could speculate that CD8α$^+$DEC205$^+$ DCs would have a specialized function in the regulation of B cell responses, similar to having specific functions in regulating T cells. For instance, CD8α$^+$ DCs have been shown to be the principal cross-presenting APC [50,52] and potent inducers of Th1

responses [49,230] as compared to other DC subsets. It is likely that specific DC subsets would have differential effects on B cell responses as well. Indeed, pDCs have been shown to promote plasmablast generation and plasma cell differentiation through production of IFNα and IL-6, respectively rather than inducing B cell survival [207]. Dubois *et al.* demonstrated that DC-derived IL-12 was important for differentiation of naive B cells into plasma and memory B cells, and IL-6 was important for inducing Ab secretion from differentiated plasma cells [231]. As $CD8\alpha^+$ and $CD8\alpha^-DCAL2^+$ but not $CD8\alpha^-DCIR2^+$ DCs are major sources of IL-12 [43,44], it is possible that enhancing the lifespan of specific DC subsets such as the $CD8\alpha^+$ subset would drive B cells to differentiate into plasma and memory B cells rather than proliferate.

Maintaining the balance of producing effective DC induction of adaptive immune responses while preventing excessive activation that could lead to immunopathology remains a challenge in the development of DC-based vaccines and therapies; much of these obstacles remain in the proper control of DC viability. The spontaneous autoimmunity and embryonic lethality of *Bim*$^{-/-}$ mice is a clear indication of how important controlling lifespan in all cells is to maintaining this balance [188]. More specifically, maintenance of a limited lifespan in DCs is crucial for preserving peripheral tolerance, as adoptive transfer of DCs with prolonged lifespan into mice on the Murphy Roths large (MRL) background accelerates the development of autoimmunity *in vivo* [181,232].

However, extending the lifespan of DCs has shown to be effective in enhancing the resulting T cell responses, supporting the rationale to enhance the longevity of DC-based vaccines and therapies. Several studies utilizing murine and human tumors demonstrated that extending the lifespan of tumor antigen-loaded DCs increased the magnitude and duration of tumor-specific CTL responses [209,210,212,233,234]. Further insight into the mechanisms that are specifically bolstered by prolonging DC lifespan would increase the chances for the success of a DC-specific therapy, while diminishing possible side-effects that may include excessive or prolonged reactivity or unexpected dampening of other cellular responses.

The results from this study illustrate a few of the vast number of determinants that are involved in mounting an effective adaptive immune response. Figure 5.1 summarizes our findings of how CD22 and Bim function in controlling immune responses. Taking these factors into account is crucial to the success of the specific outcome of a therapy or vaccine aimed at enhancing the adaptive immune response. Targeting DCs in the hopes of enhancing T cells may have unexpected effects by suppressing the B cell response and vice-versa. In most cases, a fully effective immune response to a pathogen require cooperative efforts from both B cells and T cells, and the future development of vaccines and DC cell-based therapies should take into consideration the effects DCs have on both populations in order to boost the adaptive immune response as a whole.

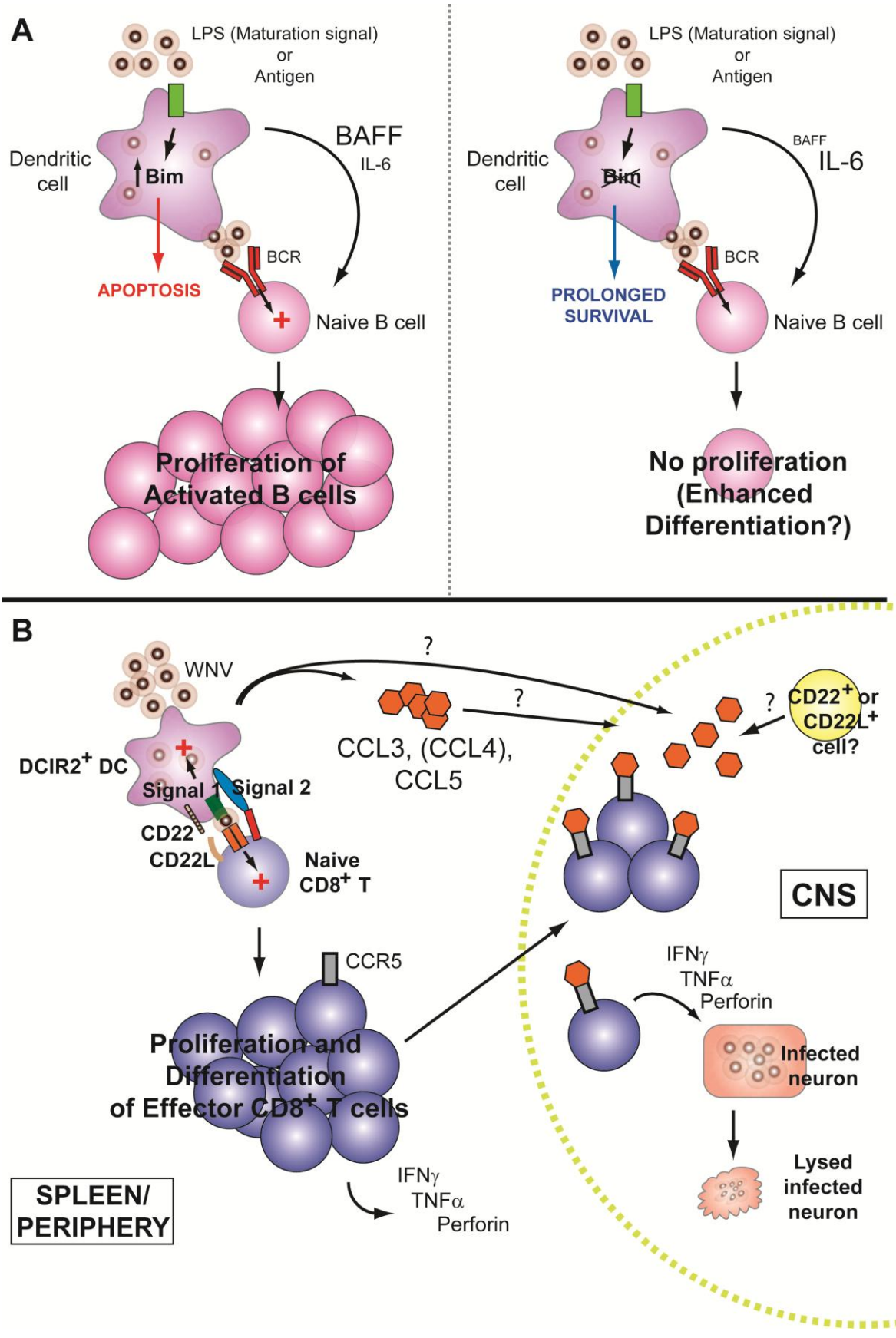
A
LPS (Maturation signal)
or
Antigen
Dendritic cell
Bim
BAFF
IL-6
BCR
APOPTOSIS
Naive B cell
Proliferation of Activated B cells
LPS (Maturation signal)
or
Antigen
Dendritic cell
Bim
BAFF
IL-6
BCR
PROLONGED SURVIVAL
Naive B cell
No proliferation (Enhanced Differentiation?)
B
WNV
?
?
CCL3, (CCL4), CCL5
?
CD22+ or CD22L+ cell?
DCIR2+ DC
Signal 1
Signal 2
CD22
CD22L
Naive CD8+ T
CNS
CCR5
IFNγ
TNFα
Perforin
Proliferation and Differentiation of Effector CD8+ T cells
Infected neuron
Lysed infected neuron
IFNγ
TNFα
Perforin
SPLEEN/ PERIPHERY

Figure 5.1. Working models of Bim and CD22 in the regulation of adaptive immune responses

A, left) Upon exposure to an antigen or maturation stimulus, Bim expression and production of cytokines like BAFF and IL-6 are upregulated within the DC. Increased production of BAFF aids in BCR-induced signaling in B cells, which together induces activating signals and initiates proliferation. Increased production of Bim induces DCs to undergo apoptosis. A, right) In the absence of Bim, survival of a DC after contact with an antigen or maturation stimulus is extended. BAFF production is dysregulated, and the DC continues to produce IL-6. Loss of BAFF from DCs inhibits BCR-induced activation and proliferation of naive B cells. Prolonged production of IL-6 may promote B cells to differentiate rather than proliferate. B) DCIR2$^+$ DCs encounter WNV in the periphery, and become activated. They in turn present peptide on MHC I complexes (Signal 1), express co-stimulatory molecules (Signal 2) and likely engage naive CD8$^+$ T cells via CD22-CD22L interactions. CD8$^+$ T cells become activated and proliferation and differentiation into effector cells capable of production IFNγ, TNFα and perforin. DCIR2$^+$ DCs are also producers of CCL3, CCL4, and CCL5, and it is unknown whether they can migrate into the CNS and produce these cytokines locally or if CCL3/4/5 produced in the periphery diffuses into the brain to recruit CD8$^+$ T cells or other CCR5$^+$ cells into the CNS. It is also possible cells within the CNS that may express CD22 or CD22L produce CCL3/4/5 locally to recruit CCR5$^+$ cells. After entering the CNS, WNV-specific CD8$^+$ T cells can lyse infected neurons to control virus spread and further neuronal destruction.

References

1. Cosenza, H. & Leserman, L.D. Cell interactions in antibody formation in vitro. I. Role of the third cell in the in vitro response of spleen cells to erythrocyte antigens. *J Immunol* **108**, 418-424 (1972).
2. Cosenza, H., Leserman, L.D. & Bowley, D.A. The third cell type required for the immune response of spleen cells in vitro. *J Immunol* **107**, 414-421 (1971).
3. Leserman, L.D., Cosenza, H. & Roseman, J.M. Cell interactions in antibody formation in vitro. II. the interaction of the third cell and antigen. *J Immunol* **109**, 587-594 (1972).
4. Steinman, R.M. & Cohn, Z.A. Identification of a novel cell type in peripheral lymphoid organs of mice. I. Morphology, quantitation, tissue distribution. *J Exp Med* **137**, 1142-1162 (1973).
5. Marland, G., Bakker, A.B., Adema, G.J. & Figdor, C.G. Dendritic cells in immune response induction. *Stem Cells* **14**, 501-507 (1996).
6. Inaba, K., Metlay, J.P., Crowley, M.T. & Steinman, R.M. Dendritic cells pulsed with protein antigens in vitro can prime antigen-specific, MHC-restricted T cells in situ. *J Exp Med* **172**, 631-640 (1990).
7. Ronchese, F. & Hausmann, B. B lymphocytes in vivo fail to prime naive T cells but can stimulate antigen-experienced T lymphocytes. *J Exp Med* **177**, 679-690 (1993).
8. Probst, H.C. & van den Broek, M. Priming of CTLs by lymphocytic choriomeningitis virus depends on dendritic cells. *J Immunol* **174**, 3920-3924 (2005).
9. Levin, D., Constant, S., Pasqualini, T., Flavell, R. & Bottomly, K. Role of dendritic cells in the priming of CD4+ T lymphocytes to peptide antigen in vivo. *J Immunol* **151**, 6742-6750 (1993).
10. Bohm, W*., et al.* Exogenous hepatitis B surface antigen particles processed by dendritic cells or macrophages prime murine MHC class I-restricted cytotoxic T lymphocytes in vivo. *J Immunol* **155**, 3313-3321 (1995).
11. Norbury, C.C., Malide, D., Gibbs, J.S., Bennink, J.R. & Yewdell, J.W. Visualizing priming of virus-specific CD8+ T cells by infected dendritic cells in vivo. *Nat Immunol* **3**, 265-271 (2002).
12. Janeway, C.A., Jr. & Bottomly, K. Signals and signs for lymphocyte responses. *Cell* **76**, 275-285 (1994).
13. Steinman, R.M. & Young, J.W. Signals arising from antigen-presenting cells. *Curr Opin Immunol* **3**, 361-372 (1991).
14. Fujii, S., Liu, K., Smith, C., Bonito, A.J. & Steinman, R.M. The linkage of innate to adaptive immunity via maturing dendritic cells in vivo requires CD40 ligation in addition to antigen presentation and CD80/86 costimulation. *J Exp Med* **199**, 1607-1618 (2004).
15. Inaba, K*., et al.* Expression of B7 costimulator molecules on mouse dendritic cells. *Adv Exp Med Biol* **378**, 65-70 (1995).
16. Luther, S.A. & Cyster, J.G. Chemokines as regulators of T cell differentiation. *Nat Immunol* **2**, 102-107 (2001).
17. Mohamadzadeh, M., Poltorak, A.N., Bergstressor, P.R., Beutler, B. & Takashima, A. Dendritic cells produce macrophage inflammatory protein-1 gamma, a new member of the CC chemokine family. *J Immunol* **156**, 3102-3106 (1996).
18. Piqueras, B., Connolly, J., Freitas, H., Palucka, A.K. & Banchereau, J. Upon viral exposure, myeloid and plasmacytoid dendritic cells produce 3 waves of distinct chemokines to recruit immune effectors. *Blood* **107**, 2613-2618 (2006).

19. Dustin, M.L. & Depoil, D. New insights into the T cell synapse from single molecule techniques. *Nat Rev Immunol* **11**, 672-684 (2011).
20. Krummel, M.F. & Davis, M.M. Dynamics of the immunological synapse: finding, establishing and solidifying a connection. *Curr Opin Immunol* **14**, 66-74 (2002).
21. Friedl, P., den Boer, A.T. & Gunzer, M. Tuning immune responses: diversity and adaptation of the immunological synapse. *Nat Rev Immunol* **5**, 532-545 (2005).
22. Benvenuti, F.*, et al.* Dendritic cell maturation controls adhesion, synapse formation, and the duration of the interactions with naive T lymphocytes. *J Immunol* **172**, 292-301 (2004).
23. Gett, A.V., Sallusto, F., Lanzavecchia, A. & Geginat, J. T cell fitness determined by signal strength. *Nat Immunol* **4**, 355-360 (2003).
24. van Stipdonk, M.J., Lemmens, E.E. & Schoenberger, S.P. Naive CTLs require a single brief period of antigenic stimulation for clonal expansion and differentiation. *Nat Immunol* **2**, 423-429 (2001).
25. Balkow, S.*, et al.* LFA-1 activity state on dendritic cells regulates contact duration with T cells and promotes T-cell priming. *Blood* **116**, 1885-1894 (2010).
26. Lanzavecchia, A. & Sallusto, F. Antigen decoding by T lymphocytes: from synapses to fate determination. *Nat Immunol* **2**, 487-492 (2001).
27. Chang, J.T.*, et al.* Asymmetric T lymphocyte division in the initiation of adaptive immune responses. *Science* **315**, 1687-1691 (2007).
28. van Kooyk, Y. & Geijtenbeek, T.B. A novel adhesion pathway that regulates dendritic cell trafficking and T cell interactions. *Immunol Rev* **186**, 47-56 (2002).
29. Smith-Garvin, J.E., Koretzky, G.A. & Jordan, M.S. T cell activation. *Annu Rev Immunol* **27**, 591-619 (2009).
30. Abram, C.L. & Lowell, C.A. The ins and outs of leukocyte integrin signaling. *Annu Rev Immunol* **27**, 339-362 (2009).
31. Clark, E.A. & Ledbetter, J.A. How B and T cells talk to each other. *Nature* **367**, 425-428 (1994).
32. Ma, D.Y. & Clark, E.A. The role of CD40 and CD154/CD40L in dendritic cells. *Semin Immunol* **21**, 265-272 (2009).
33. Moser, M. & Murphy, K.M. Dendritic cell regulation of TH1-TH2 development. *Nat Immunol* **1**, 199-205 (2000).
34. Kelsall, B.L., Stuber, E., Neurath, M. & Strober, W. Interleukin-12 production by dendritic cells. The role of CD40-CD40L interactions in Th1 T-cell responses. *Ann N Y Acad Sci* **795**, 116-126 (1996).
35. Reis e Sousa, C.*, et al.* In vivo microbial stimulation induces rapid CD40 ligand-independent production of interleukin 12 by dendritic cells and their redistribution to T cell areas. *J Exp Med* **186**, 1819-1829 (1997).
36. Pulendran, B. Modulating TH1/TH2 responses with microbes, dendritic cells, and pathogen recognition receptors. *Immunol Res* **29**, 187-196 (2004).
37. Phythian-Adams, A.T.*, et al.* CD11c depletion severely disrupts Th2 induction and development in vivo. *J Exp Med* **207**, 2089-2096 (2010).
38. Ito, T.*, et al.* TSLP-activated dendritic cells induce an inflammatory T helper type 2 cell response through OX40 ligand. *J Exp Med* **202**, 1213-1223 (2005).
39. Wang, Y.H.*, et al.* Maintenance and polarization of human TH2 central memory T cells by thymic stromal lymphopoietin-activated dendritic cells. *Immunity* **24**, 827-838 (2006).
40. Zhang, Y., Zhou, X. & Zhou, B. DC-derived TSLP promotes Th2 polarization in LPS-primed allergic airway inflammation. *Eur J Immunol* (2012).
41. de Jong, E.C.*, et al.* Microbial compounds selectively induce Th1 cell-promoting or Th2 cell-promoting dendritic cells in vitro with diverse th cell-polarizing signals. *J Immunol* **168**, 1704-1709 (2002).

42. MacDonald, A.S. & Maizels, R.M. Alarming dendritic cells for Th2 induction. *J Exp Med* **205**, 13-17 (2008).
43. Kasahara, S. & Clark, E.A. Dendritic cell-associated lectin 2 (DCAL2) defines a distinct CD8alpha-dendritic cell subset. *J Leukoc Biol* **91**, 437-448 (2012).
44. Shortman, K. & Heath, W.R. The CD8+ dendritic cell subset. *Immunol Rev* **234**, 18-31 (2010).
45. Dudziak, D.*, et al.* Differential antigen processing by dendritic cell subsets in vivo. *Science* **315**, 107-111 (2007).
46. Witmer, M.D. & Steinman, R.M. The anatomy of peripheral lymphoid organs with emphasis on accessory cells: light-microscopic immunocytochemical studies of mouse spleen, lymph node, and Peyer's patch. *Am J Anat* **170**, 465-481 (1984).
47. McLellan, A.D.*, et al.* Anatomic location and T-cell stimulatory functions of mouse dendritic cell subsets defined by CD4 and CD8 expression. *Blood* **99**, 2084-2093 (2002).
48. Carter, R.W., Thompson, C., Reid, D.M., Wong, S.Y. & Tough, D.F. Preferential induction of CD4+ T cell responses through in vivo targeting of antigen to dendritic cell-associated C-type lectin-1. *J Immunol* **177**, 2276-2284 (2006).
49. Soares, H.*, et al.* A subset of dendritic cells induces CD4+ T cells to produce IFN-gamma by an IL-12-independent but CD70-dependent mechanism in vivo. *J Exp Med* **204**, 1095-1106 (2007).
50. den Haan, J.M., Lehar, S.M. & Bevan, M.J. CD8(+) but not CD8(-) dendritic cells cross-prime cytotoxic T cells in vivo. *J Exp Med* **192**, 1685-1696 (2000).
51. Pooley, J.L., Heath, W.R. & Shortman, K. Cutting edge: intravenous soluble antigen is presented to CD4 T cells by CD8- dendritic cells, but cross-presented to CD8 T cells by CD8+ dendritic cells. *J Immunol* **166**, 5327-5330 (2001).
52. den Haan, J.M. & Bevan, M.J. Constitutive versus activation-dependent cross-presentation of immune complexes by CD8(+) and CD8(-) dendritic cells in vivo. *J Exp Med* **196**, 817-827 (2002).
53. Hou, W.S. & Van Parijs, L. A Bcl-2-dependent molecular timer regulates the lifespan and immunogenicity of dendritic cells. *Nat Immunol* **5**, 583-589 (2004).
54. Hermans, I.F., Ritchie, D.S., Yang, J., Roberts, J.M. & Ronchese, F. CD8+ T cell-dependent elimination of dendritic cells in vivo limits the induction of antitumor immunity. *J Immunol* **164**, 3095-3101 (2000).
55. Yang, J., Huck, S.P., McHugh, R.S., Hermans, I.F. & Ronchese, F. Perforin-dependent elimination of dendritic cells regulates the expansion of antigen-specific CD8+ T cells in vivo. *Proc Natl Acad Sci U S A* **103**, 147-152 (2006).
56. Ludewig, B.*, et al.* Perforin-independent regulation of dendritic cell homeostasis by CD8(+) T cells in vivo: implications for adaptive immunotherapy. *Eur J Immunol* **31**, 1772-1779 (2001).
57. Merad, M. & Manz, M.G. Dendritic cell homeostasis. *Blood* **113**, 3418-3427 (2009).
58. Kabashima, K.*, et al.* Intrinsic lymphotoxin-beta receptor requirement for homeostasis of lymphoid tissue dendritic cells. *Immunity* **22**, 439-450 (2005).
59. Kamath, A.T., Henri, S., Battye, F., Tough, D.F. & Shortman, K. Developmental kinetics and lifespan of dendritic cells in mouse lymphoid organs. *Blood* **100**, 1734-1741 (2002).
60. Kamath, A.T.*, et al.* The development, maturation, and turnover rate of mouse spleen dendritic cell populations. *J Immunol* **165**, 6762-6770 (2000).
61. Liu, K.*, et al.* Origin of dendritic cells in peripheral lymphoid organs of mice. *Nat Immunol* **8**, 578-583 (2007).
62. Parker, D.C. T cell-dependent B cell activation. *Annu Rev Immunol* **11**, 331-360 (1993).
63. Raff, M.C. T and B lymphocytes and immune responses. *Nature* **242**, 19-23 (1973).
64. Coffman, R.L. Mechanisms of helper T-cell regulation of B-cell activity. *Ann N Y Acad Sci* **681**, 25-28 (1993).

65. Klaus, S.J., Berberich, I., Shu, G. & Clark, E.A. CD40 and its ligand in the regulation of humoral immunity. *Semin Immunol* **6**, 279-286 (1994).
66. Craxton, A., Magaletti, D., Ryan, E.J. & Clark, E.A. Macrophage- and dendritic cell--dependent regulation of human B-cell proliferation requires the TNF family ligand BAFF. *Blood* **101**, 4464-4471 (2003).
67. Hoffmann, M.K. Control of B-cell differentiation by macrophages. *Ann N Y Acad Sci* **332**, 557-563 (1979).
68. Litinskiy, M.B.*, et al.* DCs induce CD40-independent immunoglobulin class switching through BLyS and APRIL. *Nat Immunol* **3**, 822-829 (2002).
69. MacLennan, I. & Vinuesa, C. Dendritic cells, BAFF, and APRIL: innate players in adaptive antibody responses. *Immunity* **17**, 235-238 (2002).
70. Inaba, K. & Steinman, R.M. Antibody responses to T-dependent antigens: contributions of dendritic cells and helper T lymphocytes. *Adv Exp Med Biol* **186**, 369-376 (1985).
71. Qi, H., Egen, J.G., Huang, A.Y. & Germain, R.N. Extrafollicular activation of lymph node B cells by antigen-bearing dendritic cells. *Science* **312**, 1672-1676 (2006).
72. Bergtold, A., Desai, D.D., Gavhane, A. & Clynes, R. Cell surface recycling of internalized antigen permits dendritic cell priming of B cells. *Immunity* **23**, 503-514 (2005).
73. Huang, N.N., Han, S.B., Hwang, I.Y. & Kehrl, J.H. B cells productively engage soluble antigen-pulsed dendritic cells: visualization of live-cell dynamics of B cell-dendritic cell interactions. *J Immunol* **175**, 7125-7134 (2005).
74. Santos, L.*, et al.* Dendritic cell-dependent inhibition of B cell proliferation requires CD22. *J Immunol* **180**, 4561-4569 (2008).
75. MacPherson, G., Kushnir, N. & Wykes, M. Dendritic cells, B cells and the regulation of antibody synthesis. *Immunol Rev* **172**, 325-334 (1999).
76. Dubois, B.*, et al.* Dendritic cells directly modulate B cell growth and differentiation. *J Leukoc Biol* **66**, 224-230 (1999).
77. Kushnir, N., Liu, L. & MacPherson, G.G. Dendritic cells and resting B cells form clusters in vitro and in vivo: T cell independence, partial LFA-1 dependence, and regulation by cross-linking surface molecules. *J Immunol* **160**, 1774-1781 (1998).
78. Wykes, M. & MacPherson, G. Dendritic cell-B-cell interaction: dendritic cells provide B cells with CD40-independent proliferation signals and CD40-dependent survival signals. *Immunology* **100**, 1-3 (2000).
79. Obayashi, K., Doi, T. & Koyasu, S. Dendritic cells suppress IgE production in B cells. *Int Immunol* **19**, 217-226 (2007).
80. Macpherson, A.J. & Uhr, T. Induction of protective IgA by intestinal dendritic cells carrying commensal bacteria. *Science* **303**, 1662-1665 (2004).
81. Gohlke, P.R.*, et al.* The receptor tyrosine kinase MerTK regulates dendritic cell production of BAFF. *Autoimmunity* **42**, 183-197 (2009).
82. Hanada, T.*, et al.* Suppressor of cytokine signaling-1 is essential for suppressing dendritic cell activation and systemic autoimmunity. *Immunity* **19**, 437-450 (2003).
83. Bergamin, F., Vincent, I.E., Summerfield, A. & McCullough, K.C. Essential role of antigen-presenting cell-derived BAFF for antibody responses. *Eur J Immunol* **37**, 3122-3130 (2007).
84. Johnson, S.*, et al.* Selected Toll-like receptor ligands and viruses promote helper-independent cytotoxic T cell priming by upregulating CD40L on dendritic cells. *Immunity* **30**, 218-227 (2009).
85. Nitschke, L. CD22 and Siglec-G: B-cell inhibitory receptors with distinct functions. *Immunol Rev* **230**, 128-143 (2009).

86. Law, C.L., Aruffo, A., Chandran, K.A., Doty, R.T. & Clark, E.A. Ig domains 1 and 2 of murine CD22 constitute the ligand-binding domain and bind multiple sialylated ligands expressed on B and T cells. *J Immunol* **155**, 3368-3376 (1995).
87. Nitschke, L., Floyd, H., Ferguson, D.J. & Crocker, P.R. Identification of CD22 ligands on bone marrow sinusoidal endothelium implicated in CD22-dependent homing of recirculating B cells. *J Exp Med* **189**, 1513-1518 (1999).
88. Law, C.L.*, et al.* CD22 associates with protein tyrosine phosphatase 1C, Syk, and phospholipase C-gamma(1) upon B cell activation. *J Exp Med* **183**, 547-560 (1996).
89. Schulte, R.J., Campbell, M.A., Fischer, W.H. & Sefton, B.M. Tyrosine phosphorylation of CD22 during B cell activation. *Science* **258**, 1001-1004 (1992).
90. Crocker, P.R., Paulson, J.C. & Varki, A. Siglecs and their roles in the immune system. *Nat Rev Immunol* **7**, 255-266 (2007).
91. Bofill, M.*, et al.* Human B cell development. II. Subpopulations in the human fetus. *J Immunol* **134**, 1531-1538 (1985).
92. Campana, D.*, et al.* Human B cell development. I. Phenotypic differences of B lymphocytes in the bone marrow and peripheral lymphoid tissue. *J Immunol* **134**, 1524-1530 (1985).
93. Dorken, B.*, et al.* HD39 (B3), a B lineage-restricted antigen whose cell surface expression is limited to resting and activated human B lymphocytes. *J Immunol* **136**, 4470-4479 (1986).
94. Erickson, L.D., Tygrett, L.T., Bhatia, S.K., Grabstein, K.H. & Waldschmidt, T.J. Differential expression of CD22 (Lyb8) on murine B cells. *Int Immunol* **8**, 1121-1129 (1996).
95. Nitschke, L., Carsetti, R., Ocker, B., Kohler, G. & Lamers, M.C. CD22 is a negative regulator of B-cell receptor signalling. *Curr Biol* **7**, 133-143 (1997).
96. Edwards, A.D.*, et al.* Relationships among murine CD11c(high) dendritic cell subsets as revealed by baseline gene expression patterns. *J Immunol* **171**, 47-60 (2003).
97. Wen, T.*, et al.* The pan-B cell marker CD22 is expressed on gastrointestinal eosinophils and negatively regulates tissue eosinophilia. *J Immunol* **188**, 1075-1082 (2012).
98. Tedder, T.F., Tuscano, J., Sato, S. & Kehrl, J.H. CD22, a B lymphocyte-specific adhesion molecule that regulates antigen receptor signaling. *Annu Rev Immunol* **15**, 481-504 (1997).
99. Miyagi, T. & Tsuiki, S. Purification and characterization of beta-galactoside (alpha 2 leads to 6)sialyltransferase from rat liver and hepatomas. *Eur J Biochem* **126**, 253-261 (1982).
100. Zhuo, Y. & Bellis, S.L. Emerging role of alpha2,6-sialic acid as a negative regulator of galectin binding and function. *J Biol Chem* **286**, 5935-5941 (2011).
101. Baum, L.G.*, et al.* Characterization of terminal sialic acid linkages on human thymocytes. Correlation between lectin-binding phenotype and sialyltransferase expression. *J Biol Chem* **271**, 10793-10799 (1996).
102. Braesch-Andersen, S. & Stamenkovic, I. Sialylation of the B lymphocyte molecule CD22 by alpha 2,6-sialyltransferase is implicated in the regulation of CD22-mediated adhesion. *J Biol Chem* **269**, 11783-11786 (1994).
103. Clark, E.A. CD22, a B cell-specific receptor, mediates adhesion and signal transduction. *J Immunol* **150**, 4715-4718 (1993).
104. Stamenkovic, I. & Seed, B. The B-cell antigen CD22 mediates monocyte and erythrocyte adhesion. *Nature* **345**, 74-77 (1990).
105. Stamenkovic, I., Sgroi, D., Aruffo, A., Sy, M.S. & Anderson, T. The B lymphocyte adhesion molecule CD22 interacts with leukocyte common antigen CD45RO on T cells and alpha 2-6 sialyltransferase, CD75, on B cells. *Cell* **66**, 1133-1144 (1991).
106. Pezzutto, A., Dorken, B., Moldenhauer, G. & Clark, E.A. Amplification of human B cell activation by a monoclonal antibody to the B cell-specific antigen CD22, Bp 130/140. *J Immunol* **138**, 98-103 (1987).

107. Pezzutto, A., Rabinovitch, P.S., Dorken, B., Moldenhauer, G. & Clark, E.A. Role of the CD22 human B cell antigen in B cell triggering by anti-immunoglobulin. *J Immunol* **140**, 1791-1795 (1988).
108. Tuscano, J., Engel, P., Tedder, T.F. & Kehrl, J.H. Engagement of the adhesion receptor CD22 triggers a potent stimulatory signal for B cells and blocking CD22/CD22L interactions impairs T-cell proliferation. *Blood* **87**, 4723-4730 (1996).
109. Craxton, A., Otipoby, K.L., Jiang, A. & Clark, E.A. Signal transduction pathways that regulate the fate of B lymphocytes. *Adv Immunol* **73**, 79-152 (1999).
110. Smith, K.G., Tarlinton, D.M., Doody, G.M., Hibbs, M.L. & Fearon, D.T. Inhibition of the B cell by CD22: a requirement for Lyn. *J Exp Med* **187**, 807-811 (1998).
111. Chan, V.W., Lowell, C.A. & DeFranco, A.L. Defective negative regulation of antigen receptor signaling in Lyn-deficient B lymphocytes. *Curr Biol* **8**, 545-553 (1998).
112. Fujimoto, M.*, et al.* B cell antigen receptor and CD40 differentially regulate CD22 tyrosine phosphorylation. *J Immunol* **176**, 873-879 (2006).
113. Greer, S.F. & Justement, L.B. CD45 regulates tyrosine phosphorylation of CD22 and its association with the protein tyrosine phosphatase SHP-1. *J Immunol* **162**, 5278-5286 (1999).
114. Ostrakhovitch, E.A., Wang, Y. & Li, S.S. SAP binds to CD22 and regulates B cell inhibitory signaling and calcium flux. *Cell Signal* **21**, 540-550 (2009).
115. Doody, G.M.*, et al.* A role in B cell activation for CD22 and the protein tyrosine phosphatase SHP. *Science* **269**, 242-244 (1995).
116. Otipoby, K.L., Draves, K.E. & Clark, E.A. CD22 regulates B cell receptor-mediated signals via two domains that independently recruit Grb2 and SHP-1. *J Biol Chem* **276**, 44315-44322 (2001).
117. Blasioli, J., Paust, S. & Thomas, M.L. Definition of the sites of interaction between the protein tyrosine phosphatase SHP-1 and CD22. *J Biol Chem* **274**, 2303-2307 (1999).
118. Sato, S.*, et al.* CD22 is both a positive and negative regulator of B lymphocyte antigen receptor signal transduction: altered signaling in CD22-deficient mice. *Immunity* **5**, 551-562 (1996).
119. Gerlach, J.*, et al.* B cell defects in SLP65/BLNK-deficient mice can be partially corrected by the absence of CD22, an inhibitory coreceptor for BCR signaling. *Eur J Immunol* **33**, 3418-3426 (2003).
120. Chen, J.*, et al.* CD22 attenuates calcium signaling by potentiating plasma membrane calcium-ATPase activity. *Nat Immunol* **5**, 651-657 (2004).
121. Poe, J.C., Fujimoto, M., Jansen, P.J., Miller, A.S. & Tedder, T.F. CD22 forms a quaternary complex with SHIP, Grb2, and Shc. A pathway for regulation of B lymphocyte antigen receptor-induced calcium flux. *J Biol Chem* **275**, 17420-17427 (2000).
122. Jacob, A., Cooney, D., Pradhan, M. & Coggeshall, K.M. Convergence of signaling pathways on the activation of ERK in B cells. *J Biol Chem* **277**, 23420-23426 (2002).
123. Sato, S., Tuscano, J.M., Inaoki, M. & Tedder, T.F. CD22 negatively and positively regulates signal transduction through the B lymphocyte antigen receptor. *Semin Immunol* **10**, 287-297 (1998).
124. O'Keefe, T.L., Williams, G.T., Davies, S.L. & Neuberger, M.S. Hyperresponsive B cells in CD22-deficient mice. *Science* **274**, 798-801 (1996).
125. Otipoby, K.L.*, et al.* CD22 regulates thymus-independent responses and the lifespan of B cells. *Nature* **384**, 634-637 (1996).
126. Poe, J.C.*, et al.* Severely impaired B lymphocyte proliferation, survival, and induction of the c-Myc:Cullin 1 ubiquitin ligase pathway resulting from CD22 deficiency on the C57BL/6 genetic background. *J Immunol* **172**, 2100-2110 (2004).
127. Samardzic, T.*, et al.* Reduction of marginal zone B cells in CD22-deficient mice. *Eur J Immunol* **32**, 561-567 (2002).
128. Petersen, L.R. & Roehrig, J.T. West Nile virus: a reemerging global pathogen. *Emerg Infect Dis* **7**, 611-614 (2001).

129. Kilpatrick, A.M. Globalization, land use, and the invasion of West Nile virus. *Science* **334**, 323-327 (2011).
130. Mukhopadhyay, S., Kuhn, R.J. & Rossmann, M.G. A structural perspective of the flavivirus life cycle. *Nat Rev Microbiol* **3**, 13-22 (2005).
131. Brien, J.D., Uhrlaub, J.L. & Nikolich-Zugich, J. West Nile virus-specific CD4 T cells exhibit direct antiviral cytokine secretion and cytotoxicity and are sufficient for antiviral protection. *J Immunol* **181**, 8568-8575 (2008).
132. Purtha, W.E.*, et al.* Antigen-specific cytotoxic T lymphocytes protect against lethal West Nile virus encephalitis. *Eur J Immunol* **37**, 1845-1854 (2007).
133. King, N.J.*, et al.* Immunopathology of flavivirus infections. *Immunol Cell Biol* **85**, 33-42 (2007).
134. Samuel, M.A. & Diamond, M.S. Pathogenesis of West Nile Virus infection: a balance between virulence, innate and adaptive immunity, and viral evasion. *J Virol* **80**, 9349-9360 (2006).
135. Johnston, L.J., Halliday, G.M. & King, N.J. Phenotypic changes in Langerhans' cells after infection with arboviruses: a role in the immune response to epidermally acquired viral infection? *J Virol* **70**, 4761-4766 (1996).
136. Johnston, L.J., Halliday, G.M. & King, N.J. Langerhans cells migrate to local lymph nodes following cutaneous infection with an arbovirus. *J Invest Dermatol* **114**, 560-568 (2000).
137. Purtha, W.E., Chachu, K.A., Virgin, H.W.t. & Diamond, M.S. Early B-cell activation after West Nile virus infection requires alpha/beta interferon but not antigen receptor signaling. *J Virol* **82**, 10964-10974 (2008).
138. Samuel, M.A. & Diamond, M.S. Alpha/beta interferon protects against lethal West Nile virus infection by restricting cellular tropism and enhancing neuronal survival. *J Virol* **79**, 13350-13361 (2005).
139. Lazear, H.M., Pinto, A.K., Vogt, M.R., Gale, M., Jr. & Diamond, M.S. Beta interferon controls west nile virus infection and pathogenesis in mice. *J Virol* **85**, 7186-7194 (2011).
140. Fredericksen, B.L., Keller, B.C., Fornek, J., Katze, M.G. & Gale, M., Jr. Establishment and maintenance of the innate antiviral response to West Nile Virus involves both RIG-I and MDA5 signaling through IPS-1. *J Virol* **82**, 609-616 (2008).
141. Suthar, M.S.*, et al.* IPS-1 is essential for the control of West Nile virus infection and immunity. *PLoS Pathog* **6**, e1000757 (2010).
142. Hildner, K.*, et al.* Batf3 deficiency reveals a critical role for CD8alpha+ dendritic cells in cytotoxic T cell immunity. *Science* **322**, 1097-1100 (2008).
143. Giordano, D.*, et al.* Nitric oxide controls an inflammatory-like Ly6C(hi)PDCA1+ DC subset that regulates Th1 immune responses. *J Leukoc Biol* **89**, 443-455 (2011).
144. Diamond, M.S., Shrestha, B., Marri, A., Mahan, D. & Engle, M. B cells and antibody play critical roles in the immediate defense of disseminated infection by West Nile encephalitis virus. *J Virol* **77**, 2578-2586 (2003).
145. Diamond, M.S.*, et al.* A critical role for induced IgM in the protection against West Nile virus infection. *J Exp Med* **198**, 1853-1862 (2003).
146. Sitati, E.M. & Diamond, M.S. CD4+ T-cell responses are required for clearance of West Nile virus from the central nervous system. *J Virol* **80**, 12060-12069 (2006).
147. Shrestha, B. & Diamond, M.S. Role of CD8+ T cells in control of West Nile virus infection. *J Virol* **78**, 8312-8321 (2004).
148. Shrestha, B., Samuel, M.A. & Diamond, M.S. CD8+ T cells require perforin to clear West Nile virus from infected neurons. *J Virol* **80**, 119-129 (2006).
149. Wang, Y., Lobigs, M., Lee, E. & Mullbacher, A. CD8+ T cells mediate recovery and immunopathology in West Nile virus encephalitis. *J Virol* **77**, 13323-13334 (2003).

150. Glass, W.G., *et al.* Chemokine receptor CCR5 promotes leukocyte trafficking to the brain and survival in West Nile virus infection. *J Exp Med* **202**, 1087-1098 (2005).
151. Suthar, M.S., *et al.* The RIG-I Like Receptor LGP2 Controls CD8+ T cell survival and fitness. *Immunity*, In Press (2012).
152. Keller, B.C., *et al.* Resistance to alpha/beta interferon is a determinant of West Nile virus replication fitness and virulence. *J Virol* **80**, 9424-9434 (2006).
153. Suthar, M.S., Brassil, M.M., Blahnik, G. & Gale, M., Jr. Infectious clones of novel lineage 1 and lineage 2 West Nile virus strains WNV-TX02 and WNV-Madagascar. *J Virol* **86**, 7704-7709 (2012).
154. Linke, S., Ellerbrok, H., Niedrig, M., Nitsche, A. & Pauli, G. Detection of West Nile virus lineages 1 and 2 by real-time PCR. *J Virol Methods* **146**, 355-358 (2007).
155. Mehlhop, E., Fuchs, A., Engle, M. & Diamond, M.S. Complement modulates pathogenesis and antibody-dependent neutralization of West Nile virus infection through a C5-independent mechanism. *Virology* **393**, 11-15 (2009).
156. Frey, A., Di Canzio, J. & Zurakowski, D. A statistically defined endpoint titer determination method for immunoassays. *J Immunol Methods* **221**, 35-41 (1998).
157. Bourne, N., *et al.* Early production of type I interferon during West Nile virus infection: role for lymphoid tissues in IRF3-independent interferon production. *J Virol* **81**, 9100-9108 (2007).
158. Engle, M.J. & Diamond, M.S. Antibody prophylaxis and therapy against West Nile virus infection in wild-type and immunodeficient mice. *J Virol* **77**, 12941-12949 (2003).
159. Torres, R.M., *et al.* Identification and characterization of the murine homologue of CD22, a B lymphocyte-restricted adhesion molecule. *J Immunol* **149**, 2641-2649 (1992).
160. Fehr, T., *et al.* Correlation of anti-viral B cell responses and splenic morphology with expression of B cell-specific molecules. *Int Immunol* **12**, 1275-1284 (2000).
161. Gjertsson, I., Nitschke, L. & Tarkowski, A. The role of B cell CD22 expression in Staphylococcus aureus arthritis and sepsis. *Microbes Infect* **6**, 377-382 (2004).
162. Shortman, K. & Liu, Y.J. Mouse and human dendritic cell subtypes. *Nat Rev Immunol* **2**, 151-161 (2002).
163. McCandless, E.E., Zhang, B., Diamond, M.S. & Klein, R.S. CXCR4 antagonism increases T cell trafficking in the central nervous system and improves survival from West Nile virus encephalitis. *Proc Natl Acad Sci U S A* **105**, 11270-11275 (2008).
164. Sitati, E., McCandless, E.E., Klein, R.S. & Diamond, M.S. CD40-CD40 ligand interactions promote trafficking of CD8+ T cells into the brain and protection against West Nile virus encephalitis. *J Virol* **81**, 9801-9811 (2007).
165. Brehin, A.C., *et al.* Dynamics of immune cell recruitment during West Nile encephalitis and identification of a new CD19+B220-BST-2+ leukocyte population. *J Immunol* **180**, 6760-6767 (2008).
166. Lefrancois, L., *et al.* The role of beta7 integrins in CD8 T cell trafficking during an antiviral immune response. *J Exp Med* **189**, 1631-1638 (1999).
167. Davison, A.M. & King, N.J. Accelerated dendritic cell differentiation from migrating Ly6C(lo) bone marrow monocytes in early dermal West Nile virus infection. *J Immunol* **186**, 2382-2396 (2012).
168. Lim, J.K. & Murphy, P.M. Chemokine control of West Nile virus infection. *Exp Cell Res* **317**, 569-574 (2011).
169. Masson, F., Mount, A.M., Wilson, N.S. & Belz, G.T. Dendritic cells: driving the differentiation programme of T cells in viral infections. *Immunol Cell Biol* **86**, 333-342 (2008).
170. Oppermann, M. Chemokine receptor CCR5: insights into structure, function, and regulation. *Cell Signal* **16**, 1201-1210 (2004).
171. Shrestha, B. & Diamond, M.S. Fas ligand interactions contribute to CD8+ T-cell-mediated control of West Nile virus infection in the central nervous system. *J Virol* **81**, 11749-11757 (2007).

172. Zhang, B., Chan, Y.K., Lu, B., Diamond, M.S. & Klein, R.S. CXCR3 mediates region-specific antiviral T cell trafficking within the central nervous system during West Nile virus encephalitis. *J Immunol* **180**, 2641-2649 (2008).
173. Engel, P.*, et al.* The same epitope on CD22 of B lymphocytes mediates the adhesion of erythrocytes, T and B lymphocytes, neutrophils, and monocytes. *J Immunol* **150**, 4719-4732 (1993).
174. Stamenkovic, I., Sgroi, D. & Aruffo, A. CD22 binds to alpha-2,6-sialyltransferase-dependent epitopes on COS cells. *Cell* **68**, 1003-1004 (1992).
175. Zeng, J.*, et al.* The generation of influenza-specific humoral responses is impaired in ST6Gal I-deficient mice. *J Immunol* **182**, 4721-4727 (2009).
176. Kim, C.H. & Broxmeyer, H.E. Chemokines: signal lamps for trafficking of T and B cells for development and effector function. *J Leukoc Biol* **65**, 6-15 (1999).
177. Castellino, F.*, et al.* Chemokines enhance immunity by guiding naive CD8+ T cells to sites of CD4+ T cell-dendritic cell interaction. *Nature* **440**, 890-895 (2006).
178. Lim, J.K.*, et al.* CCR5 deficiency is a risk factor for early clinical manifestations of West Nile virus infection but not for viral transmission. *J Infect Dis* **201**, 178-185 (2010).
179. Chappell, C.P., Draves, K.E., Giltiay, N. & Clark, E.A. Extrafollicular B cell activation by marginal zone dendritic cells T cell-dependent antibody responses. *J Exp Med* **209**, In press (2012).
180. Tischner, D., Woess, C., Ottina, E. & Villunger, A. Bcl-2-regulated cell death signalling in the prevention of autoimmunity. *Cell Death Dis* **1**, e48 (2010).
181. Chen, M.*, et al.* Dendritic cell apoptosis in the maintenance of immune tolerance. *Science* **311**, 1160-1164 (2006).
182. Chen, M., Huang, L. & Wang, J. Deficiency of Bim in dendritic cells contributes to overactivation of lymphocytes and autoimmunity. *Blood* **109**, 4360-4367 (2007).
183. Chino, T., Draves, K.E. & Clark, E.A. Regulation of dendritic cell survival and cytokine production by osteoprotegerin. *J Leukoc Biol* **86**, 933-940 (2009).
184. O'Connor, L.*, et al.* Bim: a novel member of the Bcl-2 family that promotes apoptosis. *EMBO J* **17**, 384-395 (1998).
185. Ewings, K.E., Wiggins, C.M. & Cook, S.J. Bim and the pro-survival Bcl-2 proteins: opposites attract, ERK repels. *Cell Cycle* **6**, 2236-2240 (2007).
186. Strasser, A.*, et al.* The role of bim, a proapoptotic BH3-only member of the Bcl-2 family in cell-death control. *Ann N Y Acad Sci* **917**, 541-548 (2000).
187. Strasser, A. The role of BH3-only proteins in the immune system. *Nat Rev Immunol* **5**, 189-200 (2005).
188. Bouillet, P.*, et al.* Proapoptotic Bcl-2 relative Bim required for certain apoptotic responses, leukocyte homeostasis, and to preclude autoimmunity. *Science* **286**, 1735-1738 (1999).
189. Shih, T.A., Meffre, E., Roederer, M. & Nussenzweig, M.C. Role of BCR affinity in T cell dependent antibody responses in vivo. *Nat Immunol* **3**, 570-575 (2002).
190. Goodnow, C.C.*, et al.* Altered immunoglobulin expression and functional silencing of self-reactive B lymphocytes in transgenic mice. *Nature* **334**, 676-682 (1988).
191. Horn, F., Henze, C. & Heidrich, K. Interleukin-6 signal transduction and lymphocyte function. *Immunobiology* **202**, 151-167 (2000).
192. Mackay, F., Silveira, P.A. & Brink, R. B cells and the BAFF/APRIL axis: fast-forward on autoimmunity and signaling. *Curr Opin Immunol* **19**, 327-336 (2007).
193. Steinman, R.M., Hawiger, D. & Nussenzweig, M.C. Tolerogenic dendritic cells. *Annu Rev Immunol* **21**, 685-711 (2003).
194. Lamkanfi, M., Festjens, N., Declercq, W., Vanden Berghe, T. & Vandenabeele, P. Caspases in cell survival, proliferation and differentiation. *Cell Death Differ* **14**, 44-55 (2007).

195. Eckenrode, E.F., Yang, J., Velmurugan, G.V., Foskett, J.K. & White, C. Apoptosis protection by Mcl-1 and Bcl-2 modulation of inositol 1,4,5-trisphosphate receptor-dependent Ca2+ signaling. *J Biol Chem* **285**, 13678-13684 (2010).
196. Oakes, S.A.*, et al.* Proapoptotic BAX and BAK regulate the type 1 inositol trisphosphate receptor and calcium leak from the endoplasmic reticulum. *Proc Natl Acad Sci U S A* **102**, 105-110 (2005).
197. Ludwinski, M.W.*, et al.* Critical roles of Bim in T cell activation and T cell-mediated autoimmune inflammation in mice. *J Clin Invest* **119**, 1706-1713 (2009).
198. Bossen, C. & Schneider, P. BAFF, APRIL and their receptors: structure, function and signaling. *Semin Immunol* **18**, 263-275 (2006).
199. Ng, L.G., Mackay, C.R. & Mackay, F. The BAFF/APRIL system: life beyond B lymphocytes. *Mol Immunol* **42**, 763-772 (2005).
200. Schneider, P. & Tschopp, J. BAFF and the regulation of B cell survival. *Immunol Lett* **88**, 57-62 (2003).
201. Pillai, S., Mattoo, H. & Cariappa, A. B cells and autoimmunity. *Curr Opin Immunol* **23**, 721-731 (2011).
202. Davidson, A. Targeting BAFF in autoimmunity. *Curr Opin Immunol* **22**, 732-739 (2010).
203. Mackay, F.*, et al.* Mice transgenic for BAFF develop lymphocytic disorders along with autoimmune manifestations. *J Exp Med* **190**, 1697-1710 (1999).
204. Khare, S.D.*, et al.* Severe B cell hyperplasia and autoimmune disease in TALL-1 transgenic mice. *Proc Natl Acad Sci U S A* **97**, 3370-3375 (2000).
205. Schiemann, B.*, et al.* An essential role for BAFF in the normal development of B cells through a BCMA-independent pathway. *Science* **293**, 2111-2114 (2001).
206. Gorelik, L.*, et al.* Normal B cell homeostasis requires B cell activation factor production by radiation-resistant cells. *J Exp Med* **198**, 937-945 (2003).
207. Jego, G.*, et al.* Plasmacytoid dendritic cells induce plasma cell differentiation through type I interferon and interleukin 6. *Immunity* **19**, 225-234 (2003).
208. Jego, G., Pascual, V., Palucka, A.K. & Banchereau, J. Dendritic cells control B cell growth and differentiation. *Curr Dir Autoimmun* **8**, 124-139 (2005).
209. Kim, J.H.*, et al.* 'Survival gene' Bcl-xl potentiates DNA-raised antitumor immunity. *Gene Ther* **12**, 1517-1525 (2005).
210. Ojima, T.*, et al.* Benefits of gene transduction of granulocyte macrophage colony-stimulating factor in cancer vaccine using genetically modified dendritic cells. *Int J Oncol* **31**, 931-939 (2007).
211. Hsieh, C.Y.*, et al.* IL-6-encoding tumor antigen generates potent cancer immunotherapy through antigen processing and anti-apoptotic pathways. *Mol Ther* **15**, 1890-1897 (2007).
212. Yoshikawa, T., Niwa, T., Mizuguchi, H., Okada, N. & Nakagawa, S. Engineering of highly immunogenic long-lived DC vaccines by antiapoptotic protein gene transfer to enhance cancer vaccine potency. *Gene Ther* **15**, 1321-1329 (2008).
213. Ghosh, S., Bandulet, C. & Nitschke, L. Regulation of B cell development and B cell signalling by CD22 and its ligands alpha2,6-linked sialic acids. *Int Immunol* **18**, 603-611 (2006).
214. Grewal, P.K.*, et al.* ST6Gal-I restrains CD22-dependent antigen receptor endocytosis and Shp-1 recruitment in normal and pathogenic immune signaling. *Mol Cell Biol* **26**, 4970-4981 (2006).
215. Liu, Y., Blanden, R.V. & Mullbacher, A. Identification of cytolytic lymphocytes in West Nile virus-infected murine central nervous system. *J Gen Virol* **70 (Pt 3)**, 565-573 (1989).
216. Liu, Y. & Mullbacher, A. Astrocytes are not susceptible to lysis by natural killer cells. *J Neuroimmunol* **19**, 101-110 (1988).
217. Zhang, M.*, et al.* Anti-West Nile virus activity of in vitro expanded human primary natural killer cells. *BMC Immunol* **11**, 3 (2010).

218. Hershkovitz, O*., et al.* NKp44 receptor mediates interaction of the envelope glycoproteins from the West Nile and dengue viruses with NK cells. *J Immunol* **183**, 2610-2621 (2009).
219. Skea, D.L. & Barber, B.H. Studies of the adjuvant-independent antibody response to immunotargeting. Target structure dependence, isotype distribution, and induction of long term memory. *J Immunol* **151**, 3557-3568 (1993).
220. Finkelman, F.D., Lees, A., Birnbaum, R., Gause, W.C. & Morris, S.C. Dendritic cells can present antigen in vivo in a tolerogenic or immunogenic fashion. *J Immunol* **157**, 1406-1414 (1996).
221. Chu, C.L. & Lowell, C.A. The Lyn tyrosine kinase differentially regulates dendritic cell generation and maturation. *J Immunol* **175**, 2880-2889 (2005).
222. Krebs, D.L*., et al.* Lyn-dependent signaling regulates the innate immune response by controlling dendritic cell activation of NK cells. *J Immunol* **188**, 5094-5105 (2012).
223. Yauch, L.E*., et al.* A protective role for dengue virus-specific CD8+ T cells. *J Immunol* **182**, 4865-4873 (2009).
224. Larena, M., Regner, M., Lee, E. & Lobigs, M. Pivotal role of antibody and subsidiary contribution of CD8+ T cells to recovery from infection in a murine model of Japanese encephalitis. *J Virol* **85**, 5446-5455 (2011).
225. Daridon, C*., et al.* Epratuzumab targeting of CD22 affects adhesion molecule expression and migration of B-cells in systemic lupus erythematosus. *Arthritis Res Ther* **12**, R204 (2010).
226. Sikder, M.A. & Friedberg, J.W. Beyond rituximab: The future of monoclonal antibodies in B-cell non-Hodgkin lymphoma. *Curr Hematol Malig Rep* **3**, 187-193 (2008).
227. Hoelzer, D. & Gokbuget, N. Chemoimmunotherapy in acute lymphoblastic leukemia. *Blood Rev* **26**, 25-32 (2012).
228. Johnson, T.A., Jirik, F.R. & Fournier, S. Exploring the roles of CD8(+) T lymphocytes in the pathogenesis of autoimmune demyelination. *Semin Immunopathol* **32**, 197-209 (2010).
229. Yun, T.J*., et al.* Osteoprotegerin, a crucial regulator of bone metabolism, also regulates B cell development and function. *J Immunol* **166**, 1482-1491 (2001).
230. Maldonado-Lopez, R*., et al.* CD8alpha+ and CD8alpha- subclasses of dendritic cells direct the development of distinct T helper cells in vivo. *J Exp Med* **189**, 587-592 (1999).
231. Dubois, B*., et al.* Critical role of IL-12 in dendritic cell-induced differentiation of naive B lymphocytes. *J Immunol* **161**, 2223-2231 (1998).
232. Izawa, T*., et al.* Crosstalk between RANKL and Fas signaling in dendritic cells controls immune tolerance. *Blood* **110**, 242-250 (2007).
233. Kim, J.H*., et al.* Enhancement of DC vaccine potency by activating the PI3K/AKT pathway with a small interfering RNA targeting PTEN. *Immunol Lett* **134**, 47-54 (2010).
234. Kim, J.H*., et al.* Enhancement of dendritic cell-based vaccine potency by anti-apoptotic siRNAs targeting key pro-apoptotic proteins in cytotoxic CD8(+) T cell-mediated cell death. *Immunol Lett* **122**, 58-67 (2009).